8-9-2014

Potential Stormwater Runoff Reductions by Incorporating Low Impact Development: Rocky Branch Watershed, Columbia, SC

Brett Sexton
University of South Carolina - Columbia

Potential Stormwater Runoff Reductions by Incorporating Low Impact Development: Rocky Branch Watershed, Columbia, SC

by

Brett Sexton

Bachelor of Arts
University of South Carolina, 2011

Submitted in Partial Fulfillment of the Requirements

For the Degree of Master of Earth and Environmental Resources Management in

Earth and Environmental Resources Management

College of Arts and Sciences

University of South Carolina

2014

Accepted by:

Allan James, Director of Thesis

Greg Carbone, Reader

Robin (Buz) Kloot, Reader

Lacy Ford, Vice Provost and Dean of Graduate Studies

Acknowledgements

I would like to give thanks to all of the people who have helped me on this journey. Their help and guidance does not go unnoticed and I will forever be grateful for their support. Without the help of the following people, my goals and accomplishment could not have been achieved.

I would like to take this opportunity to thank the entire faculty within the Geography Department for the countless times I walked into your office asking for assistance with or without an appointment. No matter what the circumstance I always remember leaving your office with a smile. I thank Dr. Ellis for first interesting me in graduate school and putting up with my multiple thesis topic changes. I truly appreciate the support provided by Lynn Shirley and Kevin Remington for the multiple GIS questions and software issues. I thank Dr. Hiscox and Dr. Kupfer for always keeping their office door open allowing me to stop by anytime for questions.

I would also like to extend a thank you to the Richland County GIS Department, Ken Aucoin for providing Richland County rainfall data, the United States Geological Survey for providing continuous stage data, and NOAA for RBW rainfall data. I would also like to thank Betsy Kaemmerlen for your help with the low-impact development designs and their capabilities.

To my committee members Dr. Kloot and Dr. Carbone, it is your input that helped me guide my interests and channel my focus towards urban runoff problems. Through your courses I have taken and the opportunities I have gotten to speak with you outside of the classroom you really helped me decide my thesis goals and research interests.

To Dr. Virginia Shervette, I cannot express the appreciation for your support, advice, and mentorship I have earned working with you these last couple of years. Whether the Congaree GPS ground-truthing, the electrofishing, or the office work, you always had a smile on your face and supported me no matter how down or frustrated I was. I cannot thank you enough for your friendship.

I would like to thank my advisor, Dr. Allan James, for being a friend and role model for me in the field and in the office. I cannot imagine your thoughts during the numerous drafts you had to analyze and question my methodology, but I am truly grateful for every minute working with you. Your knowledge you brought to the hydrology and spatial analysis really provided me with the skills needed in the workforce and I am eternally grateful for your mentorship.

To my parents, your love and support through this process has been incredible. Thank you for putting up with all of the bickering and doubting moments. No matter what the circumstance you guys always encouraged me to keep going and push through. I love you guys!

My deepest appreciation goes to Blair, whose constant support and love helped me push through to the end. You have been by my side from the beginning and I cannot begin to thank you for all of your needed words and inspiration over the last year. I love you so much. Thank you for always believing in me.

Abstract

Urbanization and increasing population are primary sources of water degradation, increased flood risks, and channel morphological instability. Impervious surface areas increase with urbanization and result in decreased infiltration capactities, increased stormwater runoff, and more rapid stormwater delivery, which in turn increase flood magnitudes and frequencies. Low impact development (LID) can provide volumetric detention storage to reduce flooding. This thesis reviews types of LID, their attributes and limitations, and examines how effectively they can abstract storm runoff volumes, reduce peak discharge, and delay stormwater arrival times for relatively frequent storm events in the Rocky Branch Watershed (RBW).

The RBW is 50% impervious, with some of the sub-watersheds as high as 73% impervious. The Gervais gage sub-basin, located in the headwaters of the Rocky Branch Creek, has an estimated peak discharge at the Gervais USGS gage site of 255 cfs. LID implementation provides stormwater volumetric abstractions by mimicking the preexisting natural landscape e.g., stimulating infiltration. LID volumetric abstractions within the Gervais gage sub-basin can potentially completely reduce peak discharge to zero cfs for the relatively frequent storm events; however, the purpose of this study is to mitigate the overbank flooding rather than eliminate natural flows.

Table of Contents

List of Tables

List of Figures

Chapter 1 - Introduction

Urbanization and increasing population are the main sources of water degradation (Walsh et al. 2005, Qadri 2012), increased flood risks (Leopold 1968, Burton and Pitt 2002, Hadden Loh 2012), and channel morphological instability (Chin 2006). Urban streams can cause flashier hydrographs, higher concentrations of contaminants, and reduced species richness (Arnold et al. 2010; Walsh et al. 2005). Surface-water degradation was first majorly attributed to point source pollution; however, since 1970 it has been realized a major contributor to impaired surface-water bodies is from nonpoint sources (Novotny and Olem 1994) such as construction sites, farmland, automobiles, and decomposing organic material. Healthy watersheds provide ecosystem services like clean drinking water, fishing and swimming opportunities, erosion control, flood protection, and animal habitat (Brion 2008, Hadden Loh 2012).

Impervious surface areas increase with urbanization and result in increases in stormwater runoff (Olsen et al. 2012), which in turn increase flood magnitudes and frequencies (Schueler and Holland 1994). The total runoff from a one-acre meadow during a one-inch rainstorm would fill a standard size office to a depth of about two feet (Schueler and Holland 1994); however, if the same acre was completely impervious the same amount of rainfall would completely fill the office in addition to two more (Schueler and Holland 1994). Urbanization encourages Hortonian overland flow, which is rapid runoff across the ground surface that occurs

when precipitation intensities exceed infiltration capacity. Figure 1.1 shows the typical water cycle within a watershed before and after urban development.

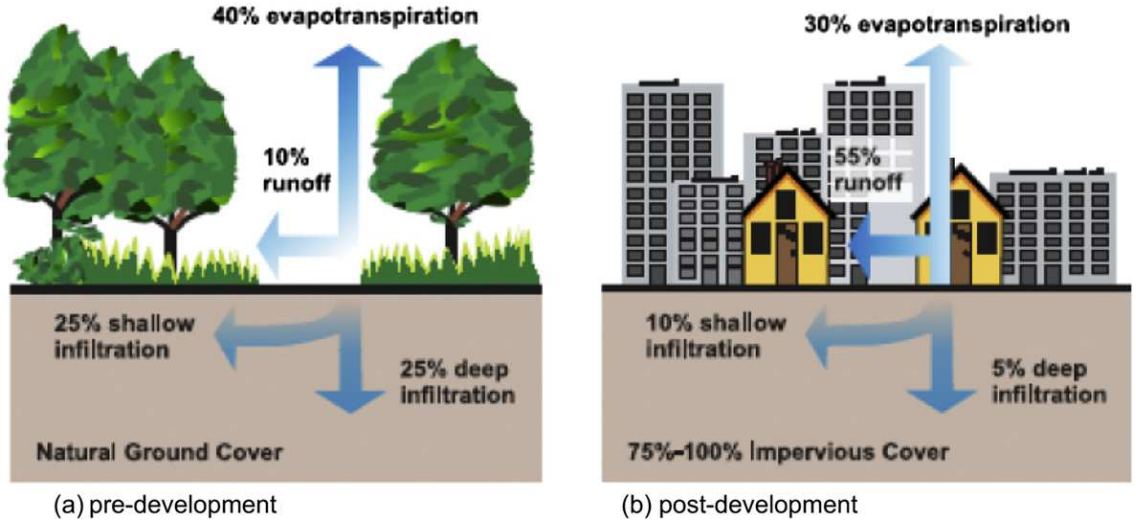

Figure 1.1. The Water Cycle for Pre-development and Post-development (Source: Olsen et al. 2012)

The Rocky Branch Watershed (RBW) located in Columbia, SC is an urbanized watershed with 50 percent impervious area. Some sub-basins within the RBW have impervious cover as high as 73 percent. RBW has rapid runoff, a well-established urban storm sewer system (USSS), and short lag times and time of concentration, which increases hydrograph response times. Highly urban areas often have low-base flows, higher peak discharges, and higher runoff volumes (Schueler 1987) for both large and small storm events. The USSS channelizes the Rocky Branch Creek (RBC) allowing for quicker flow due to lower channel roughness.

Runoff connectivity effects stormwater arrival times which will be calculated in Chapter 4. Two types of impervious cover are often described; i.e., total impervious area (TIA) and effective impervious area (EIA) (Schueler and Holland 1994). TIA is what Wooten (2008) mapped as the total area of impervious surfaces. EIA, also referred to as directly connected

impervious area (Novotny and Olem 1994), is the area of impervious surfaces that drain directly to channels or storm sewers. EIA is rarely known and has not been mapped in the RBW. Modern low-impact development (LID) can minimize the RBW runoff and stormwater arrival times by incorporating detention/retention structures.

Low-impact development

By definition, low impact development (LID) is a design strategy that encourages storage and infiltration of runoff and groundwater recharge through widely distributed, "micro-scale stormwater retention and detention areas, reduction of impervious surfaces, and the lengthening of flow paths and runoff time (Coffman, 2000)" (EPA 2000). LID employs site specific designs intended to mimic the preexisting natural landscape before development. LID techniques, pioneered by Prince George's County, Maryland in the early 1990s (EPA 2000), try to recreate surface hydrologic conditions of the natural landscape and to reduce surface imperviousness in order to increase infiltration and minimize stormwater surface runoff. This section describes bioretention cells and rain gardens, green roofs, cisterns, rain barrels, rain pillows, and permeable pavement as common examples of LID. Bioremediation and cover cropping are also discussed, which are techniques used for soil treatment and will play a role in stormwater runoff management discussed later; bioremediation and cover cropping are traditionally used for water and soil quality treatments but this thesis focuses on a volumetric analysis.

Bioretention and Rain Gardens

Bioretention cells are areas constructed with underlying drainage lines, a combination of different soil structures, and topped with a variety of native plants. They are designed to

improve water quality of stormwater runoff, restore the hydrologic condition of the surrounding area, and improve aesthetics (Zimmer 2006, Brown 2011). Rain gardens are smaller landscape features also designed to capture stormwater runoff but, unlike bioretention cells, typically do not require heavy machinery to create (Stringer 2011). Like most LID systems bioretention is a terrestrial-based water quality and stormwater reduction system designed to mimic predevelopment hydrologic regimes (Prince George's County 2007). Figure 1.2 is an illustration of the design which restores the hydrologic condition by encouraging infiltration and slowing the delivery of runoff by minimizing Hortonian overland flow. As with all LID strategies, these systems are effective when they are employed broadly across watershed areas upland of channels.

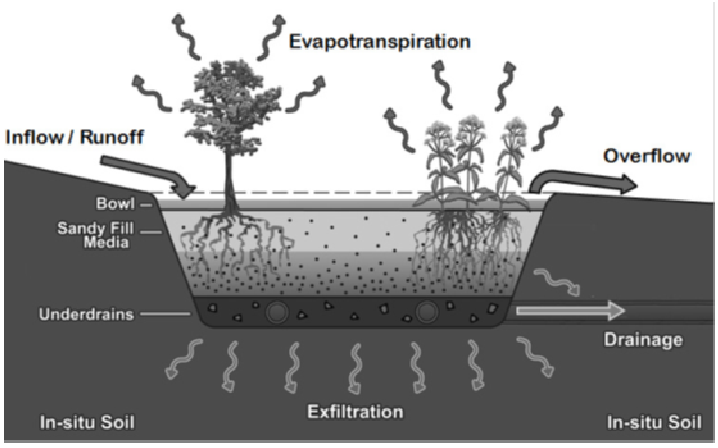

Figure 1.2. Bioretention Design (Source: Brown 2011)

Bioretention systems can be scaled for both commercial and residential benefits (Ahiablame 2012). In North Carolina, pollutant removal credits have been awarded for the construction of bioretention cells that are large enough to capture 1.5 inches (3.81 cm) in coastal counties and 1.0 inch (2.54 cm) everywhere else (Brown 2011). Florida, Kansas, Kentucky, Minnesota, Ohio, Texas, and Washington also provide stormwater utility credits (Doll and Lindsey 1999). The chemical, physical, and biological properties of soils help remove

stormwater pollutants through the four processes of settling, chemical reactions in the soil, plant uptake, and biological degradation in the root zones (Holmes 2012). In addition to pollutant removal, bioretention facilitates interception, infiltration, evaporation, transpiration, and assimilation (Prince George's County 2007). Together these functions help reduce runoff rates by increasing storage and evapotranspiration. A case study at Oak Terrace Preserve, North Charleston, South Carolina concluded that bioretention placed alongside front yards within the easement temporarily stored 5 cm of runoff (Vandiver 2010).

The design depths of each rain garden or bioretention cell depend on the slope of the drainage area. If the slope is less than 4% rain gardens can be less than 5 inches (12.7 cm) deep, between 5 and 7% slope the depth should be between 6 and 7 inches (15-18cm), and at slopes greater than 8% depth should be greater than 8 inches (20 cm) (Stringer 2011). If infiltrated water in bioretention and rain gardens can percolate completely between rain events groundwater recharge will increase. This is highly beneficial to groundwater sustainability, so many states enforce groundwater recharge requirements (Brown 2011).

Green Roofs

Green roofs are a combination of different types of vegetation systems installed on rooftops (Stringer 2011). Green roofs are constrained by flat rooftop space, but still show potential in less energy costs and stormwater runoff (USACE 2013). Figure 1.3 is an example of a green roof which is designed to compensate for the vegetation that was removed when the building was constructed (Ahiablame 2012). They are comprised of three components: subsurface drainage, growth media or soil, and vegetation on top (EPA 2000). Designed to mimic the natural landscape green roofs drastically improve permeability and aesthetics (Kloss and Calarusse 2006). Green roofs have the potential to improve air quality, minimize the urban

heat island effect, and store precipitation that would otherwise become runoff (Coffman 2000). Up to 85% of dust particles can be filtered out and removed from the air (Coffman 2000). Vegetative rooftops will mediate air temperatures allowing for cooler summers and warmer winters on buildings incorporating the design. The average rainfall retention by green roofs varies between 20% and 100% based upon rainfall intensity, duration, and depth of material. Furthermore, measurements of extensive green roofs reducing stormwater show that they intercept, retain, and evapotranspire between 34% and 69% of precipitation (Gregoire and Clausen 2011) if there is a fair amount of antecedent dry days preceding the rainfall event or the soil media has a low bulk density. A 3-inch (7.6 cm) green roof can retain approximately 0.6 inches (1.5 cm) of rain for each rainfall event and a 4-inch (10 cm) green roof can retain 50% of total rainfall over multiple storm events (Stringer 2011, Ahiablame 2012).

Figure 1.3. Green Roof in Paris, France
(Source: sustainablestormwater.org)

A 3000 ft^2 (286 m^2) rooftop in Philadelphia was fitted with a vegetated rooftop and witnessed 44 inches of rainfall within a nine month period. Only 15.5 inches (39.37 cm) of

runoff was generated; however, 90% of rainfall events in Philadelphia on average have intensities less than 2 inches (5 cm) per day (EPA 2000). Larger, more intense storm events cannot be extrapolated from the data gathered in the case study, but clear benefits are shown for smaller rain events.

Figure 1.4 is a before and after proposal in Washington, DC where buildings over 10,000 ft^2 (930 m^2) are covered by 20% vegetation. A proposed 20-year program is required to install green roofs on 20% of the city buildings over 10,000 ft^2 (Kloss and Calarusse 2006). There are 265 buildings within the RBW greater than 10,000 ft^2; therefore the potential is there.

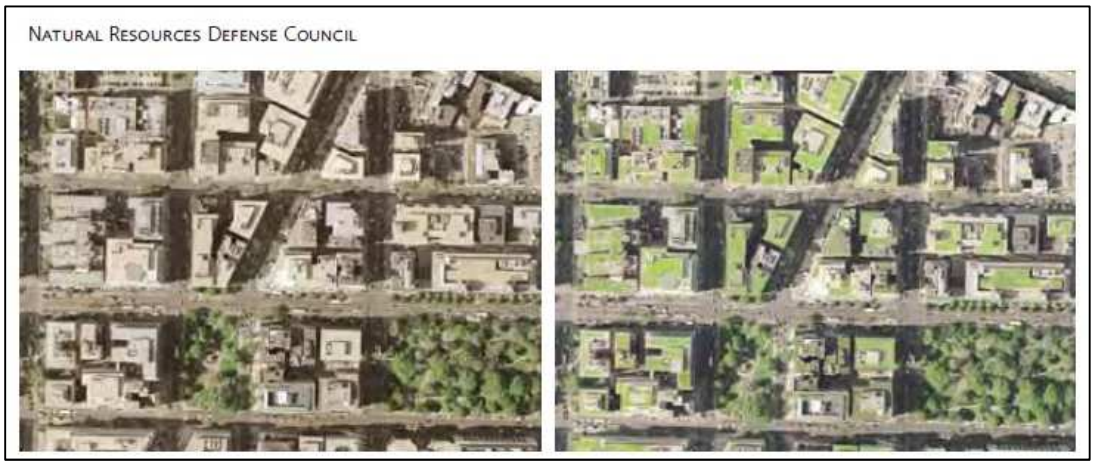

Figure 1.4 Washington, DC 20% Green Roof Program (Source: Kloss & Calarusse 2006)

Cisterns, Rain Barrels, and Rain Pillows

Cisterns and rain barrels are rainwater harvesting devices primarily used for landscaping, livestock watering, car washing, and nonpotable water uses, such as toilet flushing to provide detention storage volume (Coffman 2000, Donaldson 2009). Gutters must be installed to channel the rainwater running off the eaves of a building to these containers

(Krishna et al. 2005). Cisterns are often used on larger buildings whereas rain barrels are optimal for smaller single-family homes (see Figure 1.5).

Figure 1.5. Cistern (left) and Rain Barrel (right) (Source: Donaldson 2009)

Both are storage containers that can be placed above or below ground (Zimmer 2006). Different types of cisterns include: Fiberglass, wood, polypropylene, galvanized metal, stone, concrete, and ferrocement (a combination of steel and mortar) (Krishna et al. 2005). The wood must be a hardwood that can easily retain water, such as redwoods, fir, and cypress. The metals must be galvanized to prevent rusting from inundation. Fiberglass tanks can range from 50 to 15,000 gallons (189-56,800 liters), but are more cost efficient at the large-scale, and should be opaque to inhibit algae growth (Krishna et al. 2005). Another large-scale cistern is the wooden design which has available capacities ranging from 700 to 37,000 gallons (2,650-140,000 liters) (Krishna et al. 2005). Wooden designs are costly due to the limited choices of wood material; however, they are the best for aesthetics.

Rain barrels target smaller-scaled impervious areas due to their smaller capacities ranging usually from 20-75 gallons (76-284 liters), similar to municipal trash bins (Krishna et al. 2005). Rain barrels are typically only stored above ground, used for residential applications, and

should be equipped with mosquito screens and drain spigots (Coffman 2000, Zimmer 2006). A capacity goal when designing a cistern or rain barrel is to divert at least 10 gallons (37.9 liters) for every 1000 ft^2 (93 m^2) of impervious rooftop catchment area (Stringer 2011). Another capacity approximation to consider providing is 0.62 gallons (2.35 liters) per ft^2 (0.09 m^2) of building surface area per inch (2.54 cm) of rainfall (Krishna et al. 2005). An easy formula to use when trying to determine how large of a cistern a building needs is:

$$Volume = A*R_{ft}*0.9*7.5 \qquad \textit{Equation 1}$$

where volume is given in gallons, A is building surface area in square feet, R_{ft} is the rainfall depth in feet, *0.90* is a compensation factor allowing for evaporation, and *7.5* converts cubic feet to gallons (Donaldson 2009). For example, the Swearingen engineering building on the University of South Carolina's campus has a roof area of 67,500 ft^2 (6,271 m^2). A one-inch rainfall event on campus would create almost 38,000 gallons (144 m^3) of potential rainfall storage. Buildings this large would require multiple cisterns if a total storage of precipitation is desired.

Rain Pillows

Rain pillows are a horizontal design to fit wasted space in many homes and buildings with a gutter system. The pillows can be installed in many unused crawl spaces (Figure 1.6), basements, or above ground (Betsy Kaemmerlen written communication). Pumps are fitted to the pillow in order to apply collected rainwater to outdoor irrigation and can be designed as an automated irrigation system (RCS ND). In addition, a filtration system can be added for potable uses and treat the water to EPA drinking water standards. Rain pillows can be designed based on any buildings' footprint and can store up to 200,000 gallons (757 m^3). A variety of styles for single-family home use are available on the market with capacities ranging from 100 to 3,000 gallons (0.4 to 4 m^3) with or without plumping and pumps.

Figure 1.6. Rain Pillow (Source: RCS ND)

Permeable Pavement

Permeable pavements are blocks of asphalt with tiny areas of grass or sand separating each block. In areas with higher infiltration rates like the Midwestern United States permeable pavements do not require underlying drain systems whereas areas with slower infiltration rates drain systems are needed (Brown 2007). The permeable pavements are primarily used to reduce runoff rates; however, they can also be coupled with rainwater storage for reuse (Ahiablame 2012).

Permeable pavement can reduce runoff up to 72% from ten recent studies; however, pore spaces can become clogged (Ahiablame 2012, Sansalone et al. 2012, Yong et al. 2013). For a 1x1 m^2 permeable pavement parcel runoff reductions can be as high as 1 mm/hr (Brown 2007); the best reductions occur during the first flush of rainfall (Sansalone et al. 2012).

Bioremediation & Protective Covering

While bioremediation and protective covering are not LID practices, they can lower curve numbers (CNs), increase infiltration, minimize surface runoff, and improve water quality. This thesis does not focus on water quality but these concepts are well-known and important to discuss. Bioremediation and protective covering do not require conventional tillage (Olsen et al. 2013) and can be applied in highly urban areas similar to RBW.

Bioremediation is a set of waste-management tools for breaking down pollutants at contaminated sites. It becomes relevant to LID and conventional stormwater retention where storage of rainwater is associated with water quality issues. In particular, bioremediation can be used to pretreat stormwater before it reaches detention storage facilities or post-treat water after it is stored. Toxic organic and inorganic chemicals from urban runoff are major contributors to water contamination (Singh 2008). These chemicals found in the soil can be consumed by plants through a process called immobilization, (Kohnke and Franzmeier 1995; Novotny 2003) which is the conversion of an element from the inorganic to the organic form. The bioremediation process uses the normal functions of bacteria, fungi, and plants to break down these contaminants (Donlon and Bauder 2007).

Protective covering is traditionally designed to protect otherwise bare soil from erosion (Dabney et al 2001) and loss of plant nutrients through runoff. Covering an exposed surface area can increase hydrological storage (Novotny and Olem 1994) and increase surface roughness, which slows down stormwater arrival times. Covering bare soils or compacted grasses can also stimulate infiltration through root growth. Roots provide a pathway and habitat for soil organisms to break down organic matter (Kohnke and Franzmeier 1995), strengthening the soil structure and increasing the depth of the O and A soil horizons. Urban

permeable areas can become compacted over time by anthropogenic trampling, therefore it is important to establish a permanent root system to encourage pore space in the top soil layers. The O (organic) horizon and the A (surface soil) both contain high void space, porosity, and permeability, which is where the majority of the root system is located. These principles are well understood and commonly managed in rural and agricultural watersheds, and their applicability to urban areas should not be forgotten as a potential management tool. Although land use is much more finely fragmented in urban areas, increasing pore space and infiltration in soils within urban areas like RBW can minimize sheet flow and increase natural recharge.

Modelling Stormwater Runoff

The impacts of urbanization on hydrologic response to rainfall can be stimulated by computer models. A great variety of such models exist that range in complexity and how they operate. This study employs a few simple model simulations to explore runoff responses to scenarios of LID employment. These models, briefly introduced here, include the rational method, the curve number (CN) method, and the TR-55 modeling system that is based on the CN method. Most conventional rainfall-runoff models use measures of land use or soil properties to estimate infiltration abstractions and runoff. In urban areas, impervious surface areas may drive runoff response, as well as water quality and the health of aquatic ecosystems (Schueler, 2000; Walsh et al., 2005; 2012). Areas of impervious surfaces are analyzed in this study; therefore, to provide an index or the degree of urbanization that should help to predict runoff response.

The rational method is an empirical relation between rainfall intensity and peak flow (Hayes and Young 2006). It uses a runoff coefficient (C), rainfall intensity, and watershed area to calculate peak discharge. Runoff coefficients are determined by infiltration, depression storage,

evapotranspiration, and interception (Hayes and Young 2006) and have been tabulated for urban land uses. They range from 0 to 1.0, where 0 indicates zero runoff and 1.0 indicates all rainfall generates runoff. The rational method considers the following assumptions (Wanielista and Yousef 1993; Hayes and Young 2006):

1. Rainfall intensity is constant over the time it takes for runoff to reach the outlet from the most distant point of the watershed (time of concentration).
2. The runoff coefficient remains the same during the time of concentration.
3. The watershed area does not change during the rain event.

The runoff curve number (CN) method was developed by the USDA Natural Resources Conservation Service (NRCS), formerly known as the Soil Conversation Service (SCS), and is used to determine infiltration rates (Zhan and Huang 2004) and runoff volumes (Mishra et al. 2006; Patil et al. 2008; Soulis et al. 2009) for a single rainfall event. The hydrologic soil group, vegetation cover (Wanielista and Yousef 1993), and land-use are used to determine the CN. Figure 1.7 shows typical CN values for urban areas provided by (Cronshey 1986). CNs will be spatially assigned using standard tabulated values from (Cronshey 1986) based on the 2013 impervious surface map layers that distinguish between buildings, sidewalks and parking lots, and streets. Connectivity will affect CNs based on USSS, impervious surface area, distance to the drainage system, zoning district, and hydrologic soil group.

Cover description		Curve numbers for hydrologic soil group			
Cover type and hydrologic condition	Average percent impervious area 2/	A	B	C	D
Fully developed urban areas (vegetation established)					
Open space (lawns, parks, golf courses, cemeteries, etc.) 3/:					
Poor condition (grass cover < 50%)		68	79	86	89
Fair condition (grass cover 50% to 75%)		49	69	79	84
Good condition (grass cover > 75%)		39	61	74	80
Impervious areas:					
Paved parking lots, roofs, driveways, etc. (excluding right-of-way)		98	98	98	98
Streets and roads:					
Paved; curbs and storm sewers (excluding right-of-way)		98	98	98	98
Paved; open ditches (including right-of-way)		83	89	92	93
Gravel (including right-of-way)		76	85	89	91
Dirt (including right-of-way)		72	82	87	89
Western desert urban areas:					
Natural desert landscaping (pervious areas only) 4/		63	77	85	88
Artificial desert landscaping (impervious weed barrier, desert shrub with 1- to 2-inch sand or gravel mulch and basin borders)		96	96	96	96
Urban districts:					
Commercial and business	85	89	92	94	95
Industrial	72	81	88	91	93
Residential districts by average lot size:					
1/8 acre or less (town houses)	65	77	85	90	92
1/4 acre	38	61	75	83	87
1/3 acre	30	57	72	81	86
1/2 acre	25	54	70	80	85
1 acre	20	51	68	79	84
2 acres	12	46	65	77	82
Developing urban areas					
Newly graded areas (pervious areas only, no vegetation) 5/		77	86	91	94

Figure 1.7. Typical CN Values for Urban Areas (Source: Cronshey 1986)

A hydrologic soil group (HSG) is classified using map units that are collections of areas with similar soil components or miscellaneous areas (USDA 2007) and assigned by similarities in physical and runoff characteristics (USDA 2007). The HSGs are based on measured rainfall, runoff, and infiltrometer data and are usually grouped within a climatic region with similar textures, structures, water table depths, and runoff responses (USDA 2007); however, infiltration rate is the primary grouping factor (Pilgrim and Cordery 1993). There are four HSGs (A, B, C, and D) (Putnam 1972, Pilgrim and Cordery 1993, USDA 2007):

1. Group A soils have high infiltration rates, a low runoff probability, typically made up of less than 10 percent clay and more than 90 percent sand or gravel, and contain loams.

2. Group B soils have moderately low runoff potential when thoroughly wet, contain moderately fine to moderately coarse textures, and have a low bulk density.
3. Group C soils have a moderately high runoff potential with less than 50 percent sand and 20 to 40 percent clay. C soils are normally moderately fine to fine texture typically including sandy clay loams.
4. Group D soils have high runoff potentials with very restricted infiltration due to clay content higher than 40 percent. D soils contain shrink-swell potential, have a water table within 60 centimeters of the surface, have a drainage problem, and are mostly made up of clay loams, silty clay loams, and clays.

Using map units to list HSGs is preferred over listing them by soil series because soil series are so frequently re-defined that maintaining a single functioning list is nearly impossible (USDA 2007). Moreover, most soil maps depict soils in groups of soil series (map units) and maps of the specific soil series are not generally available.

TR-55 Runoff Model

Technical Release 55 (TR-55) is a simplified computer model widely used in the United States to calculate storm runoff volume, peak discharge, storm hydrographs, and storage volumes detention structures (Cronshey 1986). The model begins with a uniform rainfall event and calculates runoff using the runoff CN, which is then transformed into a hydrograph using unit hydrograph theory (Cronshey 1986) dependent on runoff travel times through the watershed. TR-55 is not used in this thesis because the majority of the Rocky Branch Creek is connected through the USSS.

Study Area

The Rocky Branch Watershed (RBW) is a small, urban sub-watershed of the Upper Congaree watershed with a drainage area of formerly approximate 10.3 km^2 (Wooten 2008) in 2007. After drainage divide revisions, which will be discussed later, the RBW drainage area is currently 10.82 km^2. The creek is susceptible to flash flooding due to a high impervious area of 49 percent (Wooten 2008) for the entire RBW and 51 percent (Logan et al. 1995) above the At Pickens gage. Rocky Branch Creek (RBC) is over 6.5 km long and flows through the Five Points district and the University of South Carolina (Figure 1.8). The Gregg Street, University Hill, USC Campus Northwest, and 5-Points Junction sub-divides (Figure A.1) are dominantly designated for commercial land use. The percent impervious area within the commercial zoning districts is drastically higher than in residential and industrial zones. The eastern sub-divides are primarily residential and contain a higher proportion of green space. The RBC discharges into the Congaree River above Congaree National Park so pollutants and sediments pose a threat to interests outside the RBW.

Two rain gages are located within the RBW: the University of South Carolina gage is located behind Bates House Dormitory and the Richland County gage is located on the top of the Richland County parking structure near Hampton and Harden Streets. Richland County rainfall data is provided by Ken Aucoin and have not yet been calibrated. In addition, four streamflow gages located along the RBC; however, none of the streamflow gages are fully calibrated. Three streamflow gages have been operating since October 2007 providing flow-stage data that can be used to characterize the timing of stormwater delivery and the frequency of overbank flows.

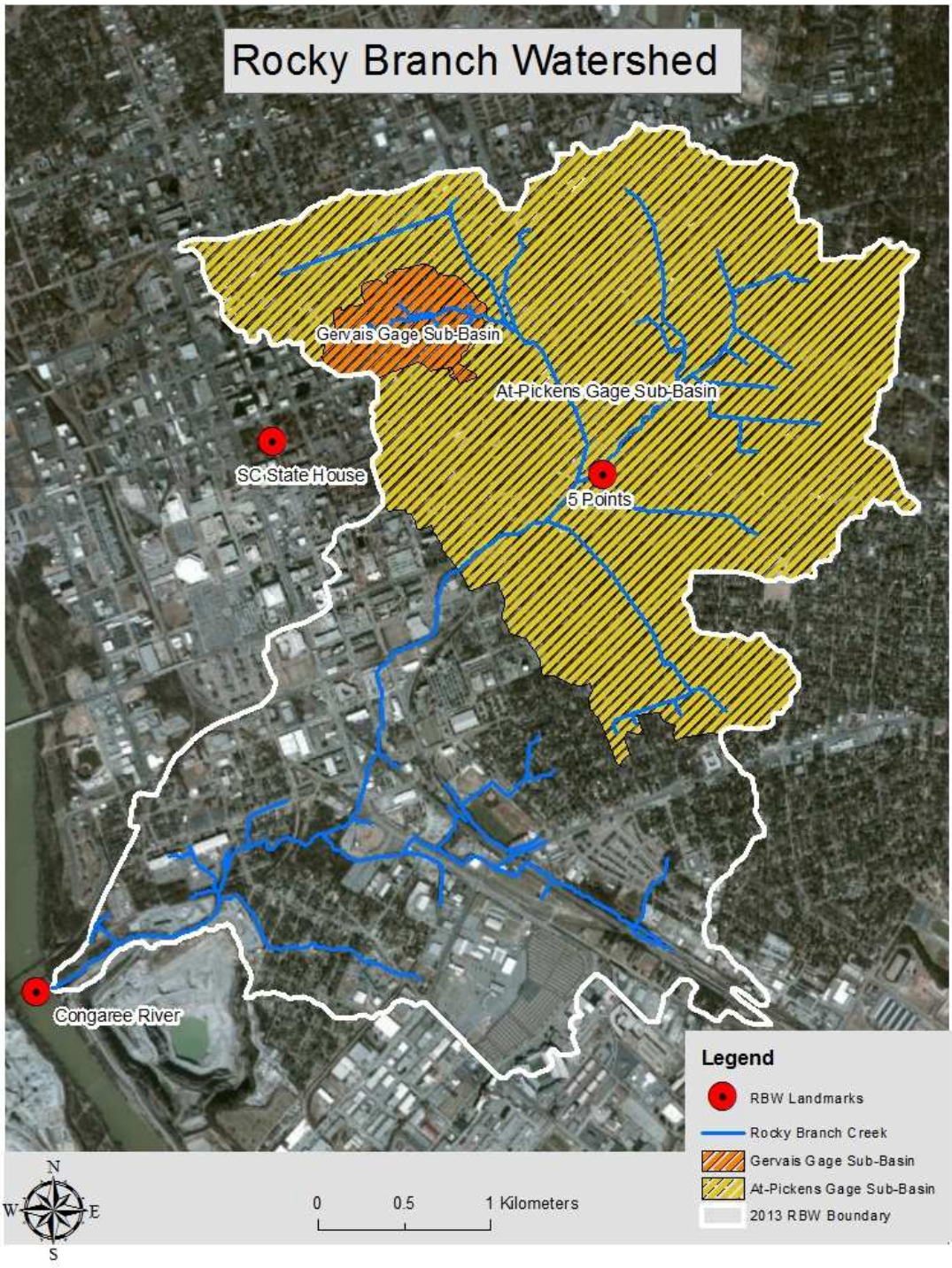

Figure 1.8. Rocky Branch Watershed

A fourth gage at Pickens Street has been discontinued, but has data dating back to 1984, for which some periods have been calibrated and provide discharge values for flows below moderate stages of flow. Figure A.2 shows the streamflow gages along the RBC and the rain gage located on the USC campus.

Objectives

This study will have three primary objectives which will be discussed in detail in Chapter 2:

1. Spatial analysis to evaluate feasibility of LID in various sub-watersheds
2. Evaluate hydrologic rainfall response by constructing model storm hydrographs within the RBW.
3. Construct a water budget analysis to determine LID treatment estimates and its effect on reducing peak discharge

Chapter 2 – Methods

This chapter presents the methodologies used to achieve each of the three thesis objectives. Additional methods and details on some of the methods are presented in subsequent chapters in the context in which they were used.

Objective 1 – Spatial Analysis to Evaluate Feasibility of LID in Various Subwatersheds

To meet objective one, existing maps were collected and updated as needed, and new spatial analyses were employed to generate a series of thematic maps and spatial data to characterize the subwatersheds. Existing data that were incorporated into the spatial dataset include storm sewer maps constructed by the City of Columbia, SSURGO digital soil data, zoning maps, impervious surfaces, and a property owner parcel map. Details on these geospatial methods are described in Chapter 3.

Revising Existing Spatial Data

Revised data layers included, remapping basin, sub-basin, and gage-basin divides based on new LiDAR data and manual interpretations of topography using the contour crenulation method on contours with a two-foot interval derived from the new LiDAR data. Several maps from Richland County and the City of Columbia were merged, since RBW overlaps both governing entities. Zoning data were collected from the City of Columbia and Richland County GIS departments and merged into four general zoning classes: low-density residential, medium

and high-density residential, commercial, and industrial. In addition, Wooten's (2008) land-use/land-cover (LU/LC) maps, including impervious surface, zoning, and parcel maps, were updated in two ways. First, based on the new basin and sub-basin drainage divides, Wooten's data were clipped where it overlapped the new watershed divide boundaries and new 2014 data were generated for impervious surfaces and zoning where the new divides extend beyond the old boundaries. Second, Wooten's impervious surface maps were updated using his methods with 2014 imagery as explained in Chapter 3. Very few losses of buildings were identified from 2007 to 2014 by these methods, but many new structures were noted by remapping.

New Thematic Maps and Cistern Analysis

New thematic maps were developed based on these maps such as: new basin, sub-basin, and gage basin drainage divides, hydrologic soil groups, impervious area property ownership, effective impervious area, and a cistern analysis. The new maps of the RBW help indicate where potential LID projects could be located in order to effectively detain stormwater runoff.

A cistern analysis was completed by calculating building rainwater runoff to determine total runoff for a single rain event. Once total runoff was determined, standard cistern and rain barrel sizes were assumed to fit various building gutter systems in order to capture 100% of the rainfall runoff. A map of the various sizes and number of cisterns per building illustrates the numbers of cisterns each building would require to compensate for the surface runoff generated by the roof. For instance, many of the residential buildings only require 100 gallon rain barrels; whereas larger university buildings require multiple larger cisterns to completely capture runoff from a 1-inch rain event.

Objective 2 – Hydrologic Analysis: Evaluating Rainfall-Runoff Response with Model Storm Hydrographs

This section briefly reviews hydrologic data available in the RBW include rainfall and discharge data that were collected at several gaging stations through time. This is followed by the methods used to compute stormflow volumes, peak discharges, and stormwater arrival times. For the purpose of building model hydrographs, stormwater volumes and peak discharges were computed. The runoff volumes and peak discharge data, along with the timing of hydrograph arrivals, constrain the shape and size of model hydrographs.

Synthetic storm hydrographs were created for specific rainfall events in order to assess the effectiveness of potential for LID to mitigate storm runoff in the At Pickens and Near Gervais sub-basins of RBW. Rainfall data are described first. The model hydrographs were generated by (1) computing storm runoff volumes by the SCS curve number method, (2) calculating flood peaks by the rational and two regional methods, and (3) constraining stormwater arrival times with computations of lag-to-peak and lag-to-centroid. Both CNs and rational coefficients were computed using spatially weighted values for the sub-watersheds based on a GIS analysis of land-use data. The model hydrographs were compared with USGS discharge hydrograph data collected at the At Pickens Street gage and USGS stage hydrograph data collected at the Gervais Street streamflow gages.

Hydrologic Data

Rainfall Data

Daily precipitation data have been collected at the USC weather station since 1943 and five-minute data were collected occasionally during 2013. In addition, uncalibrated rainfall data at a variety of time intervals have been collected since October 2012 from the top of the

Richland County parking structure near Hampton and Harden Streets, which is located very near the Gervais Street streamflow gage (Ken Aucoin, written communication). A summary of presently available rain data is given in Table 2.1. The county data were used to evalutate the timing of storm-flow arrivals at the Gervais Street gage, although the 15-minute interval streamflow data limits the constraints on timing for this small basin.

Precipitation intensities evaluated for simulations were derived from rainfall depths and durations on an intensity-duration-frequency chart developed by NOAA (2013). Rainfall recurrence intervals ranging from one to 50 years for durations ranging from 5 minutes to 2 days were computed by NOAA based on a regional analysis of precipitation data collected at several rain gages across South Carolina (Table 2.2). The analysis of rainfall values in this study assume that total rainfall from a given event occurs completely within the duration listed, so a one-inch 30-minute rainfall is assumed to have produced an intensity of one inch per hour. A rain gage is located off of South Bull Street, behind Bates House dormitory, that records five minute punch interval rainfall, but the data are only archived for 48-hour time periods. The USC rainfall data were collected periodically and used to constrain lag-to-peak discharge times at the At Pickens Street gage for developing model storm hydrographs.

Table 2.1. Available RBW Rainfall Data Summary

USC Precipitation Data		**Richland County Precipitation Data**
Daily Data	5-min Data	1-min to 15-min Data
inches	inches	inches
1943-2004	2/7/2013 to 2/8/2013	10/15/2012 to present
	7/27/2013 to 7/31/2013	
	8/6/2013	
	9/23/2013	

	9/25/2013 to 9/27/2013	

Table 2.2. Precipitation Frequency Estimates (inches) (Source: NOAA 2013)

Duration	1-yr	2-yr	5-yr	10-yr	25-yr	50-yr
5-min	0.45	0.522	0.597	0.67	0.751	0.818
10-min	0.719	0.835	0.957	1.07	1.2	1.3
15-min	0.899	1.05	1.21	1.35	1.52	1.65
30-min	1.23	1.45	1.72	1.96	2.25	2.48
60-min	1.54	1.82	2.2	2.56	2.99	3.37
2-hr	1.76	2.1	2.56	3	3.57	4.06
3-hr	1.86	2.21	2.71	3.2	3.85	4.43
6-hr	2.2	2.62	3.22	3.8	4.58	5.29
12-hr	2.57	3.07	3.78	4.49	5.45	6.33
24-hr	3	3.6	4.5	5.26	6.38	7.33
2-day	3.52	4.23	5.25	6.1	7.33	8.36

Discharge Data

Storm hydrographs were constructed for a variety of rainfall events at the Gervais Street and At Pickens Street streamflow gages using available observed discharge data at those sites. Streamflow data are currently limited for the basin. Four USGS streamflow gage sites are located on the RBC; however, none are fully calibrated (Table 2.3). Three streamflow gages have been operating since October 2007 providing flow-stage data that can be used to characterize the timing of stormwater delivery and the frequency of overbank flows. A fourth gage at Pickens Street has been discontinued, but has data dating back to 1984, for which some periods have been calibrated and provide discharge values for flows below moderate stages of flow (Table 2.4). The Civil and Environmental Engineering Department of the University of South Carolina has provided discharge data for a single storm event measured by the U.S. Geological Survey at the 02169505 gage (at Pickens Street), which can be used to accurately estimate all

discharges below 5.2 feet (Fadi Shatnawi, written communication). A series of computations were conducted to interpret and constrain discharges associated with the flow-stage data at the Gervais and At-Pickens gage sites. Channel cross sections were topographically surveyed with a rod, level, and tape at both gage sites to determine when flows top stream bank and terrace surfaces. In addition, the cross sections identify the stages at which backwater and ponding occurs due to bridges.

Table 2.3. Available Continuous Stage Data for Rocky Branch Creek (Source: USGS)

	15-min Continuous Stage			Drainage Area
USGS Gage	**Gage #**	**Start**	**End**	**km^2**
Gervais	21695045	10/24/2007	present	0.303
Above Pickens	21695048	10/1/2007	present	5.454
At Pickens	2169505	10/1/2011	1/29/2012	5.569
Whaley	2169506	10/1/2007	present	6.690

Table 2.4. At-Pickens Gage (Source: USGS)

Daily Max, Min, Mean	Stage-Q measurements	Stage-Q Storm Hydrographs
Period of Record	**Period of Record**	**Period of Record**
8/14/1984 to 12/5/1990	1984 to 1988; 2001 to present; both periods calibrated	2/7/2013 to 2/8/2013
5/13/2011 to 1/17/2012		

For the Gervais Street gage (21695045), which has only flow stage data, model storm hydrographs were simulated for floods of various return periods based on estimates of peak discharge, lag-to-centroid, and total runoff. The size of storm hydrographs is governed by peak discharge and the volume of storm runoff, whereas the shape of hydrographs is governed by the arrival times.

Runoff Volumes computed by the Curve Number Method Adjusted for Impervious Areas

Stormwater runoff volumes were computed using the standard SCS curve number (CN) method (NRCS 2010; Bedient and Huber 1988).

Runoff volumes were calculated using the following equation (Putnam 1972; Bedient and Huber 1988):

$$R = \frac{(P-0.2S)^2}{(P+0.8S)} \qquad \text{Equation 2.1}$$

where *R* is accumulated direct runoff in inches, *P* is the accumulated rainfall in inches, and *S* is the potential maximum soil retention in inches, which is a function of the SCS curve number:

$$\frac{1000}{cn'} - 10 \qquad \text{Equation 2.2}$$

where *CN* is the SCS curve number. The factors multiplied with *S* (0.2 and 0.8) are initial abstractions from interception, infiltration, and surface storage prior to runoff. Runoff volumes are computed by multiplying runoff depths by drainage area.

Curve numbers are conventionally determined, in part, by the use of hydrologic soil groups (HSGs). In urban areas, however, HSGs may not be known or may be inaccurate for computing runoff. For example, much of RBW is mapped on NRCS soil maps as "Urban Land", which does not have an associated HSG. Much of the remaining area of the catchment is mapped as a soil series variant with 'urban' used as a modifier; e.g., Vaucluse-Urban and Orangeburg-Urban. Although the HSG of Vaucluse and Orangeburg are known, these large areas of these surfaces are covered by impervious materials so infiltration is greatly impaired and hydrologic behavior is not accurately indicated by use of the HSG alone. To improve the

accuracy of hydrologic response in the RBW, the impervious surface map was utilized in the spatial weighting of curve numbers.

The runoff curve number (CN) method was developed by the USDA Natural Resources Conservation Service (NRCS), formerly known as the Soil Conversation Service (SCS), and is used to determine infiltration rates (Zhan and Huang 2004) and runoff volumes (Mishra et al. 2006, Patil et al. 2008, Soulis et al. 2009) for a single rainfall event. CNs can be assigned for urban and rural drainage areas and to various types of land-cover. The HSG, vegetation cover (Wanielista and Yousef 1993), type of land-use, and percent impervious cover are used to determine the CN (Figure 1.5).

Two types of impervious cover are often described; i.e., total impervious area (TIA) and effective impervious area (EIA) (Schueler and Holland 1994). Impervious surfaces were determined by updating a map of total impervious area (TIA) for buildings, sidewalks, and parking lots produced by Wooten (2008). Impervious surfaces were initially given a CN value of 90. Streets were given a CN of 98 based on Figure 1.7 and their high connectivity. These impervious CNs were adjusted to compensate for local runoff storage and connectivity, and represent an approximation of the effective impervious area (EIA). The EIA CN adjustments were split into three categories: hydrologic soil groups, zoning type, and 10-meter street and urban storm sewer system (USSS) buffer.

The hydrologic soil groups raised and lowered the impervious CNs. For all impervious surfaces within the A hydrologic soil group (well drained soils), EIA CN values were lowered to 85; for B soils there was no change; and for D soils (poorly drained soils) EIA CN values were increased to 95. If the centroid of the impervious surface was located within 10 meters of a street or urban storm sewer system (USSS) the EIA CN values were set to 95. Lastly, the EIA CN

values were adjusted for the four general zoning classes. If the impervious surface centroid was located within commercial zoning the EIA CN values were set to 95; Industrial EIA CN values had no change; and Residential 1 and Residential 2 EIA CN values were set to 85. Impervious area centroids were used in order to give each polygon one specific value, and not counting some impervious polygons multiple times.

Overall, EIA CN changes for three categories of impervious surface (buildings, sidewalks, and parking lots) were determined by adding the three EIA CN adjustments and then subtracting 270 (three times the initial 90 value) produced EIA CN changes varying from a decrease of 5 to an increase of 15. The EIA CN values for impervious polygons vary from 85 to 98. Areas with an increase of 10 and 15 CN were set to a CN of 98 (Table 2.5). Data from Ahiablame (2012) indicate that CNs can be reduced after LID applications are installed, but that analysis was not used in this thesis.

Table 2.5. EIA Curve Number Adjustments

TIA CN	EIA CN Adjustments	EIA CN
90	-5	85
90	0	90
90	+5	95
90	+10	98
90	+15	98

Flood Peak Discharge Computations

Flood peaks were estimated by three different methods: the rational method (CIA or CfCIA), the Putnam (1972) method, and the Bohman (1992) method.

Flood Peaks Computed by the Rational Method

As a first approximation, peak discharges were computed using the rational equation (Wanielista and Yousef 1993)

$$Q_{pk} = CIA \qquad \textit{Equation 2.3}$$

where Q_{pk} is peak discharge in cfs, C is the rational method runoff coefficient, I is the rainfall intensity in inches per hour, and A is the drainage area in acres. Rainfall intensities were derived from the IDF chart and the Rational Coefficient values were derived from spatially weighted values generated using GIS mapping. Maps of impervious surfaces in 2007 (Wooten 2008) including buildings, parking lots, roads, and sidewalks provided C runoff coefficients for the impermeable surfaces. Rational runoff coefficients were assigned to mapped surfaces according to standard rational coefficient tables (Table 2.6). Standard runoff coefficients are reported first in the table to provide the coefficient ranges. The roofs, business areas, residential areas, asphalt streets, and concrete streets were used to determine the RBW runoff coefficients. Use of higher coefficients is often recommended for urban watersheds with poor infiltration, such as RBW. Rational runoff coefficients for a given land-use/land-cover type are often given as a wide range (standard runoff coefficients in Table 2.6), with the understanding that hydrologic judgment is to be used. In this case, high runoff coefficients were chosen based on the RBW land-use/land-cover discussed in Chapter 3. The Gervais gage-basin, At Pickens gage-basin, and total RBW runoff coefficients were weighted by computing the proportion of areas of each of four LU/LC types: Buildings, parking lots/sidewalks, averaging each weighted impervious area type (Table 2.6). The weighted runoff coefficients were all above 0.8 indicating poor infiltration with high amounts of Hortonian overland flow.

Table 2.6. RBW Rational Coefficient Analysis

Ground Cover	Standard Runoff Coefficients	RBW Ground Cover	RBW Runoff Coefficients	Gervais area	At Pickens area	RBW Area
	c		c	km^2	km^2	km^2
Lawns	0.05 - 0.35	Buildings	0.95	0.05	1.02	1.66
Meadow	0.1 - 0.5	Parking Lots & Sidewalks	0.95	0.13	1.23	2.16
Unimproved areas	0.1 - 0.3	Streets	0.95	0.04	0.92	1.46
Residential areas	0.3 - 0.75	Pervious Area	0.7	0.08	2.64	5.41
Business areas	0.5 - 0.95					
Industrial areas	0.5 - 0.9	**Weighted Gervais Runoff Coefficient:**			**0.88**	
Asphalt streets	0.7 - 0.95					
Concrete streets	0.7 - 0.95	**Weighted At Pickens Runoff Coefficient:**			**0.82**	
Roofs	0.75 - 0.95					
		Weighted Total RBW Runoff Coefficient:			**0.84**	
Source: Pilgrim and Cordery 1993						

Peak discharges derived from the rational equation are often adjusted upwards for extreme floods to compensate for basin saturation through the use of a saturation factor:

$$Q_{pk} = C_f CIA \qquad \textit{Equation 2.4}$$

where C_f is a saturation factor varying from 1.1 to 1.25 for rare floods (VDOT 2002). The C_f saturation factor is best used for larger rain events in order to better account for antecedent moisture. For both gage sub-basins 1.175 was used as the saturation factor.

Flood peaks computed by the Putnam 1972 method.

Putnam 1972 presented a set of peak discharge equations for urbanized watersheds in the southeastern USA derived from a statistical regression analysis using drainage area and lag time. His peak discharge functions are given in Table 2.7, where Q_n is the peak discharge for the

flood having the reoccurrence interval indicated by the subscript in cfs, *A* is the drainage area in square miles, and *T* is the lag-time in hours.

Table 2.7. Calculating Peak Discharge
(Source: Putnam 1972)

$$Q_2 = 221 * A^{0.87} * T^{-0.60}$$

$$Q_5 = 405 * A^{0.80} * T^{-0.52}$$

$$Q_{10} = 560 * A^{0.76} * T^{-0.48}$$

$$Q_{25} = 790 * A^{0.71} * T^{-0.42}$$

Flood peaks computed by the Bohman (1992) Method.

Another method for computing peak discharges in urbanized watersheds of the Southeastern USA was presented by Bohman (1992). These equations for estimating peak discharge in urban streams are based on drainage area TIA (Table 2.8), where urbanized discharge (*UQ)* is the peak discharge in cfs, *A* is the drainage area in square miles, *TIA* is total impervious area in percent of total drainage area RQ_N is the peak discharge in cfs for an equivalent rural drainage basin in the same hydrologic area as the urban basin, and subscripts ($_N$) are the recurrence of interval of floods in years.

Table 2.8. Estimating Peak Discharge for Rural (RQ_N) and Urban (UQ_N) Streams
(Source: Bohman 1992)

RQ_N	Piedmont Rural Flood Frequency Equation		UQ_N	Estimating Equation
RQ_2	$127(A)^{0.66}$		UQ_2	$1.36(A)^{0.554}(TIA)^{1.241}(RQ_2)^{0.323}$
RQ_5	$211(A)^{0.64}$		UQ_5	$2.58(A)^{0.544}(TIA)^{1.170}(RQ_5)^{0.299}$

RQ_{10}	$267(A)^{0.64}$		UQ_{10}	$3.77(A)^{0.536}(TIA)^{1.115}(RQ_{10})^{0.291}$
RQ_{25}	$347(A)^{0.63}$		UQ_{25}	$5.84(A)^{0.524}(TIA)^{1.041}(RQ_{25})^{0.284}$
RQ_{50}	$410(A)^{0.63}$		UQ_{50}	$7.76(A)^{0.514}(TIA)^{0.987}(RQ_{50})^{0.283}$
RQ_{100}	$474(A)^{0.63}$		UQ_{100}	$10.4(A)^{0.506}(TIA)^{0.932}(RQ_{100})^{0.280}$
RQ_{500}	$615(A)^{0.63}$		UQ_{500}	$18.8(A)^{0.484}(TIA)^{0.8}(RQ_{500})^{0.281}$

Stormwater Arrival Times

The shape of model hydrographs is largely determined by the arrival times of stormwater, which may be expressed by the time-to-peak-discharge or time-to-centroid of discharge (also known as basin-lag). Most available streamflow observations were obtained at 15-minute intervals so event timing cannot be precisely determined directly. A few storm events have been observed at both streamflow gages that include rainfall measurements at five-minute intervals. Stormwater arrival times for storm hydrographs at the Gervais Street and At Pickens streamflow gages were determined by three empirical equations and compared with the observations of storm-flow events. The first method, which has been used by several municipalities for urban watersheds (Putnam 1972) to directly compute the lag time from the center of mass of the rainfall excess (centroid) to the center of mass of the resultant storm runoff is:

$$T = 0.49 \left[\frac{L}{s^{0.5}}\right]^{0.5} \left(\frac{I}{100}\right)^{-0.57}$$

Equation 2.5

where *T* is lag time in hours, *L* is length of main watercourse in miles, *s* is stream bed slope (ft/mi), and *I* is the percentage of impervious cover. Length of the main watercourse is defined as the maximum water travel distance which is the length from the outlet to the furthest watershed boundary along the flow path. Length was determined using GIS spatial analysis.

Stream bed slope was determined from the difference in elevation (ft) between an elevation point 10% from the outlet and 15% from the divide at the top of the maximum water travel path (Putnam 1972). Lastly, the percentage of the revised impervious cover was used to calculate lag-to-centroid (Putnam 1972).

Another commonly used method for calculating lag-to-centroid is based on a regional analysis of urban watersheds in the southeastern USA that employed statistical regression analysis dimensionless unit hydrographs (Bohman 1992):

$$LT = 20.2 * (L/S^{0.5})^{0.623}(TIA)^{-0.919}(RI2)^{1.129}$$

Equation 2.6

where *LT* is the average basin lag time (lag-to-centroid) in hours, *L* is the main channel length in miles, *S* is the main channel slope in feet per mile, *TIA* is the total impervious area in percent, and *RI2* is the 2-year 30-minute rainfall amount. Bohman 1992 *RI2* was originally calculated for a 2-year 2-hour rainfall but were adjusted for a 30-minute amount to accurately calculate the RBW.

Lag-to-peak times were computed using the NRCS 2010 equation which was based on data from 24 watersheds with the majority being less than 8 km^2 (2,000 acres):

$$L = \frac{(Ld^{0.8})(S+1)^{0.7}}{1900*(Y^{0.5})} \qquad \textit{Equation 2.7}$$

where *L* is the lag time from the rainfall centroid to peak discharge in hours, *Ld* is flow distance in feet, *Y* is the average watershed land slope percentage, and *S* is the maximum potential retention (Equation 2.2). The maximum potential retention uses a factor similar to the SCS CN (*cn'*), therefore, adjusted EIA CNs were used in calculations. Equation 2.7 was derived using

similar sized watersheds as RBW, but can be applied to both urban and forested areas. Flow distance (*Ld*) is defined as the longest path along which water flows from the watershed divide to the outlet (NRCS 2010), and was measured using GIS spatial analysis. The average watershed land slope percentage was calculated in two ways using GIS spatial analysis tools:

1. By drawing four lines on a topographic map perpendicular to the contour lines and determining the average weighted slope of the these lines. Lines were selected perpendicular to the LiDAR 2-ft contours within ArcMap to determine a weighted land slope in both the Gervais and At-Pickens basins.
2. By using Chow 1964 equation:

$$Y = \frac{100(CI)}{A} \qquad \text{Equation 2.8}$$

where: *Y* is the average land slope percentage, *C* is the summation of the length of the contour lines that pass through the watershed drainage area on the quad sheet or GIS, *I* is the contour interval, and *A* is the drainage area in square feet.

LiDAR-derived 0.6-m (2-ft) contour lines were clipped to each gage-basin, summed, multiplied by two for the contour interval, and divided by the drainage area.

Alternatively, lag to peak discharge can be calculated as a function of concentration T_C. An equation for estimating basin lag-time is derived by NRCS 2010:

$$Tc = \frac{(l^{0.8})(S+1)^{0.7}}{1140*(Y^{0.5})} \qquad \textit{Equation 2.9}$$

where time of concentration *Tc* is the time required for runoff to travel from the hydraulically most distant point in the watershed to the outlet in hours, *l* is flow length in feet, *Y* is the average watershed land slope percentage, and *S* is the maximum potential retention derived

from the SCS CN value (same function as Equation 2.7). Time of concentration is used in Chapter 4 to provide an estimate of lag-to-peak discharge.

Lag times computed by each of these approaches were compared with the time to peak of floods recorded by flow data at the two gages to check for consistency. Unfortunately, most of the streamflow data were measured at 15-minute intervals which is too coarse of a time interval to fully constrain lag times. Nevertheless, a few select storm events provide unequivocal evidence that flood arrival times are relatively short in these basins. Comparisons indicated that the standard NRCS method (Equation 2.7) produced lag times that are unrealistically long for the highly urbanized RBW and its gage-basins. As will be further shown in Chapter 4; however, the Putnam method (Equation 2.5) and the Bohman method (Equation 2.6) (both intended for smaller urbanized areas and based on data from southeastern U.S. watersheds similar to RBW) provided characterizations of rapid stormflow response in conformance with the observed hydrographs. Therefore, Equations 2.5 and 2.6 were compared in further analysis for the development of model hydrographs, but the NRCS method was abandoned. After storm volumes, peak discharges, and lag-times were calculated, values were compared between the various methods and evaluated based on simple triangular hydrographs.

Stormflow Hydrograph Analysis

An exploratory model hydrograph analysis was conducted for data at the Gervais Street and At Pickens gages, because streamflow data are incomplete. The Gervais Street stage observations have not been calibrated for flow magnitudes, and the At-Pickens data are calibrated only for small in-channel flow events. Storm hydrographs measured at the At-Pickens gage in the late 1980s (Logan et al. 1985) were used to develop a model hydrograph for larger events.

Relating Observed Flow Stages to Discharge by Slope-Area Method

For the purpose of constraining discharges at the two gage sites, the slope-area method; i.e., Manning Equation was used to approximate flow magnitudes:

$$Q = VA = \left(\frac{1.49}{n}\right) AR^{\frac{2}{3}}\sqrt{S}$$

Equation 2.10

where *V* is flow velocity, *A* is channel cross-section area, *n* is roughness, *R* is hydraulic radius, and *S* is energy slope. Manning's roughness coefficients for minor stream channels were initially calculated using Arcement and Schneider 1989:

$$n = (n_b + n_1 + n_2 + n_3 + n_4)*m \qquad \textit{Equation 2.11}$$

where n_b is a base value of n for the flood plain's natural bare soil surface, n_1 is a correction factor for the effect of surface irregularities on the flood plain, n_2 is a value of variations in shape and size of the flood-plain cross section (assumed to equal 0.0), n_3 is a value for obstructions on the flood plain, n_4 is a value for vegetation, and *m* is a correction factor for sinuosity of the flood plain. Values of n (Table 2.9) were expected to vary within and between the two gage site cross sections. Values of n were adjusted as needed within a reasonable range to obtain flows corresponding with the observed flow stages as described in Chapter 4.

Table 2.9. Manning's Roughness Coefficients for Stream Channels (Source: Chow 1959, Arcement and Schneider 1989)

	Minimum	Normal	Maximum
Streams on a Plain		***n***	
Clean, straight, full stage, no rifts or deep pools	0.025	0.03	0.033
Clean, winding, some pools & shoals	0.033	0.04	0.045
Same as above, but some weeds and stones	0.035	0.045	0.05
Sluggish reaches, weedy, deep pools	0.05	0.07	0.08

Very weedy reaches, deep pools, or floodways with heavy stand of timber and underbrush	0.075	0.1	0.15
Lined or Constructed Channels			
Concrete bottom with dry rubble or riprap	0.02	0.03	0.035
Gravel bottom with dry rubble or riprap	0.023	0.033	0.036
Channel Conditions			
The space between obstructions is small enough to cause the effects of several obstructions to be additive	0.02	-	0.03
The space between obstructions is small enough to cause turbulence across most of the cross section.	0.04	-	0.05

Channel cross-sections were field surveyed at the Gervais and At Pickens gage sites to allow determination of *A* and *R* for a given flow stage. No water-surface slopes have been measured for a suitable flood event, so S was approximated based on channel-bed gradients measured during the field survey at the Gervais site and measured from a combination of field survey data and ESRI (2014) imagery measurements at the At-Pickens site. Cross sections relative elevations were tied to staff gage elevations to allow determination of when flows struck the bottom of bridges or topped stream bank and terrace surfaces. The staff gage at Gervais is tied to a footbridge and the staff gage At Pickens is about three meters upstream of the Pickens Street Bridge. The cross-sections were analyzed using Cross Section Analyzer, a computer spreadsheet program by the NRCS. Based on the cross section survey this program generates a table of hydraulic variables, such as top width, cross-section area, and hydraulic radius (R), for a range of flow stages. It also allows the user to specify Manning roughness (n) values and slope of the energy grade line to estimate flow velocities and discharges at various flow stages using Equation 2.11. Stage and discharge values from the Cross Section Analyzer

output were compared with observed flow stages from the gage and with the cross sections plots to evaluate the peak discharge values predicted by the three methods described above.

Model Storm Hydrograph Analysis

Using values of peak discharge, lag-to-centroid, and total storm runoff volume, a simple triangular hydrograph was constructed for a two-year rainfall event with a rainfall duration of 30 minutes. A typical storm hydrograph is asymmetrically skewed right with a faster rising limb (Figure 2.1). A dimensionless hydrograph can be constructed in order to compare different sized storm events at a given gage site. The Soil Conservation Service dimensionless unit hydrograph is the most well-known in use (NOAA 2014). This analysis computed triangular hydrographs using lag-times from the time of center of excess rainfall to the time of center of runoff (T_C) and from the time from the beginning of excess rainfall to peak discharge (T_W) (Figure 2.1). The Putnam 1972 and Bohman 1992 methods use T_C to determine lag-times whereas the NRCS 2010 uses T_W.

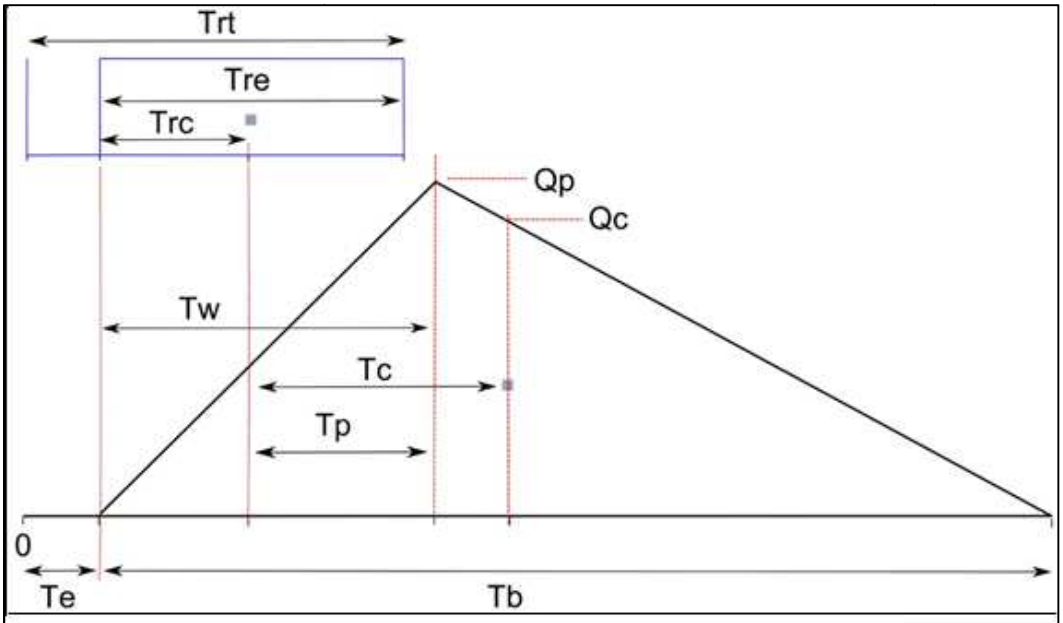

Notation

V=Volume of total storm runoff = area of triangle.
Qp=peak discharge
Qc=discharge at centroid of runoff
Tp=lag to peak, time from centroid of rainfall to peak discharge
Tc=lag to centroid, time from centroid of rainfall to centroid of runoff
Tw=watershed lag to peak
Tb=time duration of total storm runoff beginning at Te
Te=time to beginning of rainfall excess
Trt=total time of rainfall
Tre=time duration of rainfall excess = Trt-Te
Trc=time to centroid of rainfall excess; if rainfall rate is uniform, Trc=1/2 Tre

Figure 2.1. A typical triangular hydrograph

Objective 3 – Water Budgeting to Determine LID Treatment Estimates

The various scenarios of reduced LID storage volumes were evaluated by a volumetric analysis applied to the model triangular hydrographs as a first approximation. Storage volumes were subtracted from model storm hydrographs at one-minute time steps using a spreadsheet water budget to illustrate the effects of detention. The volumetric analysis was conducted with varying amounts of rainfall, LID detention, and percent area treated with LID. Rainfall inputs were assumed uniform with respect to space and time for the various precipitation recurrence

intervals. The triangular hydrographs provide continuous discharge data, so one-minute streamflow input data were generated as linear functions of time for the rising and falling limbs of the hydrographs. The simulations allowed comparisons of the effectiveness of various LID treatments in different sub-basins and testing of the three primary objectives of the study.

The water budget was used to estimate the capacity LID detention/retention storage needed to effectively reduce stormwater peak discharges. Areas within the RBW where LID will be most effective were examined by comparing the relative effectiveness across varying land-use/land-covers and soil types.

Chapter 3 - Objective 1

Revision of RBW maps:

The map of sub-basin divides used in this research is based on revision of a set of maps of watershed channels and drainage divides that was developed by Dr. Allan James between 2012 and 2013. Those maps were based on manual interpretations of topographic contours with a two-foot interval derived from recent LiDAR data. Channels were mapped using the contour crenulation method. As urban storm sewer system (USSS) maps of the basin began to become available from the City of Columbia in mid-2013, a new set of drainage divides was manually mapped in consultation with Dr. James in November, 2013 to account for extra-basin transfers where storm sewers cross topographic divides. As part of the re-interpretation of divides a flow direction grid model was derived from a LiDAR DEM using ArcGIS Hydrology tools. The revised RBW outer boundary and sub-basins were derived using the resulting flow direction grid, USSS, LiDAR shaded relief, and crenulations in the LiDAR 2-foot contours. The flow direction grid and channels from LiDAR contour crenulations received lower priority than the USSS for delineating the basin boundaries due to the USSS often flowing across low sub-basin drainage divides. Although further additions to the storm sewer maps may call for future adjustments to the mapped divides, this watershed boundary map is based on the best available topographic and storm sewer maps at the time and is considered to be the best sub-basin map of RBW available at the time of writing.

A detailed study of the RBW in 2007 included drainage divides and spatial analysis of land-use and impervious surfaces (Wooten 2008). There are substantial differences between Wooten's RBW outer and sub-basin boundaries and the boundaries revised in November, 2013; however, the total area remained similar increasing slightly from 10.33 km^2 in 2007 to 10.69 km^2 in 2013. The larger adjustments to the RBW outer boundary from Wooten's 2007 outer boundary were in the Rosewood and Fairgrounds sub-divides in the southeastern region of the RBW where the topography is relatively flat (Figure 3.1). In addition, the RBW outer divide was revised to follow the USSS in the northern headwater tributaries within the Gregg Street and MLK sub-basins, and the Olympia Village development was excluded from the RBW along the southwestern boundary.

The 2007 TIA was map was revised using a combination of ESRI and i-cubed 1-meter or better 2014 color imagery with help from the Digital Ortho Quarter Quad (DOQQ) imagery (ESRI, 2014). Different imagery and enhanced versions of DOQQs were combined into ArcMap10.2 for the world imagery base map, which is used for the TIA mapping.

Wooten's TIA data were compared with the 2013 TIA using the same 2007 boundary. Unfortunately, Wooten's TIA data could not be used for areas of the 2013 revised outer boundary. The comparisons of TIA included buildings, parking lots, sidewalks, and streets within Wooten's 2007 RBW boundary. The 2013 TIA was merged with Wooten's 2007 TIA and clipped to Wooten's 2007 RBW outer boundary. Figure A.3 indicates 2013 TIA additions to Wooten's 2007 TIA. The 2013 TIA additions totaling 145,845 m^2 were added to Wooten's 2007 TIA bringing the 2007 RBW boundary from 49.1% impervious in 2007 to 50.53% in 2013. Furthermore, if the RBW boundary remained the same since 2007 the impervious area would have increased 1.43% in roughly six years.

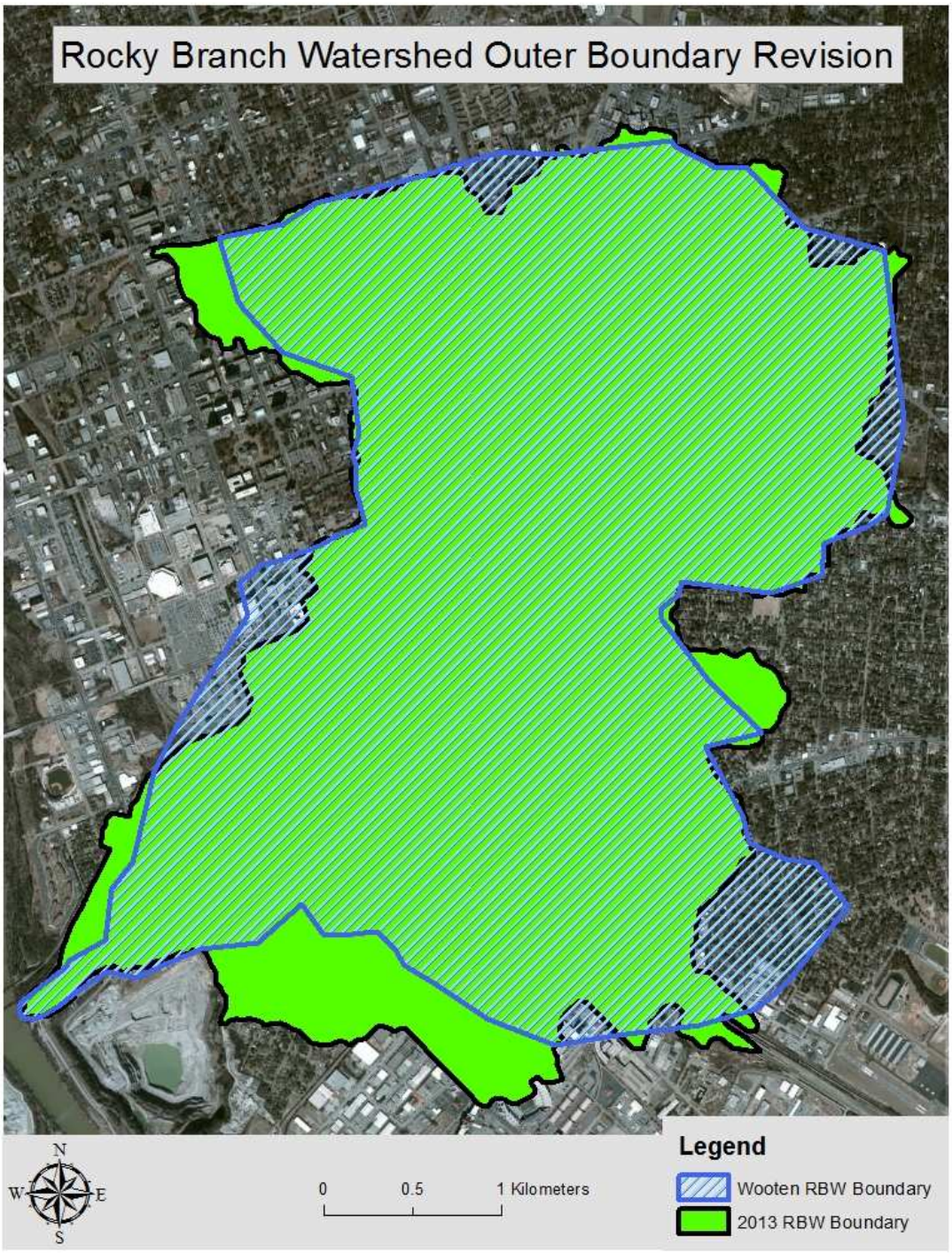

Figure 3.1. Rocky Branch Watershed Outer Boundary Revision

Because the revised 2013 RBW outer boundary was 3.37% larger and a majorly different shape than the 2007 outer boundary during TIA comparisons, the 2013 TIA should be treated

independently from Wooten's 2007 TIA in this analysis. In 2007 there were 5,447 building footprints covering an area of 1,591,307 m^2 (1.60 km^2). In 2013 there were 5,690 buildings taking up a building surface area of 1,662,190 m^2 (1.66 km^2). The sidewalks and parking lot data were grouped together and in 2007 had a total area of 2.05 km^2. In 2013 the sidewalks and parking lots had a total area of 2.16 km^2. The total area of impervious cover by streets in 2007 and in 2013 was essentially the same at 1.43 km^2 for the RBW.

RBW total impervious area in 2014 was 49.49% (Table 3.1) which is 0.39% higher than Wooten's 2007, but should be compared independently. 715 new buildings and 322 new parking lots/sidewalks were mapped using the DOQQ imagery for the 2013 TIA. In addition, streets were either extended or clipped to the 2013 RBW outer boundary.

Table 3.1. RBW Sub-divide TIA Percentages

RBW Sub-divide	Total Area (km^2)	TIA Area (km^2)	Percent Impervious
5 Points Junction	0.04	0.03	73.0
Devine Blossom	0.67	0.38	56.6
Fairgrounds	0.71	0.37	52.6
Gregg Street	1.61	1.14	70.9
Hollywood-Rose Hill	0.79	0.32	40.2
Mill Villages	0.12	0.02	20.5
Mill Villages North	0.91	0.45	49.5
MLK	2.05	0.97	47.2
North Outlet	0.17	0.01	6.0
Quarry Rim	0.07	0.01	14.9
Rosewood	2.09	0.87	41.8
South Campus	0.34	0.19	56.4
South Outlet	0.05	0.01	17.0
University Hill	0.39	0.22	57.1
USC Campus NW	0.50	0.30	59.6
Wales Garden	0.14	0.06	46.7
Wheeler Hill	0.22	0.09	39.6
TOTAL:	10.69	5.29	**49.49**

Zoning

A 2007 zoning data shapefile for the City of Columbia was provided by the City of Columbia GIS Department (Lynn Shirley, written communication). Zoning data for the Richland County portion of the RBW were re-classified to be consistent with the City of Columbia's zoning types and descriptions and to allow merging of the two datasets. A map of the Richland County zoning data was obtained from the Richland County GIS Department (RC GEO 2014) and a digitized Richland County zoning layer was created in ArcMap from the online maps and combined with the City of Columbia zoning GIS data. The re-classification was done by combining classes with parallel descriptions similar to the methodology of (Wooten 2008). The re-classified zoning districts of Richland County were merged with the City of Columbia zones into four classes: single-family and two-family residential (Residential – 1), high density residential (Residential – 2), industrial and general commercial. The four general zoning classes were grouped by similarities in size and land use from the zoning descriptions. Table 3.2 shows the City of Columbia and Richland County equivalents, zoning codes, descriptions, and the four general groups (Figure A.4).

Table 3.2. City of Columbia and Richland County Zoning Classes

Zoning Code	Zoning General Class	Zoning Classification	Description	Richland County Equivalent
RS-1	Residential 1	Single-Family Residential	Minimum lot area 15,000 sq. ft.; minimum lot width 90 ft.	RS-E; RS-LD
RS-2	Residential 1	Single-Family Residential	Minimum lot area 8,500 sq. ft.; minimum lot width 60 ft.	RS-MD
RS-3	Residential 1	Single-Family Residential	Minimum lot area 5,000 sq. ft.; minimum lot width 50 ft.	RS-HD
RD	Residential 1	Two-Family Residential	Minimum lot area of 5,000 sq. ft. for the first dwelling unit and 2,500 sq. ft. for the second, attached dwelling unit.	-

RG-1	Residential 2	General Residential	Medium and high density residential areas permitting progressively higher population densities	RM-MD
RG-2	Residential 2	General Residential	Medium and high density residential areas permitting progressively higher population densities	RM-HD
RG-3	Residential 2	General Residential	high density residential area characterized by townhouses and high-rise structures	-
C-1	Commercial	Office & Institutional District	Office, institutional, and certain types of residential uses	OI
C-2	Commercial	Neighborhood Commercial District	Commercial and service uses oriented primarily to serving the needs of persons who lives or work in nearby areas.	NC
C-3	Commercial	General Commercial District	Retail, office, and service establishments oriented primarily to major traffic arteries of predominantly commercial usage.	GC
M-1	Industrial	Light Industrial	Wholesaling, distribution, storage, processing, and light manufacturing	M-1
M-2	Industrial	Heavy Industrial	Manufacturing and industrial processes intended for distribution, storage, and processing	HI
PUD-R	Residential 1	Planned Urban Development - Residential	A unified development of large sites that allows creative site plan design	PDD
PUD-C	Commercial	Planned Urban Development - Commercial	A unified development of large sites that allows creative site plan design	PDD

LU/LC analysis:

The 2013 updated TIA from Wooten's 2008 impervious analysis were overlaid and clipped over the generalized zoning boundaries to show impervious percentages for each

general zoning district. Table 3.3 shows the zoning general classes total area, impervious surface area within each general zoning class, and the impervious percentage for each general zoning class. The industrial zone has a relatively low impervious percentage area due to the large area of railroad property in the Rosewood sub-basin and along the northwest boundary of the Vulcan quarry in the North and South Outlet sub-basins. Figure 3.2 shows the impervious areas overlaid on top of the generalized zoning boundaries.

Table 3.3. Impervious Percentage by Zoning General Class

Zoning General Class	Zoning Area	Total Impervious Area	Impervious Percentage
	km^2	km^2	
Residential 1	2.21	0.92	41.63
Residential 2	3.07	1.22	39.74
Commercial	3.99	2.6	65.16
Industrial	1.64	0.67	40.85

Both of the large industrial zoning areas located in the Fairgounds and Olympia Mills sub-basins contain the Norfolk Southern Railway, formally known as the Southern Railway in the Columbia area, and CSX Railroad, formally known as the Newberry and Laurens Railroad and the Seaboard System Railroad. Both the Norfolk Southern Railway and CSX Railroad have a variant right-of-way ranging from a few feet to a few miles. CSX stated their right-of-way rule of thumb is typically 50 feet, but can still vary in all areas. Acknowledging an approximation for a right-of-way distance a 50 foot buffer was placed around the railroad lines within the RBW and clipped out of the industrial zone in order to see if changes occur in impervious cover percentage without railroad properties included. The differences were near zero and the results were therefore left out of this discussion. All in all, exempting a 50 foot right-of-way for railroad

properties within the industrial zones has very little affect to impervious cover and the results in Table 3.2 should be used for further analysis.

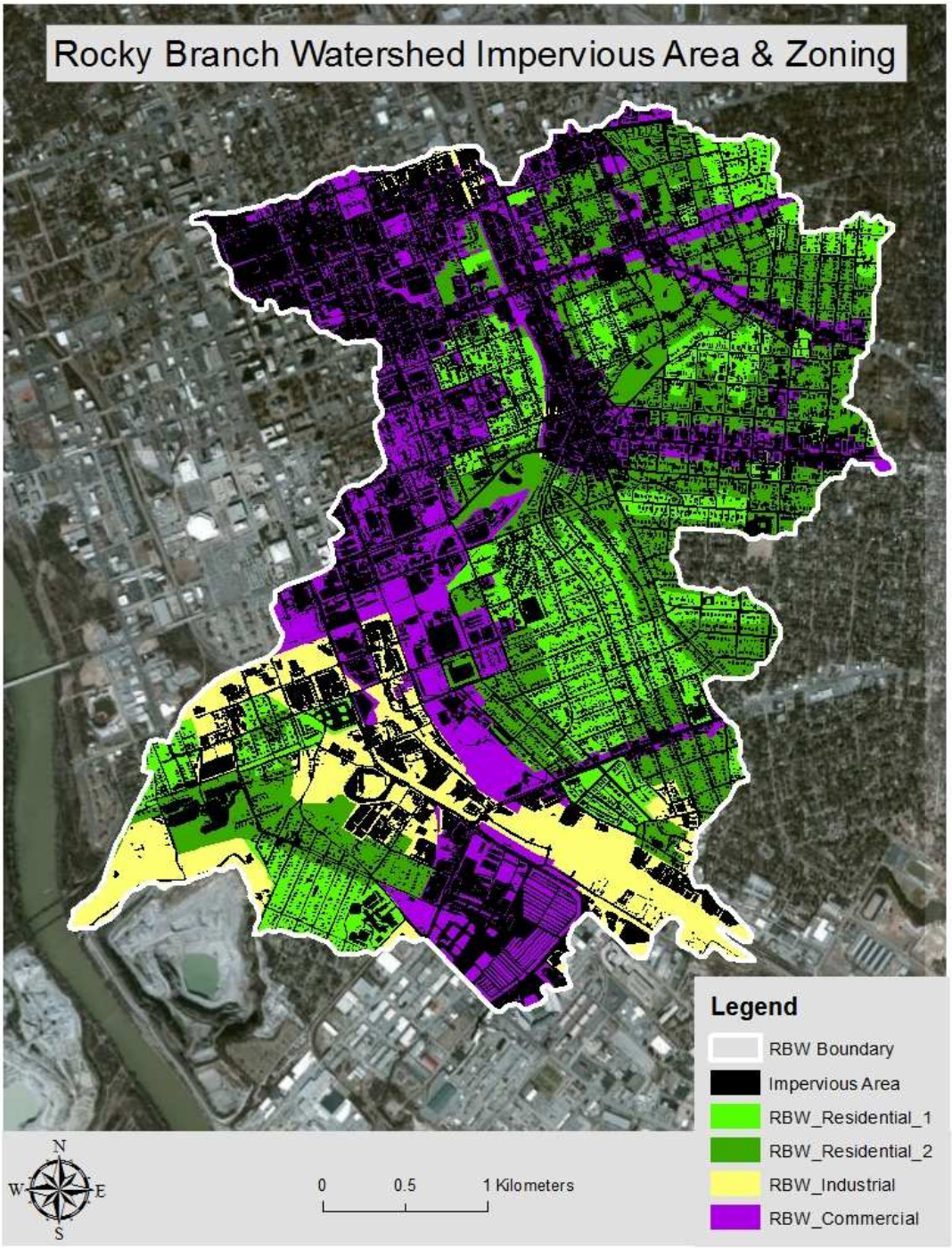

Figure 3.2. Rocky Branch Watershed Impervious Area & Zoning

Cistern Analysis

Cistern requirements for capturing the rainfall runoff from a 1-inch rain event are calculated using the runoff volume formula:

$$Volume = A*R_{ft}*0.9*7.5 \qquad Equation\ 3.1$$

where volume is given in gallons, *A* is building surface area in square feet, R_{ft} is the rainfall depth in feet, *0.90* is a compensation factor allowing for evaporation, and *7.5* converts cubic feet to gallons (Donaldson 2009).

Various cistern sizes can be used to collect the rainfall; however, for buildings larger than 9,000 ft^2 6ft x 12ft (5,076 gallon) cisterns were chosen. All buildings within RBW greater than 9,000 ft^2 are shown in Figure A.5 along with the number of 6ft x 12ft cisterns each building would require to fully capture rainfall runoff from a 1-inch uniform rainfall event. For buildings smaller than 9,000 ft^2 but larger than 1,000 ft^2 6ft x 6ft (1,269 gallons) were chosen. Figure A.5 indicates the majority of the larger buildings are located close to the RBC. For the remaining buildings smaller than 1,000 (Figure A.6) ft^2 cylindrical 100 gallon rain barrels were selected. Table 3.4 lists the largest buildings within RBW and their cistern requirements to capture 100% of a 1-inch uniform rainfall event. For example, the Olympia Mills Apartments building generates 65,086 gallons of runoff from a 1-inch uniform rainfall event calculated from Equation 3-1 and requires 13 6ft x 12ft cisterns to capture all of the runoff.

Table 3.4. RBW Buildings and Cistern Requirements from a 1-inch rainfall event

Building Size	Building Size	Building Name	Runoff from 1-in rain event	Cistern requirements from 1-in rain event
m^2	ft^2		gallons	6ft x 12ft (5,076 gallons)

16,341	175,887	Aspire Apt Complex	98,937	19.5
12,150	130,786	CofC Board of School Commission	73,567	14.5
11,408	122,790	S.C. Baptist Hospital	69,069	13.6
10,835	116,624	Olympia Mills Apts	65,601	12.9
10,585	113,930	USC Business Office	64,086	12.6
9,503	102,287	USC Treasurers Office	57,536	11.3
9,402	101,198	USC Legal Dept	56,924	11.2
8,617	92,756	USC Petigru Building	52,175	10.3
8,191	88,163	State Agriculture & Mechanical Society of S.C.	49,592	9.8
7,482	80,535	USC Business Office	45,301	8.9
7,299	78,566	Colonial Warehouse LLC	44,193	8.7
6,922	74,508	USC Russell House	41,911	8.3
6,804	73,236	Marketplace-Columbia LLC	41,195	8.1
6,719	72,325	USC Treasurers Office	40,683	8.0
6,536	70,348	Granby Mills Apts	39,571	7.8
6,422	69,123	Olympia High & Grammar School	38,881	7.7
6,361	68,468	USC Thomas Cooper Library	38,513	7.6

Hydrologic Soil Groups

The NRCS SSURGO database for Richland County was used to map the Richland County soil series for the RBW. Seven different soil series are mapped in the RBW: Dothan-Urban, Fuquay-Urban, Lakeland-Urban, Orangeburg-Urban, Toccoa, Urban Land, and Vaucluse (Figure A.7). The hydrologic soil groups (HSGs) for un-urbanized soils area recorded on the map and used to compute curve numbers. The RBW soil data were obtained by the City of Columbia and the HSGs were classified using (Lawrence 1978) and other soil county books. 55% of the soils in the RBW are classified as D soils, 30% are B soils and 15% are A soils. 49.4% of the HSGs are categorized as urban land and accounts for 91% of the D soils within the RBW.

Parcel ownership

Parcel size and ownership data were provided by the City of Columbia GIS Department (Lynn Shirley, personal communication) and spatially overlaid on the TIA buildings and parking lot data layers in order to link them with ownership. Ownership was separated into four main categories (Figure 3.3 and Table 3.5) including private, commercial, University of South Carolina, and the City of Columbia. The streets and easement sidewalks are not shown in Figure 3.3 in order to better visualize the other land uses, but sidewalks areas are included in the ownership statistics shown in Table 3.5. Table 3.5 shows the percent of impervious ownership within the RBW.

Table 3.5. Percent of RBW Impervious Areas

Ownership	Buildings	Parking Lots & Sidewalks	Streets
City of Columbia	4.4	26.9	100.0
Commercial	26.3	36.2	0.0
Private	57.5	23.4	0.0
University of South Carolina	11.8	13.5	0.0
Total	100.0	100.0	100.0

Parcel size, street width, and other factors have been used to approximate percent impervious area (Stone, 2004). Percent impervious area has also been shown to be positively related to the density of single-family homes (Stone, 2004). Similar relationships may exist for commercial and industrial land uses. These relationships may suggest planning measures to mediate the density of development and hydrologic impacts. For this study, TIA is known so

relationships between parcel size and TIA can be measured; however were not computed for this thesis.

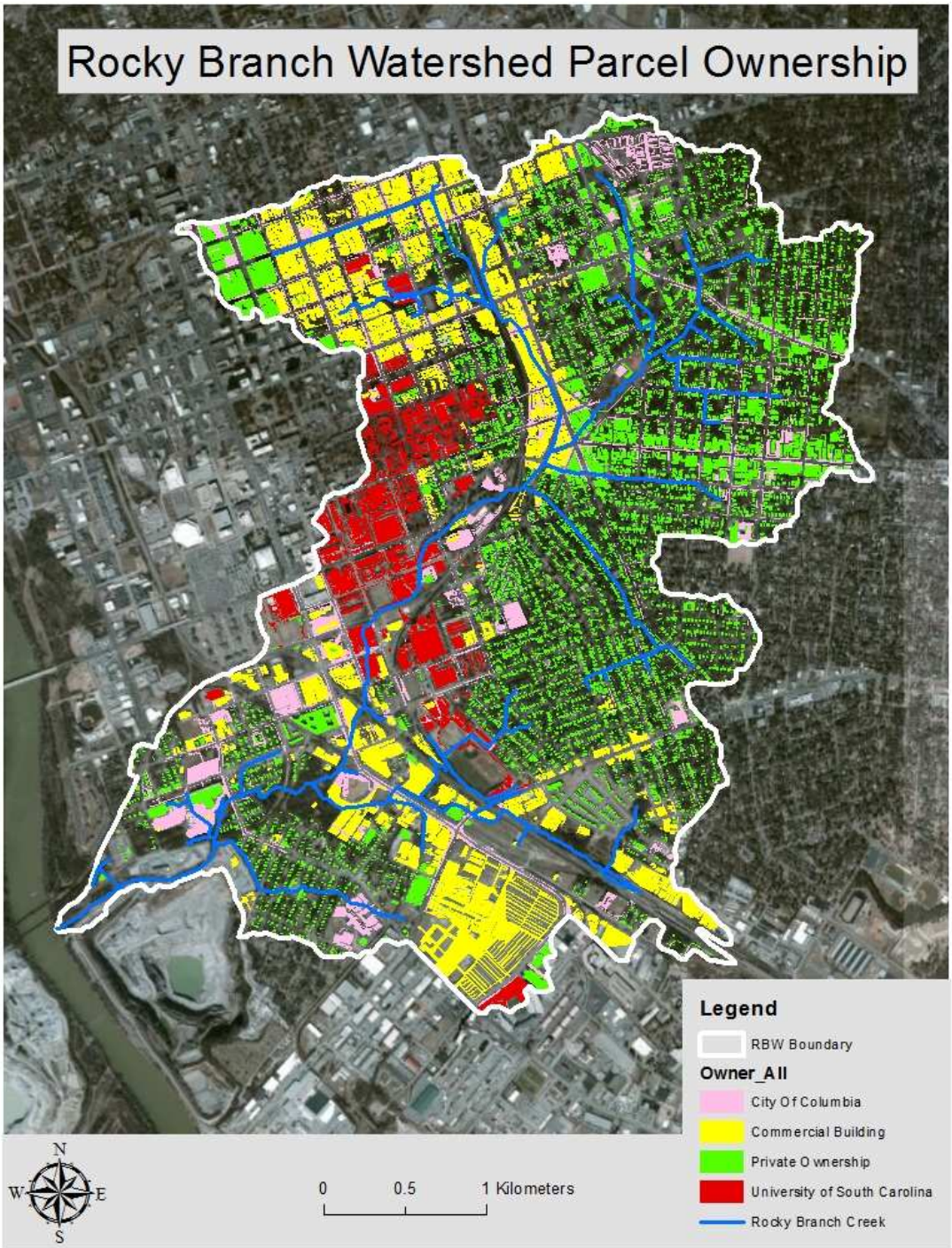

Figure 3.3. Rocky Branch Watershed Parcel Ownership

Chapter 4 – Hydrological Calculations

This chapter examines hydrologic responses in the watershed at gauge sites near Gervais Street and At Pickens Street. The goal of this analysis was to constrain estimates of the magnitude and frequency of small to moderate floods that occur every few years, and to estimate flood peak discharges, timing, and storm volumes of known recurrence intervals. These parameters are used in the evaluation of LID effectiveness in Chapter 5. Given the limited streamflow data and the limited scope of the study, which does not include rainfall-runoff simulation modeling, the development of simple synthetic model hydrographs as a first-order approximation of flood responses at two gage-sites was the goal of this analysis. In particular, triangular hydrographs are constructed based on estimates of total volume of storm runoff, peak discharge, and the timing of stormwater arrival. Runoff volumes are presented in the first section of this chapter. Presentation of the peak discharge and timing of hydrographs is split between the two gage sites. As described in Chapter 2, determining peak discharge and stormwater arrival times (Equations 2.3, 2.4, 2.5, 2.6, 2.7, and 2.9) is necessary to construct model storm hydrographs for specific storm events. Before runoff was calculated CNs were adjusted for the total RBW, Gervais gage sub-basin, and At Pickens gage sub-basin.

Adjusting Curve Number for Impervious Surface Connectivity

Total storm runoff volumes were computed for two sites (Gervais and At Pickens) using the SCS CN method based on spatially weighted curve numbers (Equations 2.1 and 2.2). Curve

numbers in the two sub-basins of RBW were adjusted for impervious surface connectivity and are referred to as EIA CNs by methods described in Chapter 2 (Table 4.1).

It has long been understood by hydrologists that the connectivity of impervious surfaces to culverts and channels is an important factor in urban storm hydrology because it drives the timing of runoff response (Martens, 1968; Putnam, 1972; Schueler 1987; Walsh et al., 2012). With spatial mapping and analysis of impervious surface and urban storm sewer systems described in Chapter 3, it is possible to map the approximate degree of connectivity of impervious surfaces in RBW using distances of the surfaces to roads and storm sewers as explained in the methods section. As explained in Chapter 2, impervious surfaces were initially assigned CNs of 90, but the CNs of well-connected impervious surfaces were increased to as much as 98. As a result of mapping, EIA CN values of 98 account for over 40 percent of the total RBW TIA above the Congaree River confluence (Table 4.1). These high CNs were assigned to all streets and to impervious polygons located in poorly drained soils, commercial zoning districts, or with centroids within 10 meters of the USSS. The EIA CNs adjusted to 95 cover an additional 37.1 percent of the total watershed. The polygons with CNs of 90 and 85, which are not well connected to roads or the USSS account for only 21 percent of the RBW TIA. This indicates that most of the runoff generated on impervious surfaces in the watershed is quickly delivered to the stream system by Hortonian overland flow and channelization.

The Gervais gage sub-basin is very densely covered with impervious surfaces with a TIA of 75.2% and these impervious surfaces were very well connected to the channel system. Gervais sub-basin EIA CN values of 98 account for over 79 percent of the TIA in the sub-basin. The EIA CNs adjusted to 95 cover an additional 19.6 percent of the sub-basin. Only approximately 1.0 percent of the TIA in the Gervais gage sub-basin is poorly connected to roads

and the USSS. Therefore, about 99 percent of the runoff from impervious areas within the Gervais gage sub-basin is quickly delivered to the stream system by sheet flow.

Impervious surface curve numbers were also adjusted for connectivity (EIA CNs) for the At Pickens gage (Table 4.1). The adjustments were similar to those of the total RBW above the Congaree River confluence. The EIA CNs that were adjusted to 98 covered 41.2% of the At Pickens gage sub-basin TIA and the EIA CNs that were adjusted to 95 covered an additional 37.4% of the sub-basin TIA. Almost 80% of the runoff generated from impervious areas within the At Pickens gage sub-basin, therefore, is well connected to the USSS or streets.

Table 4.1. EIA Analysis

	Total RBW TIA = 49.5% of RBW		**Gervais Gage Sub-basin** TIA = 75.2% of sub-basin		**At Pickens Gage Sub- basin** TIA = 44.4% of sub-basin	
EIA CN	**TIA (km^2)**	**Percent of TIA**	**TIA (km^2)**	**Percent of TIA**	**TIA (km^2)**	**Percent of TIA**
98	2.21	41.8	0.17	79.3	1.30	41.2
95	1.96	37.1	0.04	19.6	1.18	37.4
90	0.67	12.7	0.002	1.0	0.40	12.7
85	0.45	8.5	0.00	0.0	0.28	8.8
Total TIA:	5.29	100	0.22	100.0	3.17	100.0

Gervais Storm Runoff Volumes

Total storm runoff volume was computed for the Gervais gage sub-basin using the 2-year 30-minute rainfall of 1.45 inches (23mm) (Table 2.2). The storm runoff volume for the Gervais gage sub-basin was determined using a drainage area of 75.05 acres (30.37 ha) and a weighted CN of 94. The resulting volume for the 2-year 30-minute rainfall event for the Gervais gage sub-basin is 242,969 ft^3 (6,880 m^3).

As will be shown with the development of triangular hydrographs at the end of this chapter, the initial estimate of total storm runoff volume for the Gervais sub-basin is small relative to the peak discharge that is computed. To test sensitivity of the CN method to urban effects, the standard initial abstraction rate was adjusted for a second computation. Recent research indicates that the 20% initial abstraction assumed by the standard CN computational approach (0.2 in Equation 2.1) is too high for urban areas ad underestimates the volume of runoff produced (Ponce and Hawkins, 1996). An analysis of rainfall events in 134 experimental watersheds indicated that the initial abstraction ratio (Ia/S) varies between storms and between watersheds and is usually less than 0.2 (Hawkins et al. 2002). A comparison of measured rainfall and gauged runoff with runoff calculated with initial abstraction ratios of 20, 10, and 5% in ten large watersheds throughout Texas found that 10% abstraction provided the best results (Jacobs and Srinivasan, 2005); however, Lim et al. (2006) suggests an abstraction value of 5% for urban watersheds. The value of S (Equation 2.2) should also be adjusted when altering the initial abstraction (Hawkins et al. 2002):

$$S_{0.05} = 1.33 S_{0.20}^{1.15} \qquad \textit{Equation 4.1}$$

Substituting 0.05 for Ia/S and using $S_{0.05}$ in the CN equation with all the other parameters unchanged, results in an increase (9.7%) in runoff at Gervais from 242,966 ft^3 (6,880 m^3) to 266,415 ft^3 (7,544 m^3). Although this a substantial increase in runoff, runoff volumes used for subsequent calculations are based on the conventional method using the original 20% abstraction value from Equation 2.2 and not the adjusted abstraction from Equation 4.1. As a sensitivity test to indicate the maximum possible storm runoff volume for the two-year 30-minute rainfall event, CNs were temporarily set to a maximum of 99 and the resulting maximum possible runoff volume was 363,819 ft3, which is a 50% increase in storm runoff.

At-Pickens Storm Runoff Volumes

Rainfall volumes and weighted CNs were computed for each sub-basin above the At-Pickens gage (Figure A.1). USC Campus Northwest and Wheeler Hill were clipped inside of the At-Pickens gage in order to only calculate the areas within the At-Pickens gage-basin. Runoff volumes with a 20% abstraction were computed using Equation 2.1 to get a runoff percentage for each sub-basin and total runoff. The storm rainfall depth chosen for the runoff calculations were from the 2-year 30-minute event (Table 2.2).

The adjusted EIA CNs (Table 4.1) were clipped to each sub-divide and spatially weighted by dividing polygon areas by the total area of each sub-basin. The hydrologic soil groups (HSGs) determined the CN (Figure 1.7) for the pervious areas. For example, the Hollywood-Rose Hill sub-basin is the third largest RBW sub-basin above the At-Pickens gage but generates 4.69% of the total At-Pickens runoff volume. This is because it is almost completely within the B hydrologic soil group and only 31% impervious, lowering the connectivity and EIA CNs. Table 4.2 lists the sub-divides above the At-Pickens gage site, rainfall volumes assuming a uniform 30-minute 2-year event, and the resulting total storm runoff volume determined by the CN method (Equation 2.1). The Gervais gage sub-basin is also listed in Table 4.2 but is computed independently from the other sub-divides since it lies within the Gregg Street sub-basin. Rainfall volumes were computed by multiplying drainage area and storm rainfall, and using an abstraction of 20%. The storm runoff volume for the At-Pickens gage sub-basin was determined by the sum of the nine sub-basins within At-Pickens computed runoff values determined by each sub-basin's weighted CN. The resulting runoff volume for the 2-year 30-minute rainfall event for the At-Pickens gage sub-basin is 2.83 million ft^3 (263,262 m^3).

Table 4.2. RBW Sub-divides Storm Rainfall Runoff Percentages

Sub-divide	Area	Weighted CN	Storm Rainfall	Rainfall Volume	Runoff Volume	Total Runoff as Percentage of Rainfall	Percentage of Total At-Pickens Runoff
	ft^2		in	ft^3	ft^3		
Gervais	3,269,210	94	1.45	395,030	242,969	61.5	NA
Gregg Street	17,234,200	93.4	1.45	2,082,466	1,220,478	58.6	43.1
MLK	21,957,290	86.6	1.45	2,653,173	882,964	33.3	31.2
Devine-Blossom	7,125,370	82.6	1.45	860,982	200,414	23.3	7.07
Five Points	361,671	93.6	1.45	43,702	26,072	59.7	0.92
University Hill	4,057,500	90.5	1.45	490,281	227,073	46.3	8.01
Wales Garden	1,382,375	88.4	1.45	167,037	65,126	39.0	2.30
Hollywood-Rose Hill	8,419,770	77.0	1.45	1,017,389	132,837	13.1	4.69
USC Northwest	1,795,476	86.4	1.45	216,953	71,009	32.7	2.51
Wheeler Hill	223,193	84.9	1.45	26,969	7,758	28.8	0.27
Totals:	**62,556,845**	-	-	**7,558,952**	**2,833,731**	-	**100.0**

Gervais Gage Sub- basin Hydrologic Analysis

Estimates of peak discharge for the Gervais gage sub-basin are made by the rational method and evaluated by an estimate a high-stage discharge using the slope-area method. This, in turn, is followed by the analysis of stormwater timing in order to constrain hydrograph shapes and finally by development of a triangular hydrograph and dimensionless hydrograph at the Gervais gage site.

Gervais Peak Discharges by Rational Method

The rational method was used initially to calculate peak discharges based on Equations 2-3 and 2-4. The spatially weighted Gervais rational coefficient was calculated at 0.88 using values as described in Chapter 2 (Table 2.6). Peak discharges were calculated with and without a saturation factor to account for antecedent moisture conditions that most likely occur in large rain events. The saturation factor (Equation 2.4) was set to 1.175 taking the middle of the suggested range from (VDOT 2002). The rainfall intensities used from Table 2.2 were selected for rainfall durations that are equivalent to the time of concentration (Edwards 2014) of the drainage area. For the Gervais and At Pickens sub-basins the time of concentration is fairly long, which will be discussed later. Rainfall intensities with durations greater than one hour were not calculated. The Gervais sub-basin peak discharges computed by either form of the rational method (Tables 4.3 and 4.4, respectively) have low values even when increased by 17.5% using the saturation coefficient.

Table 4.3. Gervais Sub-basin Peak Discharges; (based on CIA with rainfall intensities from Table 2.2)

Duration	Recurrence Interval (1-yr)	Recurrence Interval (2-yr)	Recurrence Interval (5-yr)	Recurrence Interval (10-yr)	Recurrence Interval (25-yr)	Recurrence Interval (50-yr)
	Peak Discharges (cfs)					
5-min	2.5	2.9	3.3	3.7	4.1	4.5
10-min	7.9	9.2	10.5	11.8	13.2	14.3
15-min	14.8	17.3	20.0	22.3	25.1	27.2
30-min	40.6	47.9	56.8	64.7	74.3	81.8
60-min	102	120	145	169	197	222

Table 4.4. Gervais Sub-basin Peak Discharges with a Saturation Factor; (based on C_fCIA with C_f = 1.17 and rainfall intensities from Table 2.2)

Duration	Recurrence Interval (1-yr)	Recurrence Interval (2-yr)	Recurrence Interval (5-yr)	Recurrence Interval (10-yr)	Recurrence Interval (25-yr)	Recurrence Interval (50-yr)
Peak Discharges (cfs)						
5-min	2.9	3.4	3.9	4.3	4.9	5.3
10-min	9.3	10.8	12.4	13.8	15.5	16.8
15-min	17.4	20.4	23.5	26.2	29.5	32.0
30-min	47.7	56.2	66.7	76.0	87.2	96.2
60-min	119	141	171	199	232	261

Peak discharges were also estimated as a function of drainage area and lag time (Putnam, 1972) (cf. Table 2.7), and as a function of drainage area and TIA (Bohman, 1992) (cf. Table 2.8). The peak discharge estimates from these two methods were substantially greater than those from the CIA methods (Table 4.5 and Figure 4.1). Although the rational method is commonly used for small urban watersheds, it is not specifically calibrated for heavily urbanized environments such as the RBW. The Putnam and Bohman methods were employed, therefore, as alternatives that are based on Southeastern regional peak-flow studies of urbanized watersheds.

Table 4.5. Gervais Peak Discharge (cfs)

Q_N	Putnam	Bohman	C_fCIA				Manning Q (cfs)
			10-min	15-min	30-min	60-min	at 2-m stage = 220 cfs
Q_1	-	-	9.3	17.4	47.7	119	-
Q_2	111	255	10.8	20.4	56.2	141	-
Q_5	202	395	12.4	23.5	66.7	171	-
Q_{10}	281	482	13.8	26.2	76	199	-
Q_{25}	392	587	15.5	29.5	87.2	232	-
Q_{50}	485	660	16.8	32	96.2	261	-
Q_{100}	593	730	-	-	-		-
Q_{500}	-	850	-	-	-		-

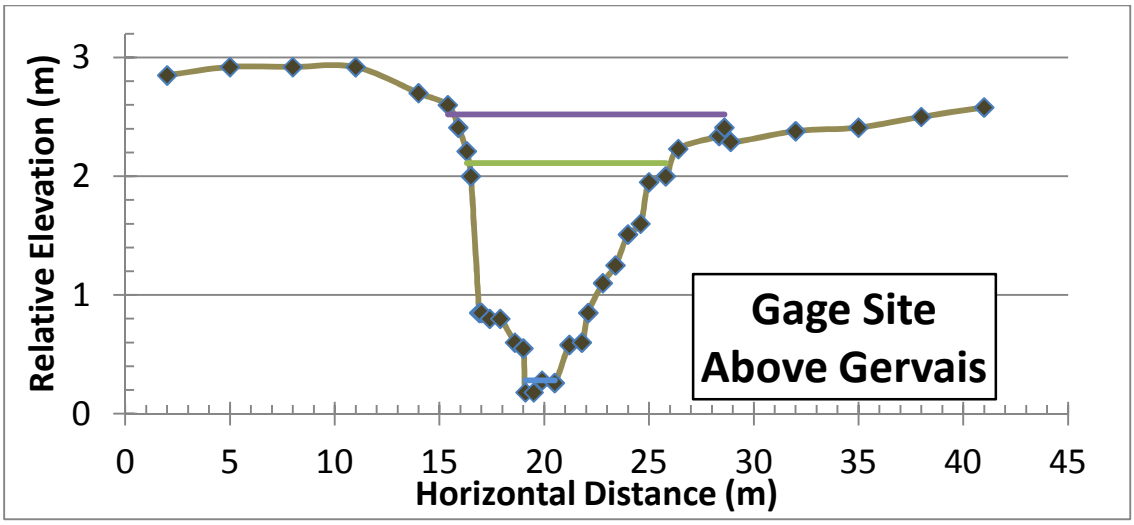

Figure 4.1. Gervais Gage Cross-Section looking downstream

Gervais Slope-Area Discharge Computations

The peak discharge estimates were compared with discharge estimates derived from the slope-area method (Manning Equation; Equation 2.10) for near bank-full flows that have been observed six times during the seven-year continuous stage record of the Gervais gage. The slope-area flow estimates are approximate but provide realistic constraints on discharges associated with observed stages at the Gervais gage. These constraints are used to assess the peak discharge estimates provided by the three peak discharge methods in Table 4.5. The 2-meter stage was chosen for the Manning discharge because higher stages strike the bottom of the bridge and go over bank.

A channel cross section was surveyed a few meters below the footbridge at the Gervais gage site on November 15, 2013 at 13:30 EST with a rod, level, and tape (Figure 4.1). The stage sensor for the gage is located immediately below the footbridge. Relative cross-section heights measured in the field were correlated to the USGS staff gage in order to compare stage data. The stage reading at that time was 1.35 feet (41.2 cm) and the depth was approximately 10 cm

at the time of the survey. USGS stage readings can be related to the cross section (Figure 4.1) by converting them to meters and subtracting 0.10 meters. This allows stage-gage records to be related to cross-section vertical coordinates and to determine when and how often flows have hit the bottom of the bridge rail or top the stream bank during the period of record. The lowest horizontal line below the one-meter relative elevation on Figure 4.1 indicates the low-flow water surface at the time of the survey, and the two broad horizontal lines between 2 and 3 meters elevation indicate the top and bottom of the footbridge rail. The footbridge has support cross beams (Figure A.8) underneath the bottom rail reaching almost to the streambed that generate substantial flow roughness as explained later. Furthermore, a stage height at the footbridge of 2.11 meters (6.92 feet) corresponds to the stage above which backwater from the bridge rail occurs. Between 2.23 and 2.6 meters (7.32 feet and 8.53 feet) flows go over the right bank. Six events since October 2007 have reached stages as high as 2.1 meter or greater hitting the base of the footbridge and one event has clearly gone over the right bank. Given the relative frequency of flows up to 2.1 meters and the inability to use the slope-area method for flows above that stage, flows were computed for stages up to 2 meters to constrain peak discharge for model hydrographs.

The slope of the energy grade line for the channel at the Gervais gage was estimated from a longitudinal profile of the bed that was measured by a rod-and-level survey (Figure A.9). If all 28 survey points of the longitudinal survey are included, extending from 22 m above to 42 m below the bridge, the best-fit line defines a slope of 0.87%. High anomalies in the bed, however, result in perturbations in the slope beyond 10 m above the bridge (5 points) and beyond 18 m below the bridge (10 points), so this slope was not used. Use of a 0.87% slope in slope-area computations resulted in unrealistically high discharge values of 303 cfs (8.58 cms at a 2-m flow stage) well in excess of the largest flows indicated by the two-year peak discharge

analyses presented in Tables 4.3 to 4.5. The slope through the shorter 28-m reach at the gage site, based on 13 survey points ranging from 10 m above and 18 m below the footbridge, defines a best-fit line with a gentler slope of 0.46%. The slope of the shorter reach (0.46%) was used, therefore, to compute flows with stages up to 2 meters.

Cross Section Analyzer (CSA) software (NRCS ND) was used to process the cross-section elevation data and compute cross-section parameters across a range of flow stages. CSA computes cross-section area, wetted perimeter, and hydraulic radius for a given stage based on the cross-section topography (Table 4.6). These parameters are independent of roughness and slope. CSA also computes mean cross-section flow velocity and discharge based on specified values of roughness and slope. The Manning roughness coefficient (*n*) initially calculated for the Gervais gage site, using values from Table 2.9 and Equation 2.11, was 0.06. This roughness was applied uniformly across the channel cross-section using 0.46% for slope. Based on a roughness of 0.06 and slope of 0.46% CSA computed discharge to be 10.4 cms (367 cfs), which is substantially greater than any of the peak flow calculations made by the empirical equations (Table 4.5).

Given that flows with a 2-m flow stage have occurred several times over the past seven years, these events are presumably smaller than a 2-year flow. This suggests that either all of the empirical estimates of peak discharge are too low or else the Manning estimate is too high. If the Manning estimate is too high either the slope in this reach is less steep or roughness is greater than the initial values. Further decreasing the slope in this location does not seem justified (Figure A.9), but increasing the Manning *n* coefficient to 1.0 for all water surface elevations may be realistic given the steel bridge reinforcement crossbeams that extend down into the flow (Figure A.8). In addition, the channel sides are secured with coarse rip-rap that

imposes a fair degree of skin friction. Using the CSA program with a roughness coefficient of 1.0 and a 0.46% slope yielded a discharge of 220 cfs (6.24 cms) and a mean flow velocity of 2 ft/s (0.63 m/s) for the 2.0 m stage flow. This discharge is much higher than all of the two-year peak discharge estimates except the Bohman estimate (Figure 4.2). It is compatible with the Bohman two-year peak discharge estimate but approximately double the estimate yielded by the Putnam method and many times greater than all of the rational equation estimates (Tables 4.5 and 4.6 and Figure 4.2). Correspondence between the slope-area discharge and Bohman peak discharge suggests that Bohman peak flow estimates are the most accurate of the three methods for the highly urbanized Gervais gage sub-basin. In short, if flows at this site are interpreted as having relatively low gradients and high roughness, then the slope-area calculations are in conformance with the highest of the peak discharge estimates (Bohman, 1992). If higher gradients or lower roughness are utilized, however, none of the estimates of peak two-year discharges are compatible with the slope-area calculations at this cross section. If the foot bridge is causing a high degree of roughness and lowering flow gradients, this could represent non-uniform flow through the reach and reduce the accuracy of the Manning estimates. In any case, high-stage field streamflow measurements are needed to calibrate the gage so that more accurate flow determinations can be made from the several years of stage data that have been collected.

Table 4.6. Gervais Gage-basin Cross-Section Analysis at 0.46% slope

Water Surface Elevation	Water Surface Elevation	Flow area	Wetted Perimeter	Hydraulic Radius	*n*	Discharge	Discharge	Velocity
M	ft	m^2	m	m		cms	cfs	m/s
0.18	0.59	0.00	0.00	0.00	0.10	0.00	0.00	0.00
0.25	0.82	0.04	0.76	0.05	0.10	0.00	0.13	0.09
0.50	1.64	0.45	2.32	0.19	0.10	0.10	3.62	0.23
0.75	2.46	1.21	4.35	0.28	0.10	0.35	12.39	0.29
1.00	3.28	2.47	6.30	0.39	0.10	0.90	31.76	0.36
1.25	4.10	4.00	7.48	0.54	0.10	1.79	63.20	0.45
1.50	4.92	5.75	8.37	0.69	0.10	3.03	107.08	0.53

1.75	5.74	7.72	9.49	0.81	0.10	4.56	161.00	0.59
2.00	6.56	9.83	10.86	0.90	0.10	6.24	220.21	0.63

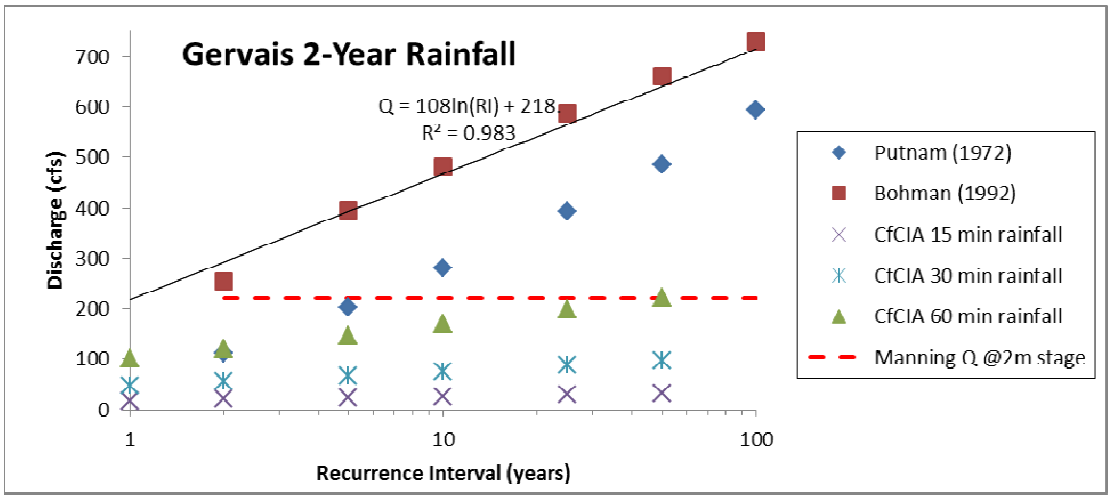

Figure 4.2. Gervais Peak Discharges estimated by rational, Putnam (1972), and Bohman (1992) methods. Dashed line is discharge at a 2-meter stage estimated by the slope-area (Manning) method.

Gervais Lag-times & Time of Concentration

The shape of storm hydrographs is largely determined by the timing of the arrival of discharge. Lag-to-centroid times were computed using Putnam 1972 (Equation 2.5), Bohman 1992 (Equation 2.6), and NRCS 2010 (Equation 2.7 for lag-to-peak).

The Gervais sub-basin is 75 acres (30.4 ha), has a main watercourse length of 0.69 miles (1.11 km), a channel slope of 144 feet per mile (2.72%), and an impervious surface area of 72.3 percent. The variables used in Equation 2.6 are similar to those in Equation 2.5 (Putnam 1972) with an additional 2-year 30-minute rainfall intensity variable taken from Table 2.4. These values result in a lag time from the centroid of rainfall to the center of runoff mass ranging from 6.1 to 8.5 minutes (Table 4.7).

The last equation used to calculate lag time was the NRCS method (Equation 2.7). For the Gervais sub-basin the flow distance to the most distant divide was 3,645 feet (1,110 meters) and the weighted CN value was 94. The average land slope using the four drawn lines perpendicular to the contours for a weighted slope was 6.75% and 8% using the Chow method (1964), which gave lag times of 12 and 11 minutes, respectively. Thus, lag times from Equation 2.7 (NRCS 2010) were longer than the calculated lag times computed by the Putnam (1972) and Bohman (1992) methods (Table 4.7). Alternatively, lag to peak discharge can be calculated as a function of time of concentration TC. Time of concentration may be considered equivalent to the time to the inflection point on the receding limb of the hydrograph (NRCS 2010). Time of concentration (Equation 2.9; NRCS, 2010) was calculated using the same variables as the NRCS (2010) lag-time computations. Using the weighted slope method, time of concentration for the Gervais gage sub-basin was 20.2 minutes and 18.6 minutes using the Chow (1964) method. Table 4.7 lists the lag-times and time of concentration for the Gervais gage sub-basin.

Table 4.7. Calculated Lag-Times and Time of Concentration for the Gervais Gage-basin

Lag-to-centroid		**Lag-to-centroid**		**Lag-to-peak**		**Time of concentration**		
Putnam method		**Bohman method**		**NRCS method**		**NRCS method**		
T	*T*	*LT*	*LT*	*L*	*L*	*Tc*	*Tc*	
(hr)	(min)	(hrs)	(min)	(hrs)	(min)	(hrs)	(min)	
0.141	8.48	0.07	6.10	0.202	12.14	0.337	20.23	**Weighted slope method**
				0.186	11.15	0.310	18.58	**Chow method**

The lag-to-peak arrivals from the three methods were compared with hydrographs and rainfall data observed at the Gervais gage site. Although most of the Gervais Street flow data were collected at 15-minute time intervals, a few storm events provide evidence of a rapid

response to flooding in this sub-basin (Figure 4.3). The July 2013 (Figure 4.3) rain event indicates a lag-to-peak of less than 15 minutes for a rainfall event of 63 mm (2.5 inches) in the Gervais Street sub-basin. USGS stage data is collected in Eastern Standard Time (EST) and were adjusted to Eastern Daylight Time (EDT) for this comparison. The rain data used in Figure 4.3 was provided by Richland County (Ken Aucoin, written communication) and was collected in 15-minute time steps during the event. Lag times were measured from seven storm events within the Gervais gage sub-basin and all responded similarly to Figure 4.3. Lag-times calculated using Putnam 1972 and Bohman 1992 are from the centroid of rainfall to the centroid of runoff mass. Therefore, lag times for the Gervais gage-basin are best estimated to be less than 15 minutes. Although 20 minutes may be an appropriate time of concentration for relatively common storms; e.g., the mean annual flood, the observed stage hydrograph and rainfall for the large well-defined July 21, 2013 storm with 63 mm (2.5 in) of rainfall indicates longer times of concentration for larger events. Based on the inflection point on the hydrograph, the time of concentration for the July 21, 2013 storm was more than an hour. Based on this analysis and the fact that the NRCS 2010 method is not intended solely for urban watersheds, further hydrograph analyses were based on lag times computed using the Putnam method (Equation 2.5) and Bohman 1992 method (Equation 2.6).

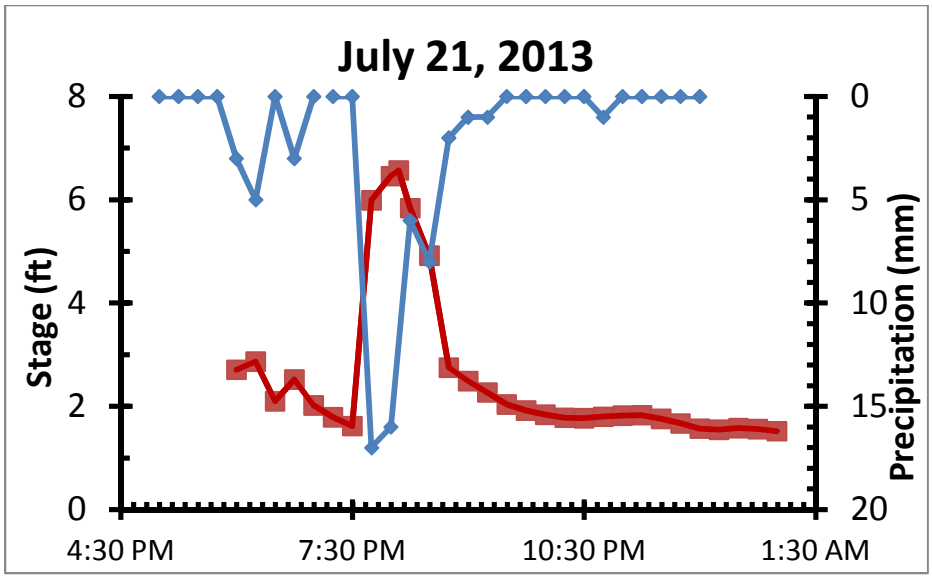

Figure 4.3. Lag-to-Peak for Gervais Gage-basin (Adjusted to EDT)

At Pickens Gage Sub-basin Hydrologic Analysis

Estimates of peak discharge are computed for the At-Pickens gage sub-basin, followed by an analysis of discharge using the slope-area method in an attempt to evaluate historic peak stages observed at the gage. This, in turn, is followed by the analysis of stormwater timing in order to constrain hydrograph shapes and to develop triangular hydrograph and dimensionless hydrograph.

At Pickens Peak Discharges

Peak discharges for the At Pickens gage sub-basin were estimated by the rational, Putnam, and Bohman methods. Peak discharges were calculated using spatially weighted rational coefficients with rainfall intensities up to the 60-minute 50-year storm (Tables 4.8 and 4.9). The saturation factor from Equation 2.4 increased all discharges by 17.5%. Studies at the site that measured discharge (Logan et al. 1985; Fadi Shatnawi, written communication) observed discharges as high as 1100 cfs (Figure A.11; Logan et al. 1985) and 1300 cfs by the

USGS (Figure A.12). These storm flows fall within the range of discharges computed by the rational method for 30-minute rainfalls with recurrence intervals greater than 2-years, or for inter-annual 60-minute rainfalls (recurrence intervals <1).

The calibration of stage-discharge relationships at the gage appear to be accurate for discharges below 350 cfs (Figure A.10; Fadi Shatnawi, written communication). However, due to backwater effects at the bridge flow stages, which are common in the historic record, cannot be converted to discharges (Tim Lanier, personal communication).

Table 4.8. At-Pickens Sub-basin Peak Discharges; (based on CIA with rainfall intensities from Table 2.2)

Duration	Recurrence Interval (1-yr)	Recurrence Interval (2-yr)	Recurrence Interval (5-yr)	Recurrence Interval (10-yr)	Recurrence Interval (25-yr)	Recurrence Interval (50-yr)
	Peak Discharges (cfs)					
5-min	45.2	52.5	60.0	67.3	75.5	82.2
10-min	145	168	192	215	241	261
15-min	271	317	365	407	458	498
30-min	742	875	1,037	1,182	1,357	1,496
60-min	1,858	2,195	2,654	3,088	3,607	4,065

Table 4.9. At-Pickens Sub-basin Peak Discharges with a Saturation Factor; (based on C_fCIA with C_f = 1.17 and rainfall intensities from Table 2.2)

Duration	Recurrence Interval (1-yr)	Recurrence Interval (2-yr)	Recurrence Interval (5-yr)	Recurrence Interval (10-yr)	Recurrence Interval (25-yr)	Recurrence Interval (50-yr)
	Peak Discharges (cfs)					
5-min	53.1	61.7	70.5	79.1	88.7	96.6
10-min	170	197	226	253	283	307
15-min	319	372	429	478	539	585
30-min	872	1,028	1,219	1,389	1,594	1,757
60-min	2,183	2,580	3,118	3,628	4,238	4,776

At-Pickens Slope-Area Discharge Computations

A channel cross-section topographic survey with a rod, level, and tape at the At Pickens gage site was tied approximately to the staff gage reading at the time of the survey (November 19, 2013 at 14:00 EST) to allow determination of when flows hit the top of the culvert beneath the Pickens Street bridge (top horizontal line on Figure 4.4), or top stream bank and terrace surfaces. The survey relative heights were related to the USGS staff gage by subtracting 0.82 meters from the corresponding USGS stage reading at the time of the survey. The Pickens Street Bridge has two concrete structural support walls forming three 2.2 x 2.2-meter box culverts where backwater occurs during flow stages above 5.2 feet (1.6 meters). An additional 14 inches (0.36 meters) is also subtracted due to a cement lip along the bottom of the culverts causing ponding, zero discharge, and acting as the control for the reach during low-flow conditions. The slope-area method was used with cross-section analyzer (CSA) software (NRCS ND) in an attempt to constrain discharge, hydraulic radius, and mean flow velocity for various flow stages. The CSA computation produced cross-section parameters shown in Table 4.10 for stages up to 11 feet (3.35 meters) near the bank tops. The bold line break above 5 feet indicates uncalibrated data and when compared to Figure A.14 the CSA overestimates discharge at higher stages and underestimates discharge at lower stages. Further analyses for the At-Pickens gage site using CSA should consider adjusting Manning roughness for the low and high stages.

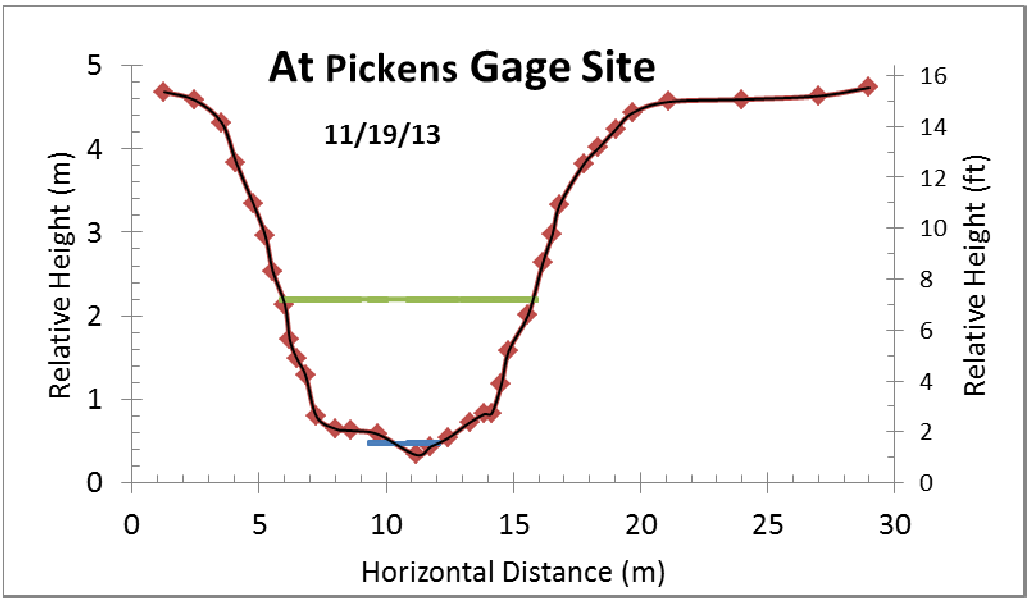

Figure 4.4. At-Pickens Gage Cross-Section looking downstream (west). High horizontal line is height of three 2.2 x 2.2-meter box culverts. Lower horizontal line is water surface at time of survey.

Table 4.10. At-Pickens Gage-basin Cross Section Analysis. Slope = 0.001 and n = 0.03

Water Surface Elevation	Water Surface Elevation	Flow area	Wetted Perimeter	Hydraulic Radius	Discharge	Discharge	Velocity
ft	m	m^2	m	m	cfs	cms	m/s
11.00	3.35	277.6	47.1	5.89	1419	40	5.11
10.50	3.20	258.0	45.6	5.66	1283	36	4.97
10.00	3.05	239.0	44.2	5.41	1154	33	4.83
9.50	2.90	220.4	42.8	5.16	1031	29	4.67
9.00	2.74	202.4	41.4	4.89	912.8	25.8	4.51
8.50	2.59	184.7	40.1	4.61	801.3	22.7	4.34
8.00	2.44	167.5	38.7	4.33	697.1	19.7	4.16
7.50	2.29	150.8	37.2	4.05	600.5	17.0	3.98
7.00	2.13	134.7	35.8	3.77	510.7	14.5	3.79
6.50	1.98	119.0	34.5	3.45	425.7	12.1	3.58
6.00	1.83	103.8	32.9	3.16	349.6	9.9	3.37
5.50	1.68	89.1	31.3	2.85	280.6	7.9	3.15
5.00	1.52	75.1	29.6	2.54	219.1	6.2	2.92
4.50	1.37	61.7	28.0	2.20	163.6	4.6	2.65
4.00	1.22	48.9	26.6	1.84	115.1	3.3	2.35
3.50	1.07	36.6	25.2	1.45	73.4	2.1	2.01
3.00	0.91	24.7	23.8	1.04	39.6	1.1	1.60
2.50	0.76	13.6	20.2	0.67	16.4	0.5	1.20

2.00	0.61	5.04	12.7	0.40	4.27	0.12	0.85
1.50	0.46	0.98	4.96	0.20	0.52	0.01	0.53
1.09	0.33	0.0	0.0	0.00	0.00	0.00	0.00

Slope-area discharge computations required estimations of roughness and slope. The Manning roughness coefficient (n) was set to 0.03 using methods described in Chapter 2. The At Pickens cross-section has coarse rip-rap, and dense vegetation along the channel walls (Figure A.13). The 0.1% slope used for the At-Pickens slope-area computation was determined using GIS spatial analysis. A digital elevation model (DEM) derived from 2-ft LiDAR was overlaid on top of the orthographic imagery (ESRI, 2014). Eleven elevations were selected from the DEM at sites along the streambed starting 200 meters upstream from the At-Pickens gage. The elevation at the gage was not used due to the cement lip discussed earlier. Discharges above a stage of 5.2 feet (1.6 meters) are affected by backwater at the bridge and should not be estimated by the Manning equation, which assumes uniform flow.

Observed stage-discharge data collected by the USGS between August, 2011 and January, 2013 (obtained from Fadi Shatnawi, written communication) were used to calibrate flows below 5.2 feet (1.6 meters). A second-order polynomial calibration was empirically derived for use as a stage-discharge rating curve:

$$Q_{cfs} = 31.7\ St_{ft}^2 - 128.1\ St_{ft} + 117 \qquad \text{(Equation 4.2)}$$

$$Q_{cms} = 9.66\ St_{m}^2 - 11.9\ St_{m} + 3.3 \qquad \text{(Equation 4.3)}$$

Comparing this calibration with the Manning estimates indicates that the Manning method over-predicted discharges at low stages and under-predicted discharges at high stages (Figure .14). Given that the Manning method should not be used for stages greater than 1.6 meters due to backwater effects, and that the empirical rating is superior below 1.6 meter stages, the

empirical calibration was used and the Manning computations were not used. Neither method should be extrapolated above 1.6 meter stages, so attempts were abandoned to develop a rating curve for interpreting high flows. Fortunately, a new gage has been established upstream that is providing additional flow data. These data could be used to reconstruct historical flows from the existing continuous stage data at the At-Pickens gage.

Peak discharge estimates at various recurrence intervals for the At-Pickens gage sub-basin were calcuated using Putnam (1972), Bohman (1992), and the rational method (Table 4.11). An evaluation of flow stages on the mean annual maximum flood series (AMFS) collected at the gage from 1985 to 2003 indicates that flows below 5.2 feet (1.6 meters) are frequently occurring events. Only two years of the twenty years or record has an annual maximum flow stage below 5.2 feet (1.6 meters). Comparisons of the peak discharge flows predicted by the various empirical equations with the AMFS at the gage are hampered by uncertainties associated with the uncalibrated discharge values given in the AMFS. Assuming the AMFS discharge values are accurate, the mean annual flood for the period was 982 cfs (23.7 cms). Flows were greater than or equal to 608 cfs in every year of the 17-year discharge record (Figure A.12). Furthermore, the three years with missing flow values were large flood years with very high peak stages and discharges that were clearly greater than average. This indicates that discharges of 371 cfs (10.5 cms) that reach the top of the culvert occur in most years. This frequency supported by two-year flow frequency magnitudes estimated by the Putnam and Bohman peak discharge estimates and by the rational method for rainfalls more than 15 minutes in duration (Table 4.11). Unfortunately, the discharge values in the AMFS or the stage-discharge relationship for high flow stages need to be confirmed before further evaluations can be made of the magnitude-frequency of peak discharges at this site.

Table 4.11. At-Pickens Peak Discharge (cfs)

Q_N	Putnam	Bohman	C_fCIA				Manning Q (cfs)
			10-min	15-min	30-min	60-min	at 5.2-ft stage = 228 cfs
Q_1	-	-	170	319	872	2,183	-
Q_2	506	478	197	372	1,028	2,580	-
Q_5	861	696	226	429	1,219	3,118	-
Q_{10}	1,144	835	253	478	1,389	3,628	-
Q_{25}	1,530	996	283	539	1,594	4,238	-
Q_{50}	1,837	1,117	307	585	1,757	4,776	-
Q_{100}	2,138	1,230	-	-	-		-
Q_{500}	-	1,434	-	-	-		-

At Pickens Lag-times & Time of Concentration

The timing of stormwater arrival was estimated by several methods and the results were compared with observations from storm hydrographs measured at the At-Pickens gage in the 1980s. The At-Pickens gage sub-basin is 1,436 acres, has a main watercourse length of 2.58 miles, a channel slope of 61 feet per mile, and a total impervious surface area of 54.5 percent. Based on these factors, the lag time to centroid (T_C) calculated by the Putnam (1972) method is 0.81 hours (48 minutes). The timing of storm hydrograph flow data collected in the 1980s (Logan et al. 1985) was analyzed by Sanjeev Joshi (written communication) by measuring the time differential between the centroid of rainfall and peak discharge. Although lag-to-peak is shorter than lag-to-centroid, the much shorter lag-to-peak times of the observed storm hydrographs suggest that the Putnam lag time is unrealistically long regardless of the magnitude of the event (Figure A.11).

The calculated T_C for the At-Pickens gage sub-basin using the Bohman (1992) method was 0.27 hours (16.3 minutes), which was a third of the time of Putnam (1972). The variables used in Equation 2.6 (Bohman method) were similar to the variables in Equation 2.5 (Putnam method) with an additional 30-minute rainfall intensity variable as explained in Chapter 2. The Bohman T_C is similar to the observed lag times to peak (Sanjeev Joshi, written communication) for moderate magnitude flows. Plotting lag-to-peak against discharge (Figure A.11) suggests lag-times at this site increase with discharge at a rate of approximately 1.4 minutes per hundred cfs. Similar effects of lag times increasing with scale have been noted elsewhere (see Figures 10.35 & 10.36 of Dunne and Leopold, 1978). While more data are needed to test and refine this relationship, the increase in lag-time with discharge is realistic and is one reason why dimensionless hydrographs are often used to compare hydrographs between storms of different magnitudes.

The NRCS method (Equation 2.7) was also used to calculate lag-to-peak time for the At Pickens sub-basin. The At-Pickens sub-basin has a 44.3 minute lag time according to the Chow 1964 method and a 61 minute lag time according to the weighted slope method.

Time of concentration (T_C) (Equation 2.9; NRCS 2010) for the At Pickens gage-basin using the weighted slope method was 1.69 hours (101 minutes) and 1.23 hours (73 minutes) using Chow 1964. Similar to the lag times calculated for At Pickens, the times of concentration calculated for At Pickens by the NRCS method are unrealistically long. Table 4.12 shows the calculated lag times and time of concentration. It is commonly assumed for unurbanized watersheds with uniform rainfall that lag-to-peak time is approximately 0.6 times the time of concentration. Thus, the lags-to-peak corresponding to the calculated 101 and 73 minute times of concentration would be approximately 61 and 44 minutes, which is essentially identical to the

lag-to-peak values estimated directly by the NRCS method. Both of the lag-to-peak times for At-Pickens computed by either method are much longer than the observed storm-flows at the site. This may be because the NRCS method is applicable to a broad set of watersheds (NRCS 2010) including heavily forested areas, and may not be sensitive to heavily urbanized impervious areas.

In summary, based on comparisons with observed hydrographs, the lag-to-centroid results produced by the Putnam (1972) and Bohman (1992) methods were more realistic than the NRCS (2010) method.

Table 4.12. Calculated Lag-Times and Time of Concentration for the At-Pickens Gage-basin

Lag-to-centroid		**Lag-to-centroid**		**Lag-to-peak**		**Time of concentration**		
Putnam method		**Bohman method**		**NRCS method**		**NRCS method**		
T	*T*	*LT*	*LT*	*L*	*L*	*Tc*	*Tc*	
(hr)	(min)	(hrs)	(min)	(hrs)	(min)	(hrs)	(min)	
0.812	48.74	0.27	16.30	1.016	60.99	1.694	101.64	**Weighted slope method**
				0.738	44.30	1.231	73.84	**Chow method**

Model Storm Hydrograph Analysis

Triangular hydrographs for the 2-year, 30-minute rainfall were created for moderate floods at the Gervais gage sub-basin based on the peak discharge, lag-times, and total runoff volumes calculated earlier. The storm-flow duration of the hydrographs were computed by dividing total storm runoff volume by peak discharge. The model hydrograph is shown in Figure 4.5 and based on the Bohman (1992) method for computing peak flow and lag-time. The high peak discharge (255 cfs) is supported by the slope-area computations of frequently occurring flow stages.

This hydrograph indicates a rapid receding limb that defines a negatively skewed hydrograph. Negatively skewed hydrographs area not conventional, but have been noted in the literature. A negatively skewed hydrograph may result from an unrealistically low calculated runoff volume, or too long of a lag-to-peak. Even if total storm runoff is increased to the maximum possible runoff using an unrealistically high basin-wide CN of 99, the triangular hydrograph based on empirically derived lag time and peak discharge is negatively skewed. A watershed composed of mostly impervious areas with a high Hortonian overland flow can generate a slightly negatively-skewed hydrograph response (Sellinger 1996). Negative skewness can also result from the watershed shape. Fan-shaped watersheds pointed towards the outlet can generate negatively skewed hydrographs (Subramanya , 2013) because stormwater travel times are longer in the tributaries furthest from the outlet. Watershed shape does not appear to be the cause of negative hydrography skewness in this case. Nonetheless, all three computed lag-times (Equations 2.5, 2.6, and 2.7) support the negatively skewed hydrograph. The lag time used in Figure 4.5 was the shortest time computed from empirical equations and was geometrically determined using the lag-to-centroid computed by the Bohman (1992) method and converting lag-to-centroid to lag-to-peak by solving for similar right triangles, which gave a lag-to-peak of 10 minutes. A shorter lag-to-peak time is difficult to justify for the 30-minute rainfall and would indicate peak discharge occurring before uniform rainfall had ceased. There are reasons to suspect, however, that the CN method underestimated the total storm runoff volume. As described early in this chapter, adjusting runoff for a smaller initial abstraction increased runoff by 9.7% but had little effect on the shape of the hydrograph. The volumetric analysis for water budgeting in the Gervais basin described in Chapter 5 used a synthetic hydrograph based on the runoff volumes computed using 20% abstractions and a weighted curve number of 94.

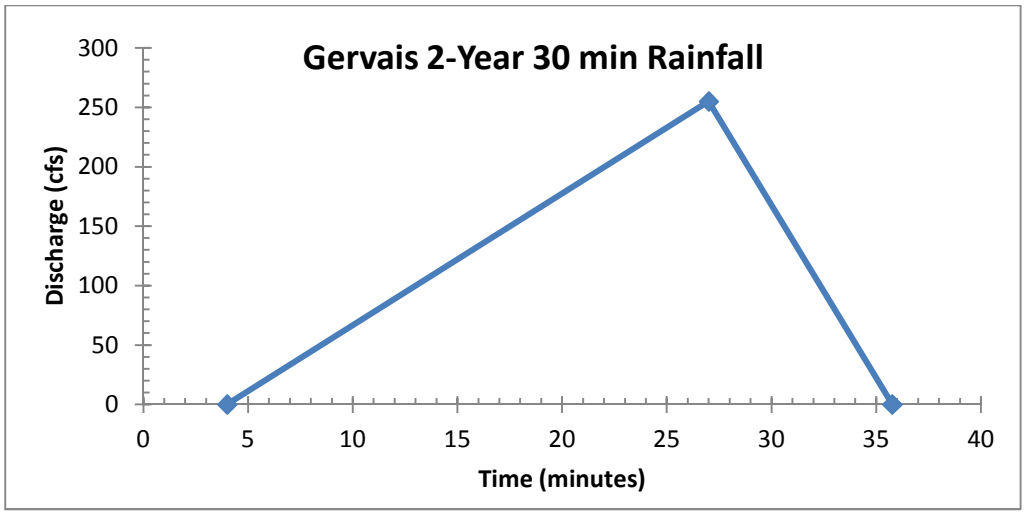

Figure 4.5. Gervais Model Hydrograph

Dimensionless hydrographs are constructed to compare different size storm events by dividing time over time-to-peak along the x-axis and dividing discharge over peak discharge along the y-axis. Figure 4.6 indicates a dimensionless hydrograph for a 2-year 30-minute rainfall event at the Gervais gage site.

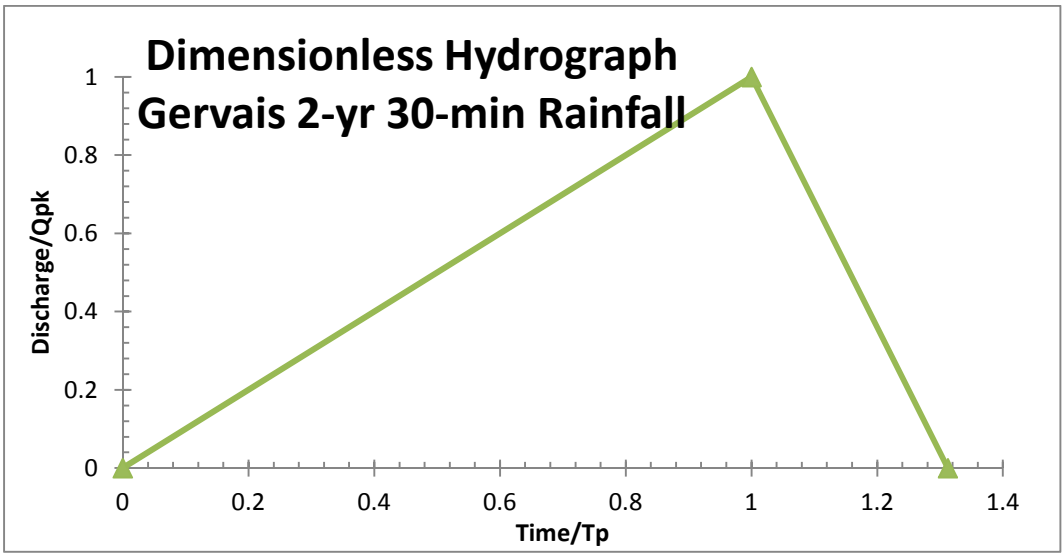

Figure 4.6. Gervais gage site dimensionless unit hydrograph for a 2-year 30-minute rainfall event

Summary Discussion

Total storm runoff was computed for several sub-basins using the weighted curve-number method and with curve numbers adjusted for impervious surface connectivity. The Gervais sub-basin is highly urbanized with a TIA that covers 75.2% of the basin surface. Approximately 98.6% of the impervious surface area in the basin is well connected to storm sewers or channels and were assigned CNs from 95 to 98. This resulted in a relatively high total runoff volume of 242,969 ft^3 (6,880 m^3) for the 2-year, 30-minute rainfall event from the Gervais gage sub-basin. This amounts to an average runoff depth of 0.89 inches (23 mm) for the 1.45 inch (37 mm) rainfall event; or a runoff index (runoff/rainfall) of 62%. The larger At-Pickens sub basin is less densely urbanized than the basin with a TIA of 44.4%. Some 78.6% of the TIA in the At-Pickens basin is well connected to storm sewers and channels and was assigned CNs from 95 to 98 resulting in a total runoff volume for the 2-year, 30-minute rainfall event of 2,833,731 ft^3 (80,304 m^3). Runoff averages a depth of 0.544 inches (14 mm) across the At-Pickens sub basin. This gives a runoff index of 37%, which is substantially less than the Gervais sub basin, reflecting the smaller TIA and less-dense urbanization of the residential neighborhoods that comprise many of the sub basins above the At-Pickens site.

Discharges at the Gervais cross-section can be constrained somewhat with available data, although streamflow measurements are needed to calibrate the gage. Slope-area (Manning) discharge computations, using a relatively low gradient and high roughness, indicate that discharge at a stage of 2 meters is in conformance with the two-year peak flood estimate computed by the Bohman (1992) method. Estimates of peak discharge derived from the other empirical methods were too low to be matched by slope-area methods at frequently occurring flow stages. By all indications, the two-year hydrograph at the Gervais gage site are negatively

skewed. While gage-calibration is needed to confirm this relationship, rainfall-runoff models should seriously consider the potential for this non-conventional hydrograph shape.

Moderate magnitude discharges at the At-Pickens gage below 1.7 m stages can be modeled with the slope-area method. Roughness would need to be adjusted to refine the modeled values presented here. Instead, the calibration developed from stage-discharge data collected in 2011 to 2013 was used for moderate flows. No means of calibrating flows above a stage of 1.7 m has been devised. Several storm hydrographs observed in the early 1980s provide an empirical means of interpreting storm hydrographs.

Chapter 5 – Water Budgeting to Determine LID Treatment Estimates

LID runoff abstraction in the RBW can potentially lower peak discharge, increase lag-times, and minimize total runoff volumes in the watershed. A sensitivity analysis was conducted by computing a water budget using the Gervais triangular hydrograph. Runoff volumes were subtracted from the hydrograph as LID abstraction was implemented.

Water Budgeting

The Gervais gage sub-basin triangular hydrograph generated for a 2-year, 30-minute rainfall provided continuous discharge data that was used for a water-budget analysis. As described in Chapter 4, the hydrograph was computed using the SCS curve number method and Bohman (1992) lag-to-centroid (Figure 4.5). It has a peak discharge of 255 cfs (7.2 cms) and a total storm runoff volume of 242,901 ft^3 (6,833 m^3). One-minute streamflow input data were generated as linear functions of time for the rising and falling limb of the hydrograph.

Various scenarios of total LID volume were simulated and the LID-storage volume was subtracted from volumes of the hydrograph input as long as storage remained available assuming no losses from LID-storage.

To allow for manipulations of the spatial area of the basin that was subjected to LID treatment, total runoff volume was reduced to various percentages of treated area. The percent basin area treated determines how much of the total runoff can effectively be reduced. If only 10% of the sub-basin is treated with LID assuming a uniform spatial distribution of

rainfall, the runoff at the outlet can only be minimized by 10% regardless of the amount of LID implemented. In that case, LID storage is slower to fill because only 10% of the runoff goes into storage. On the other hand, the influence of storage on total runoff at the outlet is reduced and may have little influence on peak discharge. Altering the percentage of the basin treated accounts for situations where certain parts of the basin contribute runoff to the outlet that is not affected by LID; that is, runoff from the untreated areas is not reduced. Untreated areas may represent an entire tributary or the lower floodplains of main channels where LID is not usually effectively implemented. With spatially uniform rainfall the sensitivity of total outflow from the basin to LID treatment will be proportional to the area that is treated. One way to reduce flood peaks in cases with large percentages of untreated runoff would be to implement conventional detention or retention structures in the lower basin to store untreated runoff.

The volumetric water budget is constructed to subtract potential LID storage from the inflow runoff volume (adjusted for percent area treated) until storage is filled. The budget was computed in one-minute intervals and LID storage decreased the total runoff volume until the potential storage was completely used or the percent runoff treated threshold was met. A matrix was constructed of the budget results for a range of percent basin treated from 10% to 100% (Table 5.1). The maximum values of LID storage potential in the second column indicate the potential volume that can be abstracted from storm runoff, which is simply the product of available potential storage and the percentage treated. For example, if only 10% of the Gervais sub-basin is treated with LID the maximum potential storage that can be used for abstraction from the 2-year, 30-minute storm is 24,290 ft^2. This matrix shows that the effectiveness of increasing LID storage is limited by the area of the basin that is controlled by mitigation.

The volumetric water budget analysis was used to simulate the effects of LID storage on peak instantaneous discharge for the two-year, 30-minute storm hydrograph at Gervais. These simulations were conducted on a variety of percentages of the sub-basin treated and the maximum effective LID storage volume for that percent (from Table 5.1). Adjusted peak discharges were computed for each volume of effective storage. Table 5.2 shows the change in peak discharge as total available LID storage increases for the Gervais gage sub-basin during a 2-year 30-minute event. LID storage used in Table 5.2 indicates the maximum effective storage capacity for the given percent areas. In addition to peak discharges changing, lag-times can increase once the runoff volume under the rising limb is abstracted (Figure A.15).

Table 5.1. Potential Discharge Reductions from LID Implementation for 2-year, 30-minute storm event

Percent Area Treated	LID Storage Used	Original Peak Discharge	Adjusted Peak Discharge	Change in Peak Discharge	Percent Reduction in Peak Discharge
	ft^3	cfs	cfs	cfs	
10%	24,290	255	227	28	10.8%
20%	48,580	255	202	53	21.8%
30%	72,870	255	177	78	31.7%
40%	97,160	255	152	103	41.6%
50%	121,451	255	126	129	50.5%
60%	145,741	255	101	154	61.4%
70%	170,031	255	76	179	71.3%
80%	194,321	255	51	204	80.2%
90%	218,611	255	25	230	91.1%
100%	242,901	255	0	255	100%

Under the given assumption that LID storage will be used by the first available runoff, this seemingly simple water budget simulation reveals a spatial complexity of the response in peak discharge. This complexity is introduced when only a proportion of the catchment is treated. First, LID storage must be of sufficient storage volume so it will not be filled before the

arrival of the peak discharge. Increasing LID storage volume will prolong the period of runoff reductions for a given precipitation intensity and percent area treated. Thus, increasing LID storage will enhance peak discharge reductions up to a point. Second, the optimal volume of LID storage for a given rainfall event depends on the percentage of the catchment being treated. Increasing the percent area can increase reductions in peak discharge if there is adequate storage because more of the total basin runoff will be treated. For cases of limited storage, however, increasing the area treated by storage directs more runoff to the storage sites during the rising limb of hydrographs. This may result in reducing or eliminating the effect on peak discharge.

In summary, changes in peak discharge differ for each amount of available storage. If the available storage capacity is relatively low it is better to treat a lower percentage of the watershed area to prolong the storage process. The storage process must last as long as the time-to-peak in the storm model hydrograph or else the peak discharge is unaffected. If a higher percentage of the watershed is treated with LID, but the amount of potential storage is relatively low, the storage capacity fills much faster and could potentially fill up before the time-to-peak occurs.

LID Implementation into the RBW

Spatial analysis of where LID implementation has the highest effectiveness can be shown in Table 4.2. All of the sub-basins above the At-Pickens gage, including the 5-Points, Wales Garden, Wheeler Hill, South Campus, Mill-Villages North, and Mill-Villages sub-basins, contribute to the RBW flooding. Table 4.2 indicates that 70% of the runoff above the At-Pickens gage occurs within the Gregg Street and MLK sub-basins. Runoff and volumetric simulations in the Gervais sub-basin, a very heavily urbanized area within the Gregg Street sub-basin, serve as

examples of the sensitivity and effectiveness of runoff to LID implementation. Implementing LID into the Gervais gage sub-basin could be highly effective for mitigating flood water generated in these sub-basins. Based on runoff depths, Gregg Street, Five Points, University Hill, Wales Garden, and USC Northwest could also be sub-basins where LID would be effective. The Hollywood-Rose Hill sub-basin is large but it generates a relatively low mean depth of runoff, so LID is likely to be least effective in reducing flood generation.

Disconnecting the impervious areas with higher EIA CNs is an effective spatial approach to where LID should be implemented. LID such as bioretention and cisterns can disconnect parking lots and buildings from the USSS. The CN values in the LID implementation analysis are treated differently from the adjusted EIA CNs because LID minimizes connectivity.

Gervais Gage Sub-basin LID Implementation using the Water Budget Analysis

Runoff volumes from building rooftops within the Gervais gage sub-basin were computed using the SCS curve number method (Equation 2.1). Building footprint areas (shown in Figure 5.1) were taken from the revised 2013 TIA data. The CN values used for the buildings were 98 (Figure 1.7). The rainfall intensity used in the analysis is the 2-year 30-minute rainfall event (Table 2.2). The total runoff volume generated for the 135 buildings within the Gervais gage sub-basin for a 2-year 30-minute rainfall event was 63,477 ft^3 (1797 m^3).

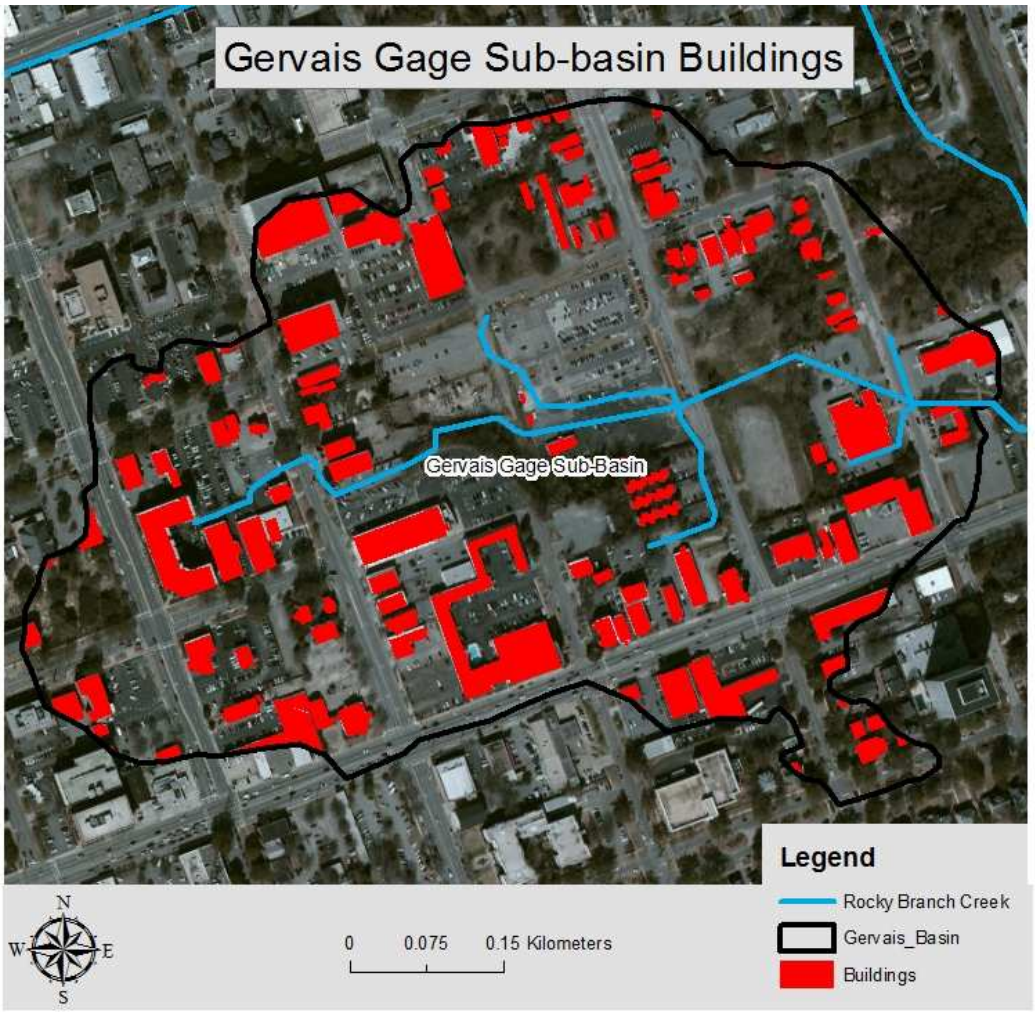

Figure 5.1. Gervais Gage Sub-basin Building Coverage

The water budget analysis was run using the runoff volume generated from the Gervais gage sub-basin buildings. The building runoff is a higher volume runoff per unit area than the Gervais gage sub-basin due to different CNs used and should be treated independently from the water budget analysis. However, the Gervais building runoff volume can be used in the water budget as a realistic maximum LID abstraction volume. If 63,477 ft^3 of runoff is abstracted using LID such as cisterns, rain barrels, rain pillows, and green roofs peak discharge can be lowered. If only 1% of the basin is treated peak discharge will be reduced by 1%. Table 5.2 shows the change in peak discharge as percent area treated increases. The highest percent change in

discharge using the Gervais buildings runoff volume occurs when 30% of the sub-basin is treated. Increasing the percent area treated decreases the change in peak discharge after 30% because the storage begins to fill up too quickly, prior to the arrival of peak discharge.

Table 5.2. Change in Peak Discharge by Abstracting Runoff Volume from the Gervais Gage Sub-basin Buildings

Percent Area Treated	LID Storage Used	Original Peak Discharge	Adjusted Peak Discharge	Change in Peak Discharge	Percent Change in Peak Discharge
	ft^3	cfs	cfs	cfs	
1%	2,429	255	252	3	1%
5%	12,145	255	242	13	5%
10%	24,290	255	230	25	10%
20%	48,580	255	204	51	20%
30%	63,477	255	179	76	30%
31%	63,477	255	176	79	31%
32%	63,477	255	190	65	25%
33%	63,477	255	197	58	23%
34%	63,477	255	208	47	18%
35%	63,477	255	226	29	11%
36%	63,477	255	226	29	11%
37%	63,477	255	235	20	8%
38%	63,477	255	255	0	0%

Runoff volumes generated from parking lots and sidewalks within the Gervais gage sub-basin were also computed for the 2-year 30-minute rainfall event. The runoff volumes were computed the same as the buildings using 98 for the CNs. The Gervais gage sub-basin parking lots and sidewalks generate 142,679 ft^3 (4,040 m^3) of total runoff for the 2-year 30-minute rainfall event. One parking lot within the Gervais gage sub-basin owned by the University of South Carolina is 159,121 ft^2 (48,500 m^2) generating 16,322 ft^3 (462 m^3) of runoff for the 2-year 30-minute rainfall (Figure 5.2).

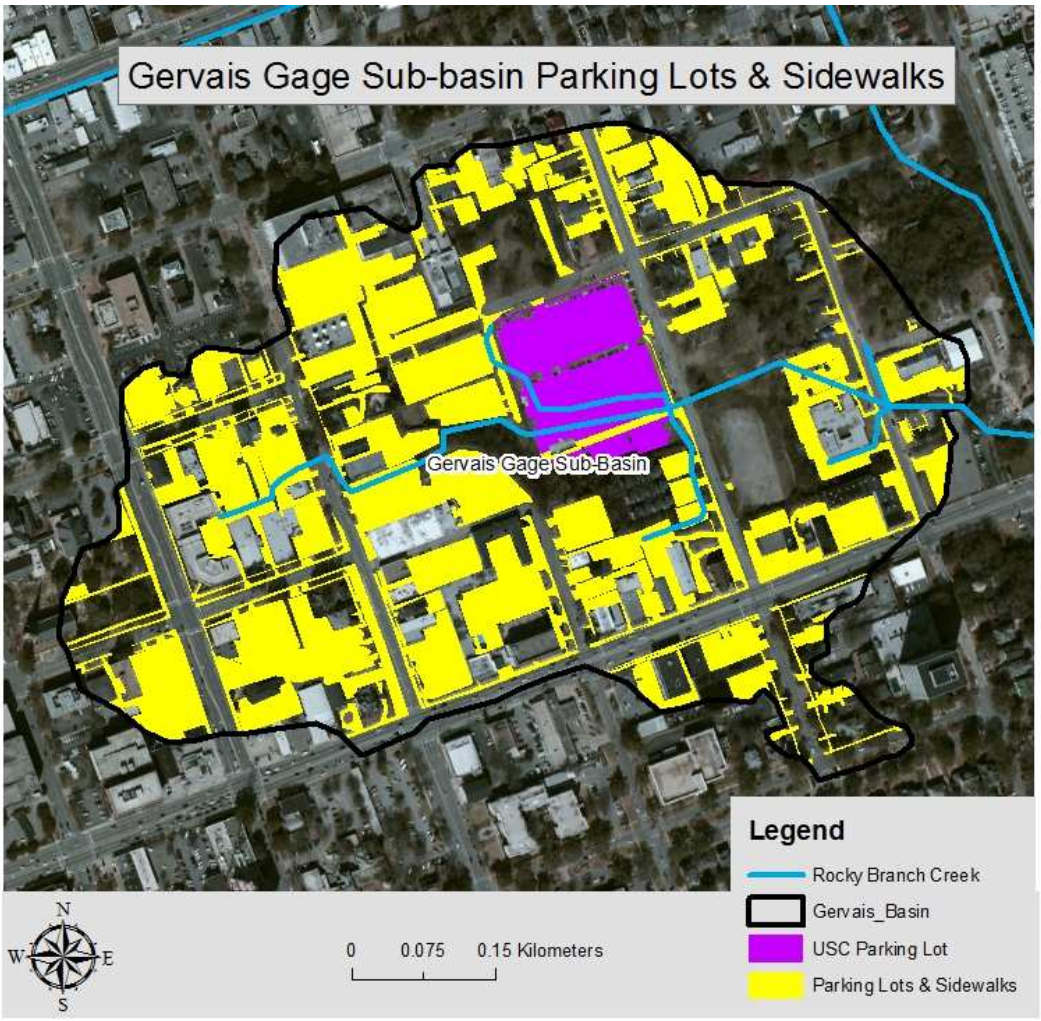

Figure 5.2. Gervais Gage Sub-basin Parking Lots and Sidewalks

Disconnecting the runoff generated from the parking lots will have a higher impact than sidewalks because sidewalks within the RBW generally have a vegetative buffer from the streets and USSS already established. Implementing buffers between the impervious parking lots and USSS using bioretention, rain gardens, and porous pavement can serve as examples of well-known LID detention designs.

Implementing LID into the Gervais gage sub-basin is best done using a conglomeration of LID designs. The designs must also disconnect large impervious areas such as buildings and parking lots from the streets and USSS. Targeting the largest buildings (buildings over 5,000 ft^2)

and parking lots (parking lots over 10,000 ft^2) to disconnect impervious surfaces from the USSS using LID implementation has the potential to abstract 116,168 ft^3 (3,290 m^3) from the Gervais gage sub-basin during the 2-year 30-minute rainfall event. There are 29 buildings over 5,000 ft^2 (142 m^2) and 27 parking lots over 10,000 ft^2 (283 m^2) located within the Gervais gage sub-basin. A cistern capable of holding runoff generated from a 5,000 ft^2 building is 3,800 gallons (14,385 L) or a diameter of 18 feet and a height of 6 feet (Krishna et al. 2005).

Changes to peak discharge within the Gervais gage sub-basin were computed using the water budget for the larger buildings and parking lots runoff volume (116,168 ft^3 or 3,290 m^3). The adjusted peak discharge, using a percent area treatment of 50%, after a potential abstraction of all of the runoff volume generated from the larger buildings and parking lots was reduced to 127 cfs (3.6 cms) or approximately 50% of the original Bohman (1992) peak discharge of 255 cfs (7.2 cms).

Constructing a detention pond near the outlet could be designed to complement LID by capturing some of the peak discharge after LID abstraction. Total abstraction in the larger buildings and parking lots (116,168 ft^3 (3,290 m^3) has the potential to reduce the peak discharge by about 50%. A detention pond required to capture the rest of the resulting runoff would need to be 126,757 ft^3, approximately one and a half Olympic-size swimming pools or three acre-feet. Figure A.16 shows a three acre-foot detention pond located near the outlet which would need to be designed with an inlet to fill only above a given stage. Otherwise, the pond would fill up before the time-to-peak since it captures a large percent area treated. The hydrograph response from only using the detention pond near the outlet is shown in Figure A.17.

Converting Parking lots to Fallow Land

Another method for decreasing urban surface runoff is decreasing the amount of existing impervious area. One example is converting parking lots to open grassland. A simple

simulation of such a conversion in the Gervais basin was made by altering curve numbers to represent various percentage areas converted from parking lot to fallow land. The CNs for impervious surfaces converted to open grassland were reassigned from 98 to 84 (Figure 1.7). This reduction in CNs is modest, since they are all located in a D hydrologic soil group. Greater reductions could be achieved by conversion of parking lots to fallow land over more permeable soils. In spite of the relatively impermeable soils, weighted CNs based on converting highly connected impervious parking lots to open grassland are substantially lower in the Gervais gage sub-basin (Table 5.3). Table 5.3 also shows the reductions in total storm runoff volume for the 2-year 30-minute storm event that would be achieved by converting a percentage of the parking lots in the Gervais gage sub-basin to open fallow land. This analysis suggests that simply converting 20% of the area of parking lots to fallow land with grass cover--without any investment in LID or detention structures whatsoever—could reduce storm-flow volumes by almost 10%. In some urban basins with abandoned paved areas, such an approach may be a viable strategy for reducing flooding at minimal cost.

Table 5.3. Total Runoff Response from Converting Parking Lots to Fallow Land in the Gervais Gage Sub-basin

Percent Parking Lot Converted	Weighted EIA CN	Total Runoff (ft^3)	Percent Change in Runoff
0	94.0	242,969	0
10	93.4	232,023	4.5
20	92.8	219,941	9.5
30	92.1	208,769	14.1

The CNs assigned to the open grassland were 84 (Figure 1.7) since they are located in a D hydrologic soil group. However, the open grassland CN is still substantially lower than the highly

connected impervious parking lots in the Gervais gage sub-basin and can minimize total runoff volumes.

Discussion

Peak discharges can be lowered by implementing LID and detention ponds over a small area of the watershed in order to extend the storage capacities. Based on the assumptions of the volumetric analysis; e.g., all runoff for the treated area will go to available LID storage until that storage is filled. If the potential storage from LID is smaller using a smaller treatment area is best to reduce peak discharge (Table 5.2) whereas if more potential storage is available the treatment area can effectively be increased. The water budget analysis determined that peak discharges can potentially decrease from LID abstraction with a low percentage treatment area as long as storage capacities outlast the time-to-peak. Treating a high percentage of the watershed with a relatively small LID abstraction capacity results in storage capacity being rapidly filled and increases the time delay to the start of the hydrograph rising limb (Figure A.17), but may not change the peak discharge. If storage capacity is filled during the rising limb, the peak discharge will remain the same.

Disconnecting the main sources of stormwater runoff e.g., buildings and parking lots is an effective way to decrease peak discharge, increase peak stormwater arrival times, and extend the hydrograph. Peak stormwater arrival times increase (Figure A.15) with continued LID storage after the total runoff volume under the rising limb of the hydrograph is abstracted. In addition to increased lag-to-peak time, decreased peak discharge occurs when LID storage is sufficient to last through the rising limb. The Bohman (1992) method (Table 2.8) computed an estimated peak discharge of 255 cfs (7.2 cms) for the 2-year 30-minute Gervais gage sub-basin.

Implementing LID into the larger buildings and parking lots within the Gervais gage sub-basin can decrease the estimated peak discharge of this flood by as much as 50%.

The use of conventional stormwater detention structures can complement storage by LID methods. Constructing an additional three acre-foot detention structure (Figure A.16) near or at the outlet of the sub-basin can capture much of the remaining runoff from untreated areas to store total runoff from a 2-year 30-minute rainfall event. However, the goal is not to completely reduce peak discharge, but to demonstrate the capability to reduce it for frequent floods; i.e., the 2-year 30-minute rain event. Some stormwater runoff is necessary in urbanized streams for biological and natural functions, including water quality.

Chapter 6 – Conclusions

Urban watersheds with high surrounding impervious areas increase hydrograph response times, raise peak discharge, and generate larger runoff. The Rocky Branch Watershed has a flashy hydrologic response due to a highly impervious area with urban soils. Consequently, the stream has experienced high flow-stages since 1984 according to the At-Pickens flow-stage gage data provided by the USGS. The RBW is 49.5% impervious and is zoned 65% commercial with relatively steep slopes. Surface flows generated from the impervious area are well connected through the urban storm sewer system (USSS) which runs throughout the watershed.

Spatial analysis of the RBW was conducted to characterize hydrologic and land-use variables. The watershed drainage divides and impervious area data from Wooten (2008) were revised before hydrologic analyses could be computed. Digital maps of soils, zoning, parcel ownership, urban storm sewer system (USSS), drainage divides, and impervious surfaces, were analysed with a GIS and used to adjust curves numbers and to interpret results of the runoff and peak discharge analysis.

Buildings, parking lots, and sidewalks were given CN values of 90 and adjusted accordingly to compensate for local runoff storage and connectivity. The adjusted CNs (EIA) were adjusted for hydrologic soil type, zoning, and a USSS 10-meter buffer around the storm sewer system. EIA CNs indicate that only approximately 1% of the total impervious area (TIA) in the Gervais gage sub-basin is poorly connected to the USSS and roads. The larger At-Pickens gage sub-basin has approximately 20% of the TIA poorly connected.

Discharges were computed at two sites using empirical equations by the Putnam (1972), Bohman (1992), slope-area, and rational methods for storms equal to or larger than a 30-minute 2-year event (Table 2.2). Rocky Branch Creek at the Gervais gage site is a headwater tributary with rip-rapped channel walls and a pedestrian bridge causing high Manning roughness values. Discharge and lag-times were then computed in order to construct a model storm hydrograph for the Gervais gage sub-basin. Only the Bohman (1992) method produced a 2-year discharge large enough to be compatible with the Manning results, so this was used to estimate a peak discharge of 255 cfs (7.2 cms).

Some studies show that the conventionally assume initial abstraction rate of 20% used by the SCS CN method is too big for urbanized areas. A preliminary computation indicates the difference in total stormwater runoff between a 20% and 5% abstraction results in an approximately 10% increase in total runoff for the Gervais gage sub-basin. Calculated lag-to-centroid response times for the Gervais and At-Pickens gage sub-basins reveal a rapid rising limb in the hydrograph. Triangular model storm hydrographs were generated for the Gervais gage sub-basin using calculated peak discharges and total volume runoff from the SCS CN method (Equation 2.1) indicating an even faster receding limb, which gives hydrographs a negatively skewed shape.

Flow data for Rocky Branch Creek at the At-Pickens gage include both stage and discharge. Attempts to compute large flood discharges were not successful, so discharges could not be determined for high flow stages. Some storm hydrographs for the site are available from the published literature and were used to constrain lag-to-peak times, but limited information is available for large overbank floods at the site. Peak discharges above 1100 cfs (31 cms) have been observed by the USGS and Logan et al. (1985); however, peak discharge cannot currently

be calibrated above a 5.2-ft (1.6 m) stage due to backwater at the Pickens Street Bridge. A stage-discharge rating curve was computed for flows below 5.2-ft stages. Compared to this calibration curve, flow estimates computed by the Cross-Section Analyzer (CSA) software using the slope-area method (Manning Equation) over-predicted discharges at low stages and under-predicted discharges at moderately high stages (Figure A.14). Lag-to-centroid times computed by Putnam (1972) and Bohman (1992) were more realistic than the NRCS (2010) method for the At-Pickens gage.

Low-impact development and detention structures were lumped together in a water budget analysis to show potential changes in peak discharge as LID is implemented into the watershed. Volumetric reductions depend on the percent area of the watershed treated and the amount of abstraction by LID. The water budget analysis demonstrates that peak discharge can only be reduced if abstraction outlasts the time-to-peak. If the potential available abstraction is relatively small it is better to have a low percent area treated to prolong the storage.

Written Communications

Betsy Kaemmerlen. Landscape Architect at Fuss & O'Neill. Columbia, South Carolina

Fadi Shatnawi. PhD student in Water Resources in the Civil and Environmental Engineering Department of the University of South Carolina.

Lynn Shirley. GIS Manager. Department of Geography of the University of South Carolina

Ken Aucoin, Emergency Planner-Chief Meteorologist, Richland County Emergency Services, 1410 Laurens St., Columbia, SC 29204. Aucoink@rcgov.us

Tim Lanier. Hydrologist for the United States Geological Survey (USGS) in Columbia, SC. thlanier@usgs.gov

Sanjeev Joshi. Graduate research student in the Geography Department at the University of South Carolina.

Works Cited

Ahiablame, L. M. 2012. Development of methods for modeling and evaluation of low impact development practices at the watershed scale. Unpublished Ph.D. Dissertation, Purdue University, Indiana.

Arcement Jr, G. J., and V. R. Schneider. 1989 "Guide for Selecting Manning's Roughness Coefficients for Natural Channels and Flood Plains". United States Geological Survey Water-supply Paper 2339.

Arnold, Chester L., C. Bellucci, K. Collins, R. Claytor. 2010. "Responding to the first impervious cover-based TMDL in the nation." *Watershed Sci Bull.* (11-18)

Bedient, Philip B., and Wayne Charles. Huber. "Chapter 2: Hydrologic Analysis."Hydrology and Floodplain Analysis. 3rd ed. Reading, MA: Addison-Wesley, 1988. 79-167. Print.

Bohman, L.R., 1992, Determination of flood hydrographs for streams in South Carolina: Volume 2. Estimation of peak-discharge frequency, runoff volumes, and flood hydrographs for urban watersheds: U.S. Geological Survey. 44-46.

Brown, C. R. 2007. Characteristics of solids removal and clogging processes in two types of permeable pavement. Unpublished M.Sc. Thesis, University of Calgary, Canada.

Burton, A. and R. Pitt. 2002. Stormwater Effects Handbook: A Toolbox for Watershed Managers, Scientists, and Engineers. Lewis Publishers

Chow, V. T. 1959. *Open-Channel Hydraulics*. New York: McGraw-Hill. 680 pp.

Coffman, L. 2000. Low-Impact Development Design Strategies, an Integrated Design Approach. EPA 841-B-00-003. Prince George's County, MD. Department of Environmental Resources.

Cronshey, Roger. Urban hydrology for small watersheds. US Dept. of Agriculture, Soil Conservation Service, Engineering Division, 1986.

Dabney, S. M., Delgado, J. A. and Reeves, D. W.(2001). 'Using Winter Cover Crops to Improve Soil and Water Quality'. Communications in Soil Science and Plant Analysis,32:7,1221 — 1250

Doll, A. and G. Lindsey. 1999. Credits Bring Economic Incentives for Onsite Stormwater Management. Water Environment Federation.

Donaldson, S. (Ed.) 2009. Low Impact Development in Northern Nevada: Rainwater Harvesting. Pages 1-4 in Univ. Nevada, Reno. University of Nevada Cooperation Extension.

Donlon, Dana L., and J. W. Bauder. 2007. "Bioremediation of Contaminated Soil." Montana State University-Bozeman. Web. Date accessed: March 31, 2014 <http://waterquality.montana.edu/docs/methane/Donlan.shtml>.

Dunne, T., and Leopold, Luna B., 1978, Water in Environmental Planning, San Francisco, W.H. Freeman Co. 818 pp.

Edwards, Ken. "LMNO Engineering. Fluid Flow Calculations: Pressure Pipes, Channels, Hydrology, Ground Water." *Fluid Flow Calculations*. LMNO Engineering, 10 Feb. 2014. Web. 2 Mar. 2014. <http://www.lmnoeng.com/index.shtml>.

Environmental Systems Research Institute (ESRI), 2014. World Imagery, Map Service. http://services.arcgisonline.com/ArcGIS/rest/services/World_Imagery/MapServer. Last Accessed March 14, 2014.

EPA. 2000. Low Impact Development, A Literature Review, EPA841-B-00-005.

Gregoire, Bruce G. and John C. Clausen. 2011. Effect of a modular extensive green roof on stormwater runoff and water quality, Ecological Engineering, Volume 37, Issue 6, June 2011, Pages 963-969, ISSN 0925-8574.

Hadden Loh, T. 2012. Understanding urban development and water quality through scenarios. Ph.D. The University of North Carolina at Chapel Hill, United States -- North Carolina.

Hawkins, R.H., Jiang, R., Woodward, D.E., Hjelmfelt, A.T., Van Mullem, J.A. and Quan, D.Q. (2002). "Runoff Curve Number Method: Examination of the Initial Abstraction Ratio", Proceedings of Second Federal Interagency Hydrologic Modeling Conference, Las Vegas, Nevada, 2002.

Hayes, Donald C., and Richard L. Young. "Comparison of Peak Discharge and Runoff Characteristic Estimates from the Rational Method to Field Observations for Small Basins in Central Virginia." (2006).

Holmes, A. C. 2012. Design and implementation processes of low impact development in the Dallas - Fort Worth area. Unpublished M.L.A. Thesis. University of Texas Arlington.

Jacobs, J.H. and R. Srinivasan, 2005. Effects of Curve Number modification on runoff estimation using WSR-88D rainfall data in Texas watersheds, *Journal of Soil and Water Conservation*, 60 (5) 274-278.

Kohnke, H. and D. P. Franzmeier. 1995. Soil Science Simplified 4edition. Waveland Press Inc.

Kloss, C. and C. Calarusse. 2006. Rooftops to Rivers. Natural Resources Defense Council, New York.

Krishna, H., B. Chris, G. Jan, and C. Stephen. 2005. The Texas Manual on Rainwater Harvesting Austin, Texas.

Lawrence, C. B. 1978. Soil survey of Richland County, South Carolina. National Cooperative Soil Survey. Soil Conservation Service, U.S. Dept. Agriculture

Leopold, L. 1968. Hydrology for Urban Land Planning: A guidebook on the hydrologic effects of urban land use. USGS Circular 554.

Lim, K. J., Engel, B. A., Muthkrishnan, S., and Harbor, J. (2006). "Effects of initial abstraction and urbanization on estimated runoff using CN technology." *J. Am. Water Resour. Assoc.*, 42(3), 629-643.

Logan S.W., Eckenwiler M.R., Bohman L.R, 1995. Selected hydrologic data for urban watersheds in South Carlina, 1983-90. U.S. Geological Survey Open-File Report, 95-351.

Mishra, S.K., J.V. 2006. Tyagi, V.P. Singh, Ranvir Singh, SCS-CN-based modeling of sediment yield, Journal of Hydrology, Volume 324, Issues 1–4, 15 June 2006, Pages 301-322.

Natural Resources Conservation service (NRCS). ND. Soil Survey Geographic (SSURGO) Data for the Southwest Columbia 7.5 Minute Quadrangle. Downloaded from DNR GIS Clearinghouse.

NOAA (National Oceanic Atmospheric Administration). 2014. "Unit Hydrograph Technical Manual." Nohrsc.noaa.gov. National Operational Hydrologic Remote Sensing Center. Web.

Novotny, Vladimir, and Harvey Olem. Water Quality: Prevention, Identification, and Management of Diffuse Pollution. New York: Van Nostrand Reinhold, 1994. Print.

Novotny, Vladimir. "Chapter 6. Soil Pollution and Its Mitigation." Water Quality: Diffuse Pollution and Watershed Management. Hoboken, NJ: J. Wiley, 2003. 275-77. Print.

Olson, Nicholas C., John S. Gulliver, John L. Nieber, Masoud Kayhanian. 2013. Remediation to improve infiltration into compact soils. Journal of Environmental Management. Volume 117. Pages 85-95.

Patil, J. P., et al. "Evaluation of modified CN methods for watershed runoff estimation using a GIS-based interface." Biosystems engineering 100.1 (2008): 137-146.

Pilgrim, David H., and Ian Cordery. "Chapter 9 Flood Runoff." *Handbook of Hydrology*. Ed. David R. Maidment. New York: McGraw-Hill, 1993. 9.1-.26. Print.

Ponce, V.M., and R.H. Hawkins. 1996. Runoff Curve Number: Has it Reached Maturity? Journal of Hydrologic Engineering, ASCE 1(1):11-18.

Prince George's County, M. 2007. Bioretention Manual in E. S. Division, editor. Department of Environmental Resources

Putnam, A. L. 1972. Effect of urban development on floods in the Piedmont Province of North Carolina. USGS (U.S. Geological Survey).

Qadri, S. M. 2012. Urbanization and its Impacts on Water Quality: The Need for Green Infrastructure. Dissertation. Southern University and A & M College, Baton Rouge.

Rainwater Collection Solutions (RCS). No Date (ND). "The Original Rainwater Pillow". http://www.rainwaterpillow.com/. Last Accessed March 31, 2014.

"RCGEO 2.0 Mapping." RCGEO 2.0 Mapping. Richland County GIS Department, n.d. Web. 15 Jan. 2014. <http://www3.richlandmaps.com/rcgeoportal/>.

Sansalone, J., X. Kuang, G. Ying, V. Ranieri, Filtration and clogging of permeable pavement loaded by urban drainage, Water Research, Volume 46, Issue 20, 15 December 2012, Pages 6763-6774.

Schueler, T. 1987. Controlling urban runoff: A practical manual for planning and designing urban best management practices. Metropolitan Washington Council of Governments. Washington, D.C., 272 pp.

Schueler, T.R. and Holland, H.K. 1994. The importance of imperviousness. Watershed Protection Techniques 1(3): 100-111.

Sellinger, Cynthia E. 1996. "Computer Program for Performing Hydrograph Separation Using the Rating Curve Method." NOAA Technical Memorandum ERL GLERL-100. National Oceanic and Atmospheric Administration, n.d. Web. 05 June 2014.

Singh, S., Seung Hyun Kang, Ashok Mulchandani, Wilfred Chen, Bioremediation: environmental clean-up through pathway engineering, Current Opinion in Biotechnology, Volume 19, Issue 5, October 2008, Pages 437-444.

Soulis, K. X., et al. "Analysis of the runoff generation mechanism for the investigation of the SCS-CN method applicability to a partial area experimental watershed." *Hydrology & Earth System Sciences Discussions* 6.1 (2009).

Stone, B. Jr. 2004. Paving over paradise: how land use regulations promote residential imperviousness. Landscape and Urban Planning 69: 101–113.

Stringer, A. F. 2011. Design guidance on low impact development practices for stormwater management and control in Oklahoma. Unpublished M.S. thesis. Oklahoma State University.

Subramanya, K. *Engineering Hydrology*. New Delhi: Tata McGraw Hill Limited, 2013. Web. 07 July 2014.

United States. Army Corps of Engineers (USACE). Assistant Chief of Staff For Installation Management . Army Low Impact Development Technical User Guide. N.p., 4 Jan. 2013. Web. 11 Apr. 2014.

USDA. 2007. Hydrology National Engineering Handbook: Hydrologic Soil Groups Pages 1-14 *in* NRCS, editor. USDA.

USDA NRCS. 2010. National Engineering Handbook, Part 630, Hydrology. Chapter 15: Time of Concentration. Washington, DC: USDA National Resources Conservation Service.

USDA NRCS. ND (No Date). Cross-Section Hydraulic Analyzer. Washington, DC: USDA National Resources Conservation Service. http://go.usa.gov/0Eo. Date Accessed: March 27, 2014.

Vandiver, A. E. 2010. Investigation of low impact development for Coastal South Carolina: Oak Terrace Preserve. Unpublished PhD. Dissertation. University of South Carolina.

VDOT. 2002. VDOT Drainage Manual: Chapter 6 - Hydrology. Virginia Department of Transportation

Walsh, C.J., Roy, A.H., Feminella, J.W., Cottingham, P.D., Groffman, P.M., and Morgan, R.P. 2005. The urban stream syndrome: current knowledge and the search for a cure. Journal of the North American Benthological Society 24, 706–723.

Walsh, C. J., Fletcher, T. D., and Burns, M. J. 2012. Urban stormwater runoff: a new class of environmental flow problem. PLoS ONE, 7(9) e45814. doi:10.1371/journal.pone.0045814

Wanielista, Martin P., and Yousef A. Yousef. "Chapter 3: Hydrographs." *Stormwater Management*. New York: J. Wiley, 1993. 70-76. Print.

Wooten, J. 2008. Assessing the Restoration Feasibility of Rocky Branch Creek: An Integrated Watershed Management Approach. Unpub. M.S. Thesis, Masters in Earth and Environmental Mangagement University of South Carolina.

Yong, C.F., D.T. McCarthy, A. Deletic, Predicting physical clogging of porous and permeable pavements, Journal of Hydrology, Volume 481, 25 February 2013, Pages 48-55, ISSN 0022-1694, http://dx.doi.org/10.1016/j.jhydrol.2012.12.009.

Zhan, X., Min-Lang Huang. 2004. ArcCN-Runoff: an ArcGIS tool for generating curve number and runoff maps, Environmental Modelling & Software, Volume 19, Issue 10, October 2004, Pages 875-879, ISSN 1364-8152, http://dx.doi.org/10.1016/j.envsoft.2004.03.001.

Zimmer, C. A. 2006. Low-impact development practices for stormwater management: Implications for urban hydrology. Unpublished M.S. Thesis. University of Guelph, Canada.

Appendix A: Additional Spatial and Hydrologic Figures

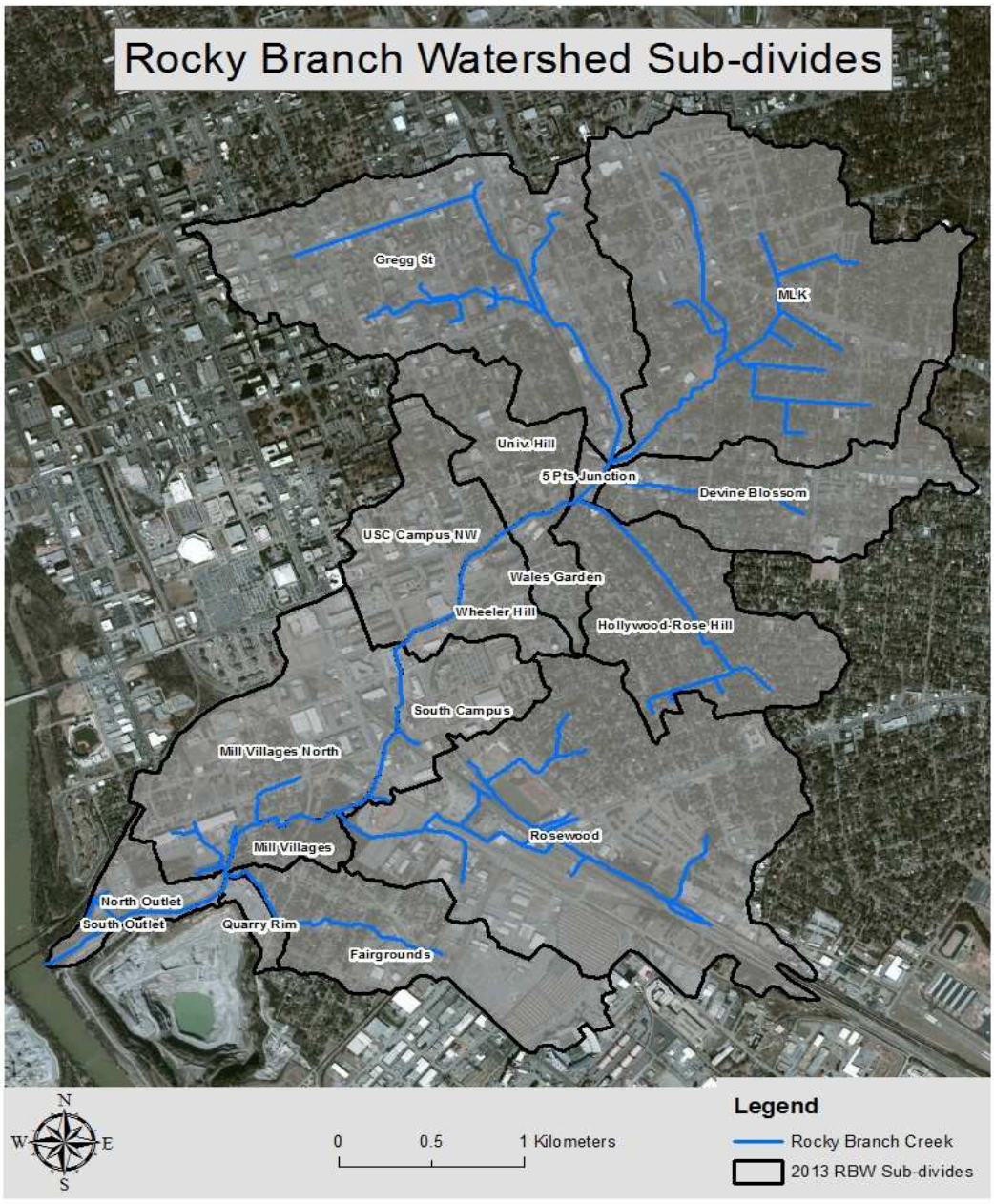

Figure A.1. Rocky Branch Watershed Sub-divides

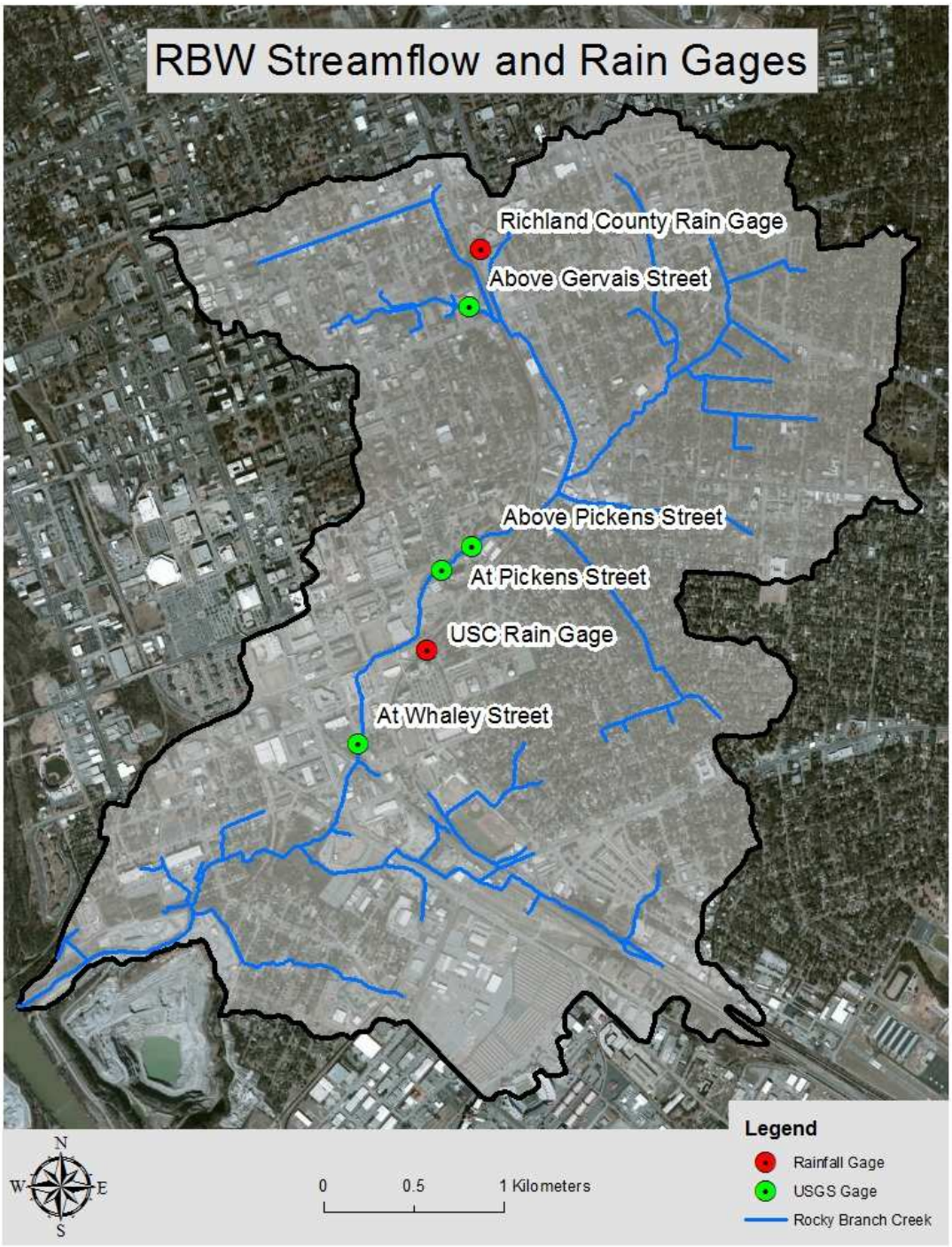

Figure A.2. Rocky Branch Watershed Gages

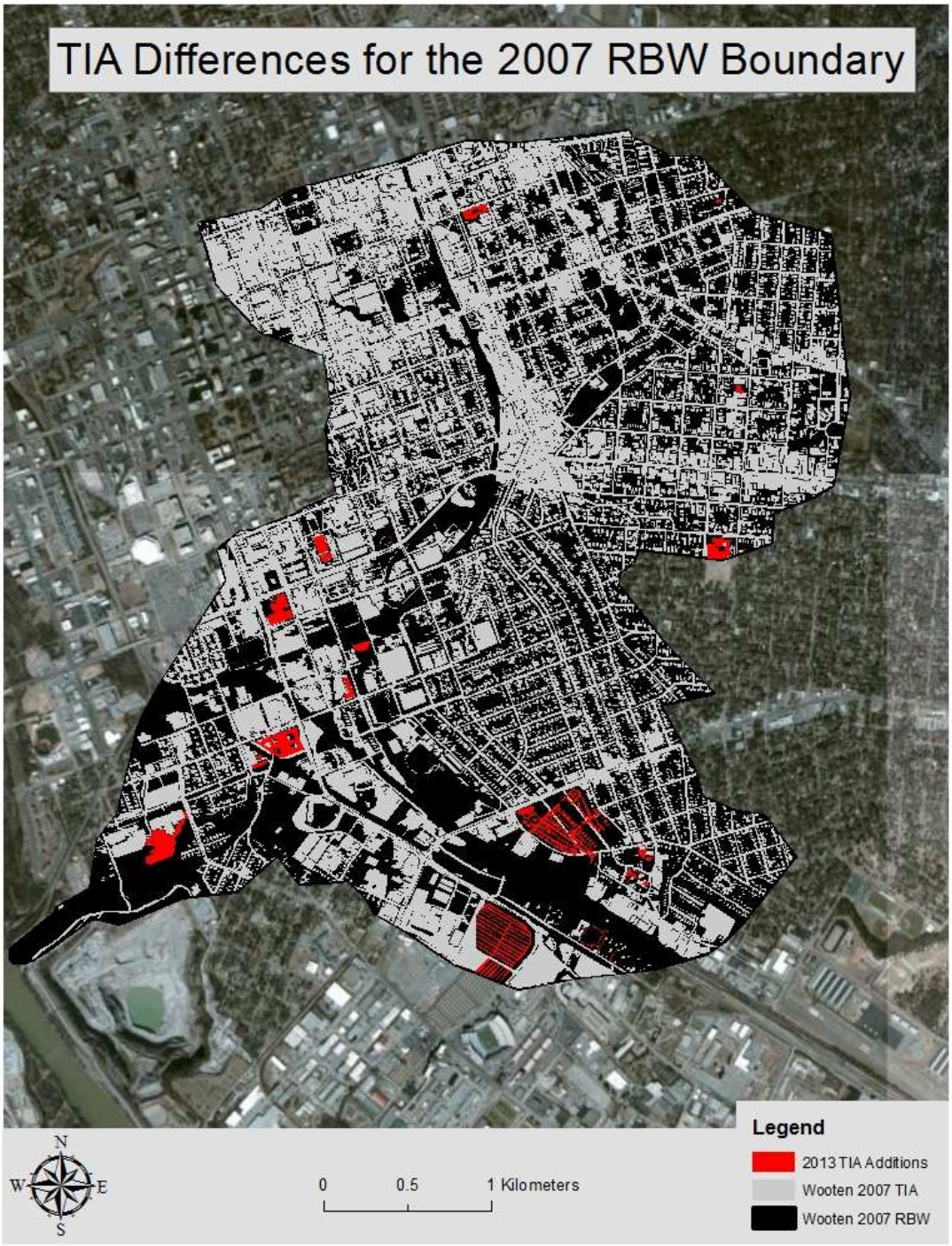

Figure A.3. RBW Total Impervious Area Differences using the 2007 Outer Boundary

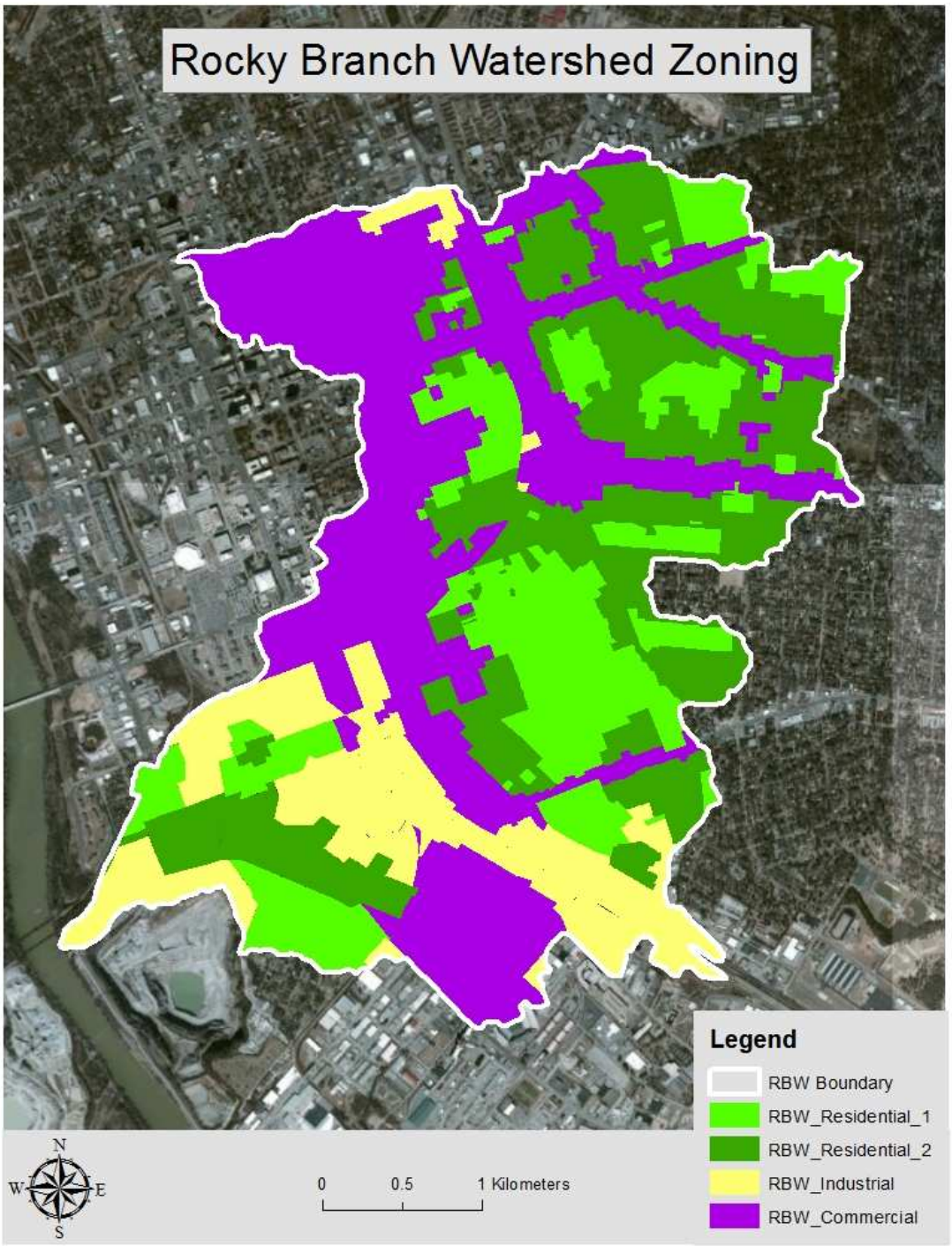

Figure A.4. 2013 Rocky Branch Watershed Zoning

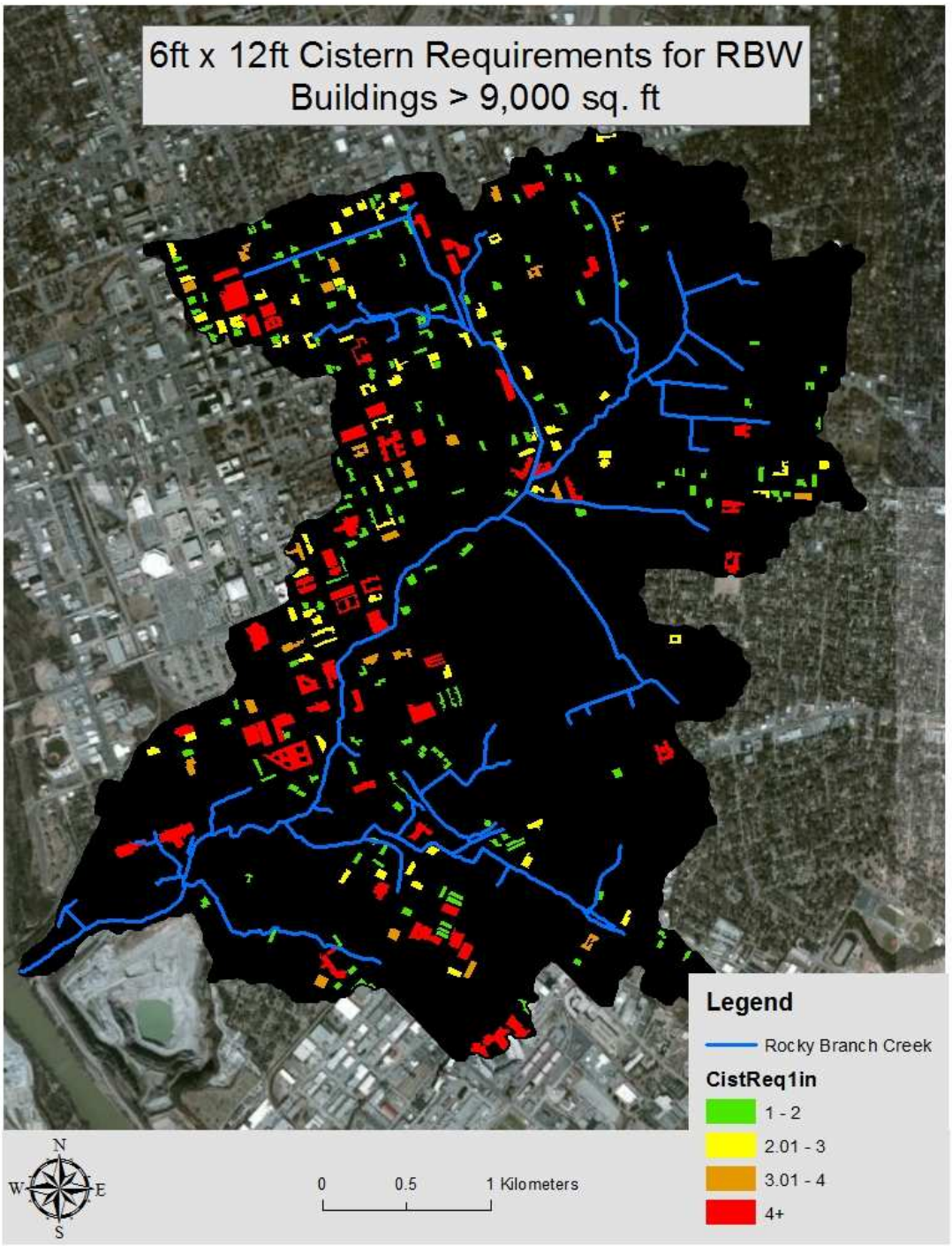

Figure A.5. 6ft x 6ft Cistern Requirements for RBW Buildings Larger than 9,000 sq. ft for a 1-inch uniform rainfall event

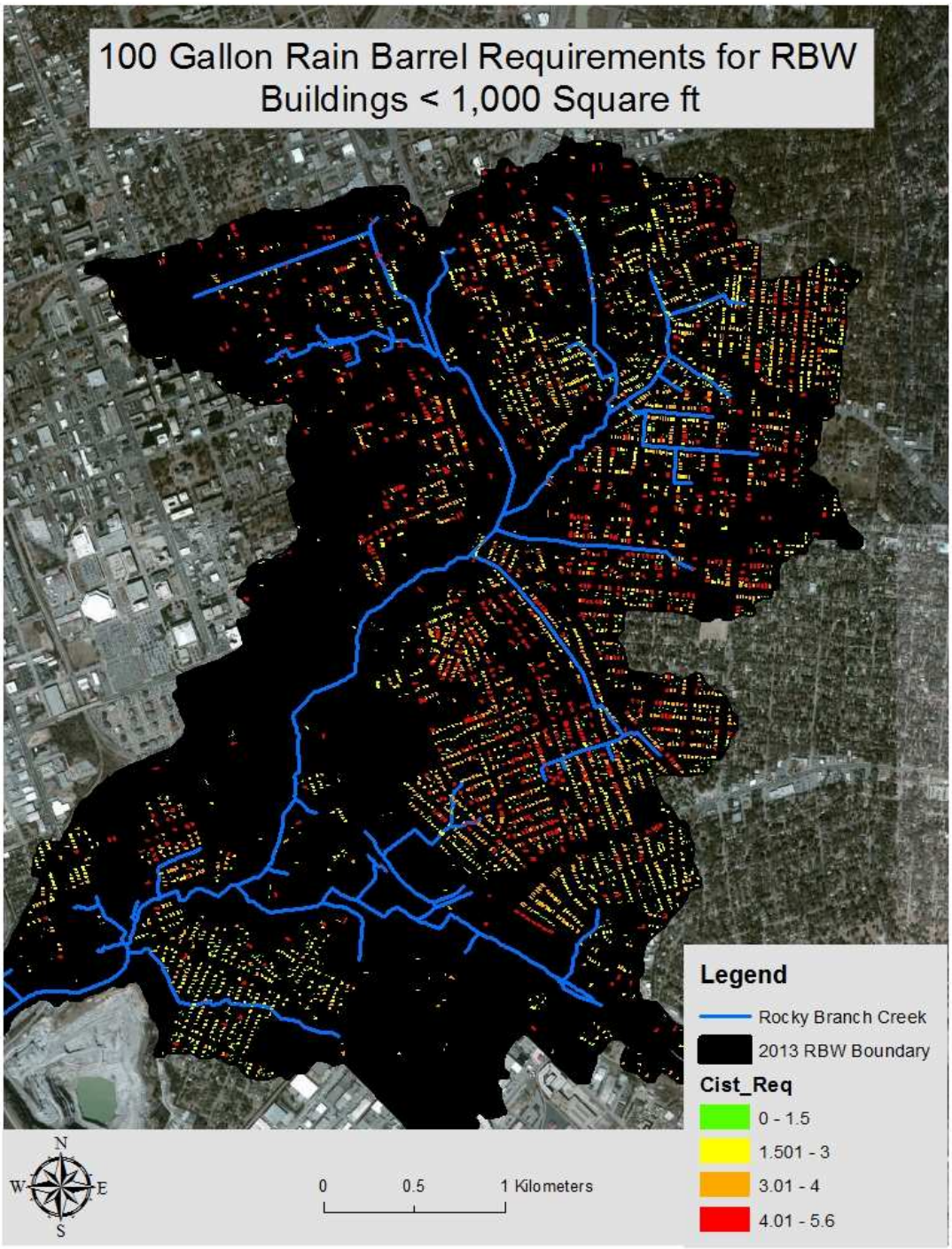

Figure A.6. Rain Barrel (100-gal) Requirements for RBW Buildings Smaller than 1,000 sq. ft for a 1-inch uniform rainfall event

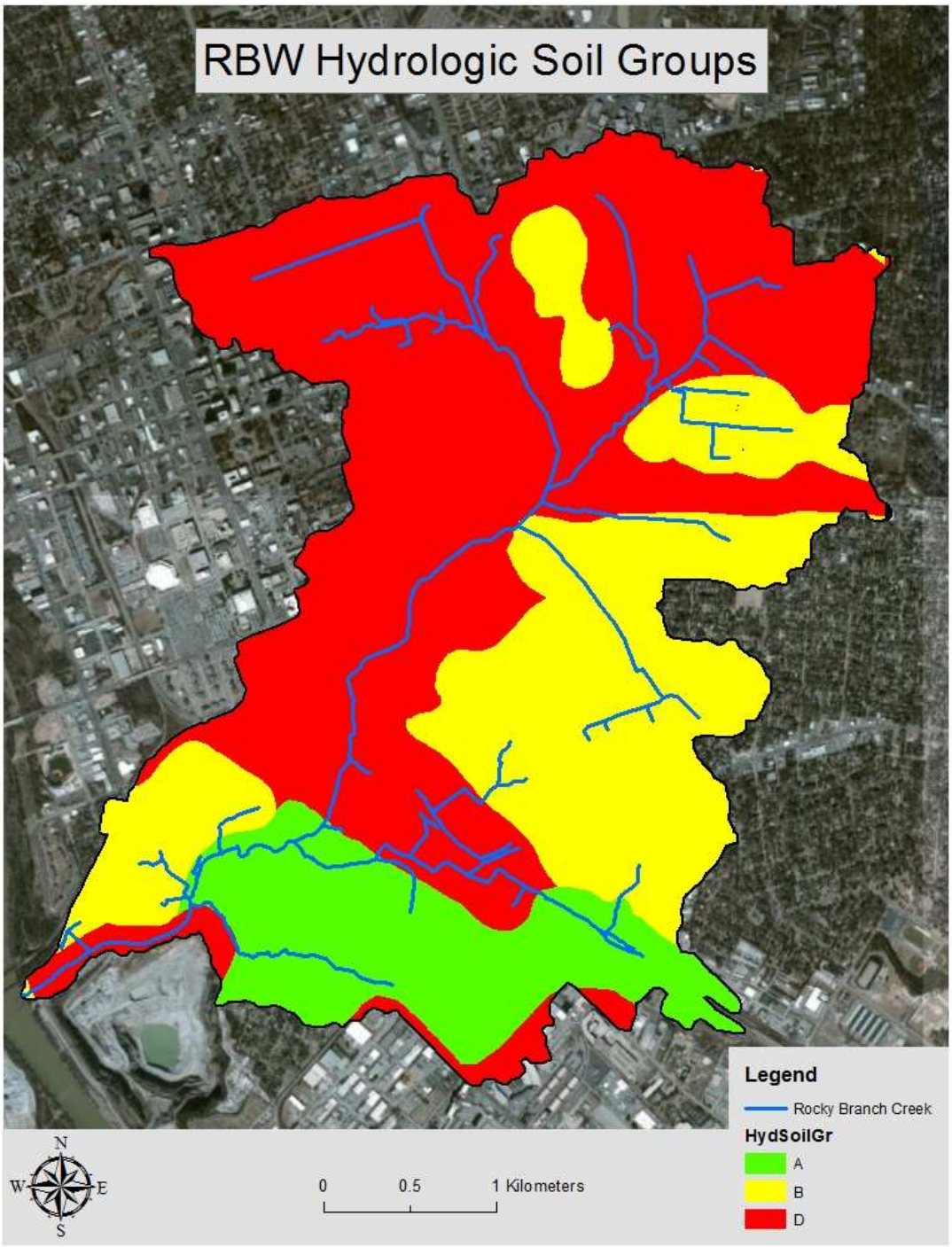

Figure A.7. Rocky Branch Watershed Hydrologic Soil Groups

Figure A.8. Gervais Gage Site Cross-Section;
(A) view upstream (B) view downstream

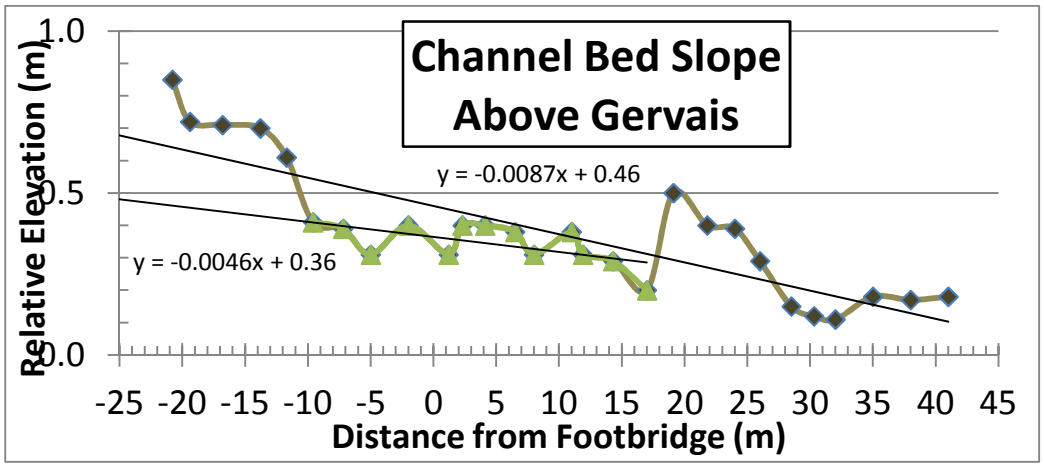

Figure A.9. Gervais Slope Profile

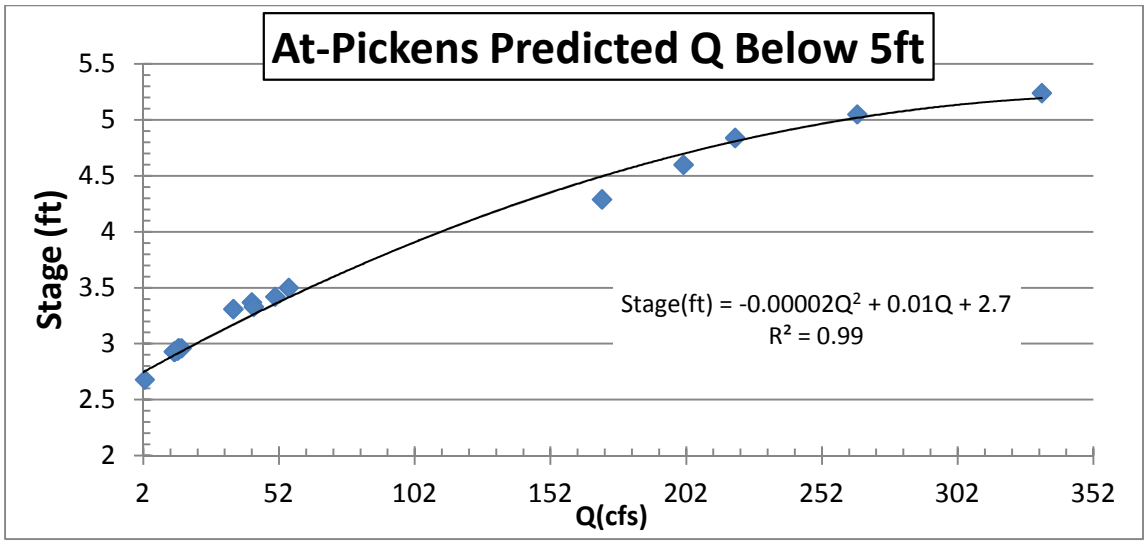

Figure A.10. Predicted Discharge Below 5ft for the At-Pickens Gage Site (Fadi Shatnawi, written communication)

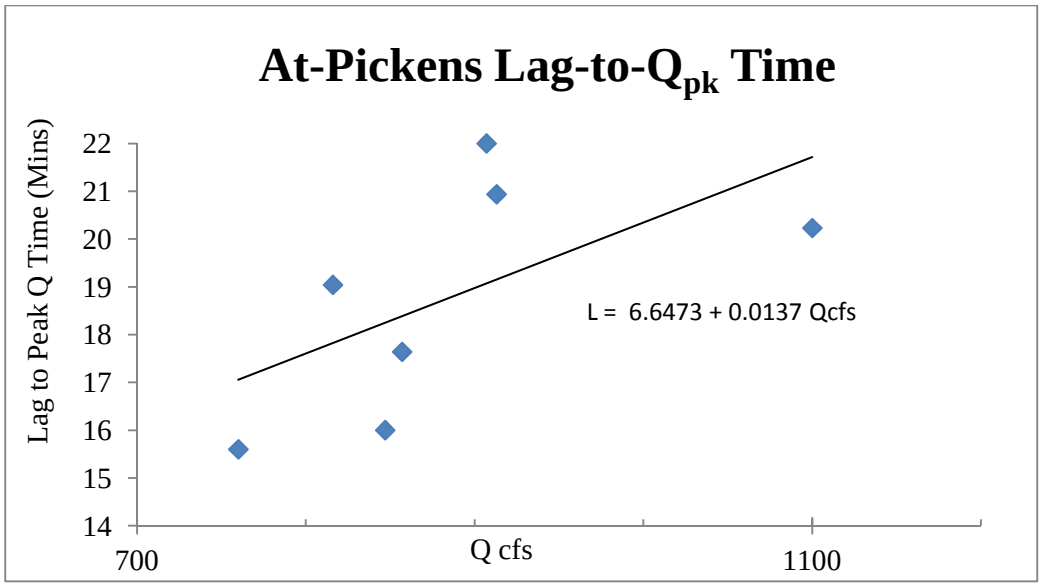

Figure A.11. At-Pickens Discharge Data (Logan et al. 1985; Sanjeev Joshi, written communication)

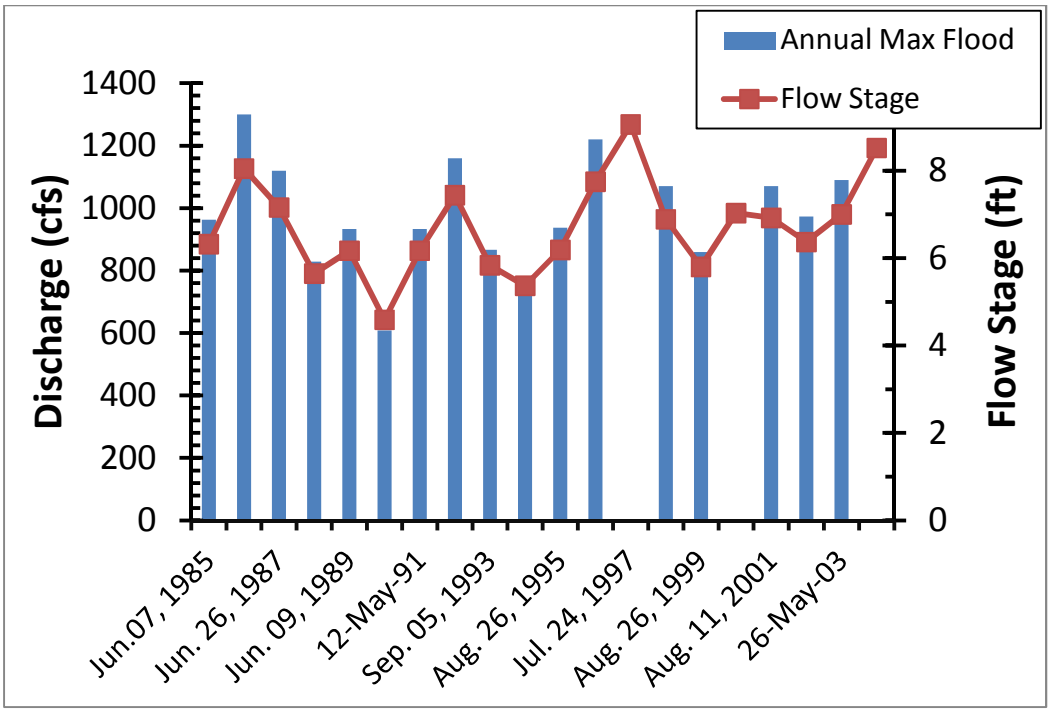

Figure A.12. USGS Annual Peak Discharges for At-Pickens Gage (uncalibrated). http://nwis.waterdata.usgs.gov/usa/nwis/peak/?site_no=02169505

Figure A.13. At-Pickens Gage Site Cross Section.
(A) View upstream from Pickens Street Bridge.
(B) View downstream towards bridge box culverts with stilling well of gage on the right bank

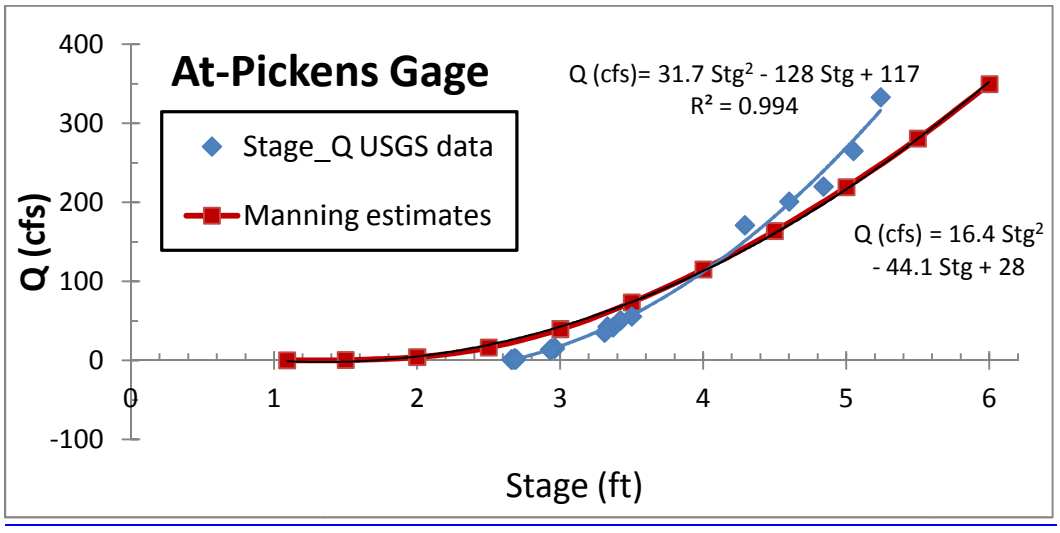

Figure A.14. Stage-discharge calibration curves for At-Pickens gage.

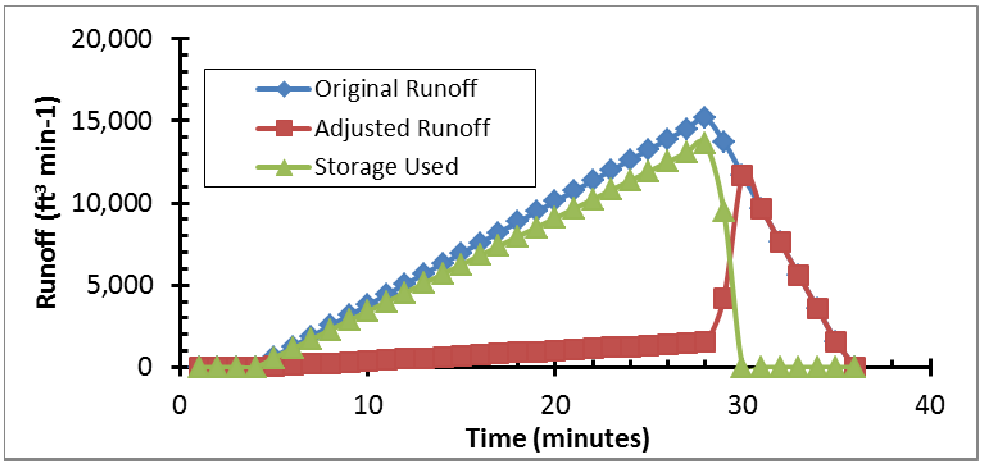

Figure A.15. Gervais hydrograph runoff analysis for the 2-year 30-minute rainfall event after 180,000 ft^3 LID abstraction

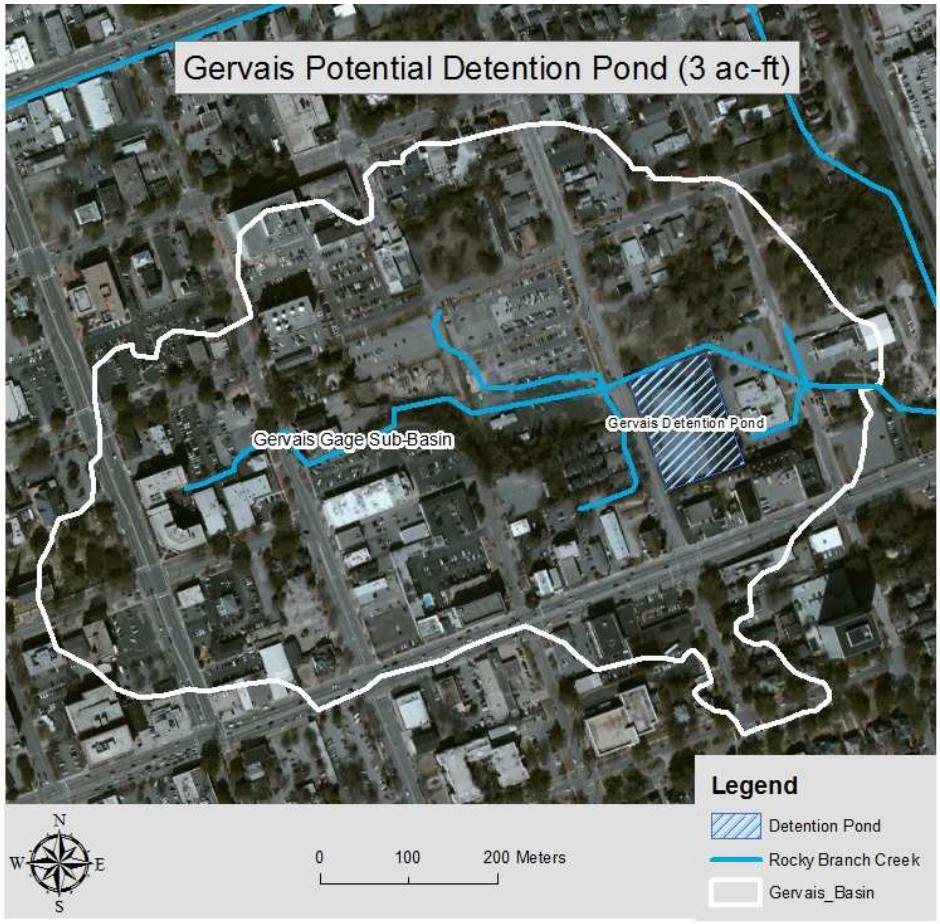

Figure A.16. Potential Gervais Detention Pond

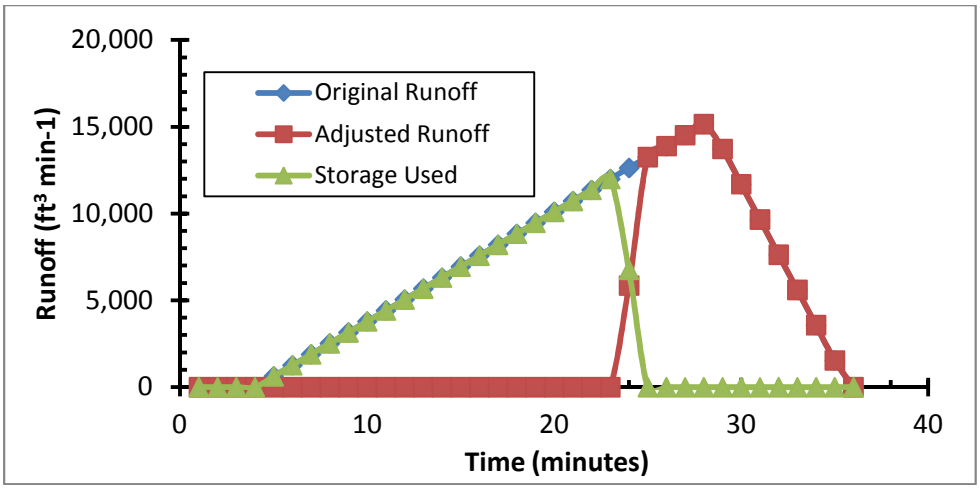

Figure A.17. Gervais hydrograph runoff analysis for the 2-year 30-minute rainfall event after 126,757 ft^3 abstraction and 100% watershed area is treated